

MATHEMATICAL MODELS FOR PREDICTING AND MITIGATING THE
SPREAD OF CHLAMYDIA SEXUALLY TRANSMITTED INFECTION

AN ABSTRACT
SUBMITTED ON THE JANUARY 9, 2022
TO THE DEPARTMENT OF MATHEMATICS
OF THE SCHOOL OF SCIENCE AND ENGINEERING OF
TULANE UNIVERSITY
IN PARTIAL FULFILLMENT OF THE REQUIREMENTS
FOR THE DEGREE OF
DOCTOR OF PHILOSOPHY
BY

ASMA AZIZI BOROOJENI

APPROVED: _____

JAMES MAC HYMAN
CHAIRMAN

PATRICIA KISSINGER

LISA FAUCI

KUN ZHAO

SCOTT MCKINLEY

Abstract

Chlamydia trachomatis (Ct) is the most common bacterial sexually transmitted infection (STI) in the United States and is major cause of infertility, pelvic inflammatory disease, and ectopic pregnancy among women. Despite decades of screening women for Ct, rates continue to increase among them in high prevalent areas such as New Orleans. A pilot study in New Orleans found approximately 11% of 14 – 24 year old of African Americans (AAs) were infected with Ct. Our goal is to mathematically model the impact of different interventions for AA men resident in New Orleans on the general rate of Ct among women resident at the same region. We create and analyze mathematical models such as multi-risk and continuous-risk compartmental models and agent-based network model to first help understand the spread of Ct and second evaluate and estimate behavioral and biomedical interventions including condom-use, screening, partner notification, social friend notification, and rescreening. Our compartmental models predict the Ct prevalence is a function of the number of partners for a person, and quantify how this distribution changes as a function of condom-use. We also observe that although increased Ct screening and rescreening, and treating partners of infected people will reduce the prevalence, these mitigations alone are not sufficient to control the epidemic. A combination of both sexual partner and social friend notification is needed to mitigate Ct.

MATHEMATICAL MODELS FOR PREDICTING AND MITIGATING THE
SPREAD OF CHLAMYDIA SEXUALLY TRANSMITTED INFECTION

A DISSERTATION
SUBMITTED ON THE JANUARY 9, 2022
TO THE DEPARTMENT OF MATHEMATICS
OF THE SCHOOL OF SCIENCE AND ENGINEERING OF
TULANE UNIVERSITY
IN PARTIAL FULFILLMENT OF THE REQUIREMENTS
FOR THE DEGREE OF
DOCTOR OF PHILOSOPHY
BY

ASMA AZIZI BOROOJENI

APPROVED: _____

JAMES MAC HYMAN
CHAIRMAN

PATRICIA KISSINGER

LISA FAUCI

KUN ZHAO

SCOTT MCKINLEY

Acknowledgement

Foremost, **Thanks to merciful God** for all the countless gifts dedicated me and to my parents for their love and for supporting me spiritually throughout my PhD and my life.

I would like to express my heartiest gratitude to my advisor Prof. **James Mac Hyman** for his sincere guidance, his continuous support of my Ph.D study and research, his patience, motivation, enthusiasm, and immense knowledge. Mac you are more than an advisor for me: with your way of teaching I grew up both personally and professionally. You are the very best advisor any lucky student can have.

I also would like to thank my thesis committee members: Profs. Patricia Kissinger, Lisa Fauci, Scott Mcckinley and Kun Zhao, for their encouragement, insightful comments, and hard questions. My sincere thanks also goes to Norine Schmidth, Dr. Charles Stocker, and Dr. Martin , for leading me working on this project projects.

And an special thank to all my friends and fellows specially to Martha Dryer, Jeremy Dewar, Zhuolin Qu, Justin Davis, and Ling Xue and all those, too many to name.

This work was supported by the endowment for the Evelyn and John G. Phillips Distinguished Chair in Mathematics at Tulane University, grants from the National Institutes of Health National Institute of Child Health and Human Development, NCHID/NIAID (R01HD086794), Office of Adolescent Health, OAH (TP2AH000013), the National Institute of General Medical Sciences program for Models of Infectious

Disease Agent Study (U01GM097658), and by grants from the National Science Foundation (DMS1263374).

List of Tables

2.1	Variables and parameters of the model	21
2.2	Sensitivity index of \mathcal{R}_0 with respect to parameters of the model	27
2.3	Sensitivity index of endemic point with respect to parameters of the model	29
2.4	\mathcal{R}_0 for different scenarios	31
2.5	Sensitivity indices of equilibrium points with respect to screen- ing rates	32
3.1	Model parameters	44
3.2	Condom-use fraction based on age and risk	45
3.3	Condom-use scenarios	52
4.1	Joint-degree table from data	59
4.2	Joint-degree probability	60
4.3	Joint-degree probability distribution	61
4.4	The number of sexual acts based on number of partners for women	62
4.5	Number of acts per partner per unit time	63
4.6	Probability distribution for men's age	64
4.7	The Contact file of social network	65
4.8	Parameters of the model and their baseline values	77

4.9	Notification scenarios	92
A.1	Properties of the real and randomly generated Romance networks	113
A.2	Properties of real Romance network and of the networks generated by the ED_{\max} algorithm, configuration model and Havel Hakimi algorithm.	114
B.1	Notations table	122

List of Figures

1.1	Ct vs gender	3
1.2	Ct vs region	3
1.3	Ct vs age	4
1.4	Screened females for Ct	5
1.5	Concept of \mathcal{R}_0	6
1.6	Components of partner notification	11
2.1	The number of acts per partnership per unit time vs number of partners	22
2.2	Sensitivity of basic reproduction number	27
2.3	Prevalence of Ct for different screening scenarios	31
(a)	Different scenarios	31
(b)	Optimized scenario	31
3.1	Components of the transmission rate $\lambda(t, r)$	38
3.2	Biased mixing function	40
3.3	\mathcal{R}_0 vs preference level ϵ	48
3.4	Infected fraction vs risk r and preference level ϵ	50
(a)	$3D \epsilon = 0.1$	50
(b)	$2D \epsilon = 0.1$	50
(c)	$3D \epsilon = 0.6$	50

(d)	$2D \epsilon = 0.6$	50
(e)	$3D \epsilon = 0.9$	50
(f)	$2D \epsilon = 0.9$	50
3.5	Total infected fraction vs condom-use	51
3.6	Ct prevalence vs time for different condom-use scenarios	53
4.1	Bar plot for number of partners	58
4.2	Bar plot of	58
(a)	Number of partners for men	58
(b)	Number of partners for women	58
4.3	Bar plot of age distribution of men	64
4.4	Bar plot of age distribution	65
(a)	For partners of men	65
(b)	For primary partners of men	65
4.5	Box plot for size of giant component and bi-component	68
4.6	Box plot for number of connected components	68
4.7	Redundancy coefficient vs degree	69
4.8	Box plot of age distribution for social friends and sexual partners of men	70
4.9	Biomedical intervention flow diagram	74
4.10	Prevalence of Ct vs time	76
4.11	Ct dynamic on network	79
(a)	Prevalence of Ct vs time for different networks	79
(b)	Prevalence of Ct vs time at baseline	79
4.12	Bar plot of distributions for	80
(a)	Degree Centrality	80
(b)	Betweenness Centrality	80
(c)	Closeness Centrality	80

4.13	Difference between degree and closeness scores	80
4.14	Distance reachability for nodes with different degree and close- ness scores	83
(a)	Degree vs Closeness Centrality	83
(b)	Distance-Reach distribution	83
(c)	Reachability Probability within 20 Distance	83
4.15	Prevalence vs screening rate for men	85
(a)	Prevalence of Ct vs time for different networks	85
(b)	Prevalence of Ct vs time at baseline	85
4.16	Interval for rescreening	86
4.17	Quasi-steady state vs rescreening rate	87
4.18	Prevalence vs partner treatment	88
(a)	Prevalence of Ct at quasi-stationary state vs fraction of partners notified	88
(b)	Prevalence of Ct vs time at baseline	88
4.19	Prevalence vs partner screening	89
(a)	Prevalence of Ct at quasi-stationary state vs fraction of partners notified	89
(b)	Prevalence of Ct vs time at baseline	89
4.20	Prevalence vs partner treatment and screening	90
4.21	Prevalence of Ct vs time for scenarios 1-7	91
(a)	Partner screening	91
(b)	Partner treatment	91
A.1	Rewiring with 3 swaps	103
A.2	Rewiring with 2 swaps	103
A.3	Romance contact network	112
A.4	Bar plot of distribution for properties of generated networks	115

(a)	Clustering coefficient	115
(b)	Redundency coefficient	115
(c)	Size of giant component	115
(d)	Number of connected components	115
A.5	Giant components of romance network	116
(a)	Romance Network	116
(b)	ED _{max} Algorithm	116
(c)	Configuration Model	116
(d)	Havel Hakimi model	116
B.1	Schematic of step 1	120

Contents

Acknowledgement	ii
List of Tables	iv
List of Figures	vi
1 Chlamydia Trachomatis	1
1.1 History of Ct	2
1.2 Symptoms and Causes	4
1.3 Control and Prevention	5
1.3.1 Behavioral approach: reducing to exposure and transmission .	7
1.3.2 Biomedical approach: reducing infection period	9
1.4 Mathematical Approaches to Control Ct	10
2 Multi-risk Compartment Model	14
2.1 Ct Transmission Model Overview	15
2.1.1 Transmission rate	17
2.1.2 Partnership formation	18
2.1.3 Probability of transmission per partner	20
2.2 Basic Reproduction Number	22
2.3 Sensitivity Analysis	25
2.3.1 Sensitivity indices of \mathcal{R}_0	26

2.3.2	Sensitivity indices of endemic equilibriums	28
2.4	Screening Scenarios	30
2.5	Discussion and Conclusion	33
3	Continuous Risk-based Model	34
3.1	Ct Transmission Model Overview	35
3.1.1	Transmission rate	36
3.1.2	Partnership formation	37
3.1.3	Probability of transmission per partner	41
3.2	Parameter Estimation	44
3.2.1	Population distribution	44
3.2.2	Condom-use	44
3.3	Numerical Simulations	45
3.3.1	Basic reproduction number \mathcal{R}_0	46
3.3.2	Endemic equilibrium	47
3.3.3	Condom-use scenarios	49
3.4	Discussion and Conclusions	52
4	Network Model	56
4.1	The New Orleans Sexual Activity Survey Data	57
4.1.1	Distributions for number of partners	57
4.1.2	Distribution for number of partners of partners	59
4.1.3	The number of sexual acts per partner	62
4.1.4	Age distribution	63
4.2	The New Orleans Social Activity Data	64
4.3	Network Generation	66
4.3.1	Analysis of generated networks	67
4.3.2	Age distribution of the network	69

4.4	Ct Transmission Model Overview	70
4.4.1	The force of infection	71
4.4.2	Recovery from infection	71
4.4.3	Model initialization	75
4.5	Numerical Simulations	76
4.5.1	Dynamic of Ct on networks	77
4.5.2	Analysis of infected population at quasi-steady state	78
4.5.3	Mitigation efforts for controlling chlamydia	82
4.6	Discussion and Conclusion	93
A	Generating Bipartite Networks with a Prescribed Joint Degree Dis-	
	tribution	98
A.1	Bipartite Network	100
A.2	Some Definitions Related to Bipartite Network	104
A.3	Generating Bipartite Network	106
A.4	Rewiring Approach	110
A.5	Romance Network	111
B	Sexual Activities Hidden in Social Organization: A Preferential At-	
	achment Mechanism for Human Sexual Network Formation in So-	
	cial Network Context	117
B.1	Degree and joint-degree distribution and <i>BJD</i> matrix for a sexual network	118
B.2	Social network embedding sexual network	118
B.3	Generating Bipartite Sexual Network	119
B.3.1	The algorithm	119
B.3.1.1	Phase 1: extension and revision of SocNet	119
B.3.1.2	Phase 2: main algorithm	121

B.3.1.3	Phase 3: correcting BJD	125
References		127

Chapter 1

Chlamydia Trachomatis

Chlamydia trachomatis (Ct) is an infection from the family of Sexually Transmitted Infections (STIs), which are transmitted through sexual acts and they can be caused by bacteria or viruses. Here, sexual act means any type of sexual intercourse including oral, vaginal, and anal sex. STIs are one of the most common causes of illness and even death worldwide, and therefore, are a major public health issue. These infections exert a high emotional toll on suffered individuals, as well as an economic burden on public health system. The World Bank estimated that among women aged 15 – 44 year old, STIs (excluding HIV) are the second most common causes of healthy life lost after maternal morbidity [1].

There are more than 20 different STIs including chlamydia, gonorrhea, syphilis, herpes, viral hepatitis, and HIV affecting men and women of all backgrounds and economic levels. However, because of lack of an effective notification system in many countries and also lack of symptom in most of these STIs, the size of the global burden of STIs is uncertain. In this Chapter we are going to review a background and feature of the most prevalent bacterial STI i.e Ct.

1.1 History of Ct

Chlamydia is an infection caused by a kind of bacteria called *Chlamydia trachomatis* (Ct) that is passed during sexual act, usually thorough vaginal and anal intercourse. Ct was first discovered in 1907 by german parasitologist Stanislaus von Prowazek. Genus part of the name, Chlamydia, comes from the Greek word *chlamys*, which means cloak and the species part of the name, *trachomatis* is also Greek and means rough or harsh [2].

Most of Ct cases do not show any symptom, for that reason it sometimes called *Silent infection*, for the cases showing symptom, its symptoms are similar to some other infections, therefore, it was not recognized as a sexually transmitted disease till 1980.

Today Ct is the most common and the most spread bacterial STI in the world. In 1997 there were 537,904 reported diagnoses, however, by 2009 the annual total had more than doubled to 1,244,180. In the United States over 2.8 million cases of Ct are reported each year [3]. Based on Center of Disease Control and Prevention (CDC) report, about three million American women and men become infected with Ct every year. Spreading of Ct among African Americans, AAs, was eight times bigger than whites and rates among American Indians/Alaska Natives and Hispanics are also higher than among whites [4]. The Figure (1.1) shows the rate of reported infected cases by gender in years 1994-2014 and Figure (1.2) is reported cases by region in 2014 in the United States.

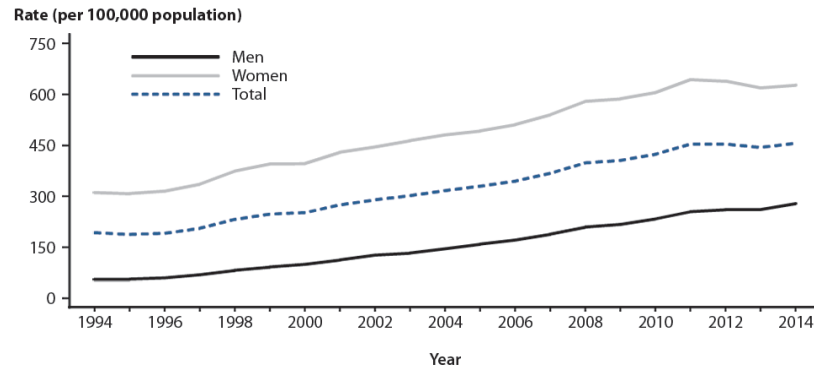


Figure 1.1: Rates of Reported Cases by gender in United States in years 1994 – 2014 [4].

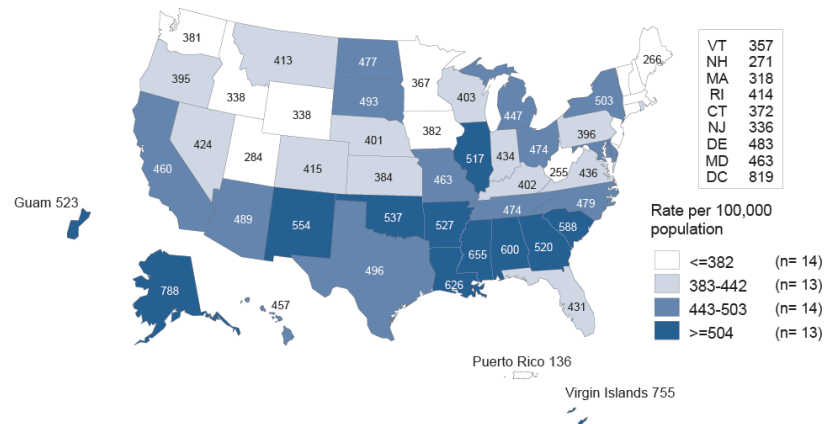


Figure 1.2: Rates of Reported Cases by region in United States in 2014 [4].

Ct mostly affects young people, individuals ages 15 – 25 years old. CDC estimates that adolescent and young adults, people ages 15 – 25 years old, make up around one quarter of the sexually active population, but account for 67% of the Ct infections that occur in the United States [4]. In 2013, the rate among 15 – 19 year old people was 1852.1 cases per 100000 and the rate among 20 – 25 year old people was 2451.6 cases per 100000. As shown in Figure (1.3), among women, the highest age-specific rates of reported Ct in 2013 were among those aged 15 – 19 years (2941.0 cases per 100000 women) and 20 – 25 years (3651.1 cases per 100000 women) [4].

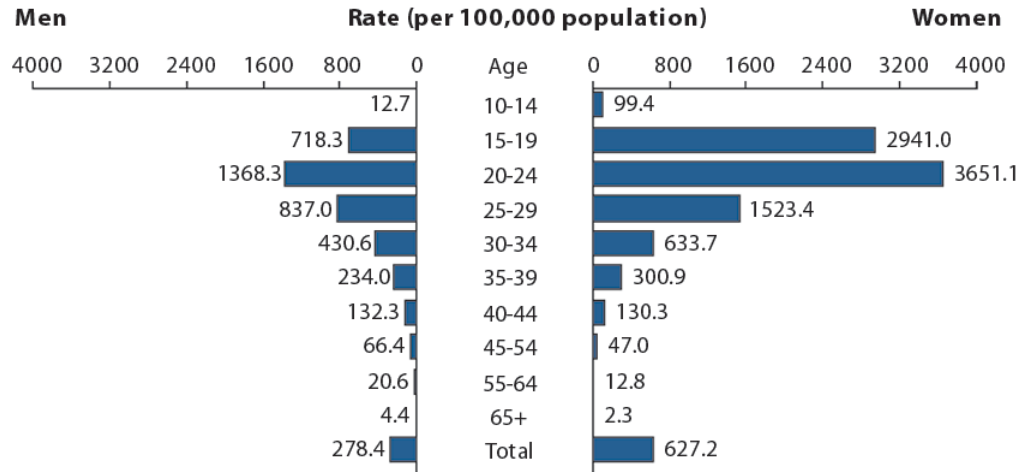


Figure 1.3: Ct Rates of Reported Cases by Age Group and Sex, United States, 2016 [4].

1.2 Symptoms and Causes

Ct is known as a silent infection because most of the infected people are asymptomatic and lack abnormal physical examination findings: about 70% – 95% of women and 90% of men with Ct have no symptoms [5, 6]. However, in the case infected people show symptoms, they are different for women and men.

Infected women with Ct may experience abdominal pain, abnormal vaginal discharge, bleeding between menstrual periods, low-grade fever, painful intercourse, pain or a burning feeling while urinating, swelling inside the vagina or around the anus, the urge to urinate more than usual, vaginal bleeding after intercourse, and yellowish discharge from the cervix [4]. Infected men may experience pain or a burning feeling while urinating, pus or watery or milky discharge from the penis, swollen or tender testicles, and swelling around the anus [4].

Ct infections are associated with a spectrum of clinical diseases, urethritis and including epididymitis among men, and cervicitis, salpingitis, and acute urethral syndrome among women [7]. Although at the early stage of Ct the damages go unnoticed,

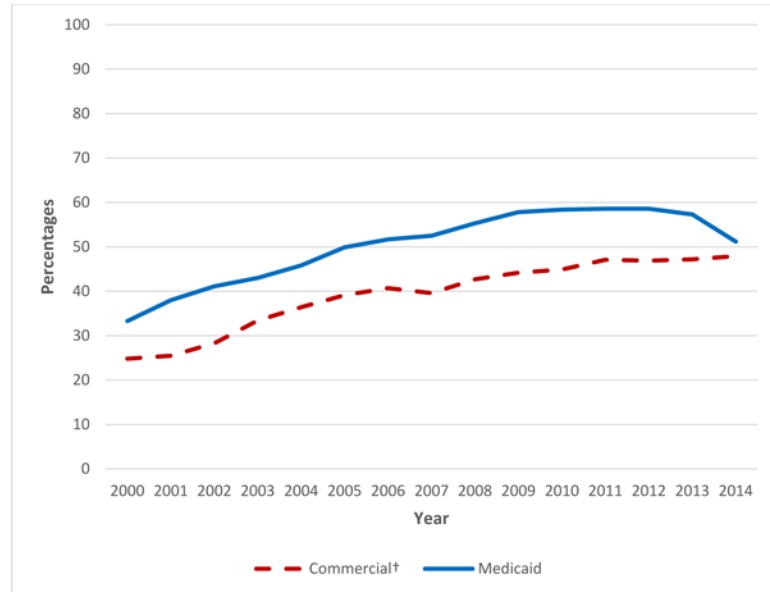


Figure 1.4: Percentage of sexually active female aged 16–24 years who were screened for Ct infection, by health plan type and year, United States, 2000–2014

but Ct can lead to serious health problems, that is, because Ct is silent infection, it can sometimes cause other diseases.

Ct is a major cause of infertility, pelvic inflammatory disease (PID), and ectopic pregnancy among women with estimated annual cost exceeds five billion dollars [8–16], and has been associated with increased HIV acquisition and transmission [8,10,12–19]. Untreated, an estimated 16% of women with Ct will develop PID [8], and 6% will have tubal infertility [13]. In pregnant women, untreated Ct has been associated with pre-term delivery, as well as ophthalmia neonatorum (conjunctivitis) and pneumonia in the newborn [20].

1.3 Control and Prevention

The rate of spread of Ct in a population is determined by three factors [21]:

1. the probability of acquiring the infection by susceptible individuals, i.e the efficiency of transmission (β),

2. the rate of exposure of susceptible persons to infected partners (c), and
3. the length of time that persons are infected and are able to transmit infection (τ).

There is an important concept in epidemiology- called basic reproduction number and shown by \mathcal{R}_0 - which states on average how many infections result from one infected person in a wholly susceptible population. For the very simple model this value is calculated as $\mathcal{R}_0 = \beta c \tau$. If this value is greater than one, then Ct can increase in the community. But, if it is less than one, then the rate of spread of the Ct will die out. The pattern of spread for when $\mathcal{R}_0 \leq 1$ and $\mathcal{R}_0 > 1$ is shown Figure (1.5).

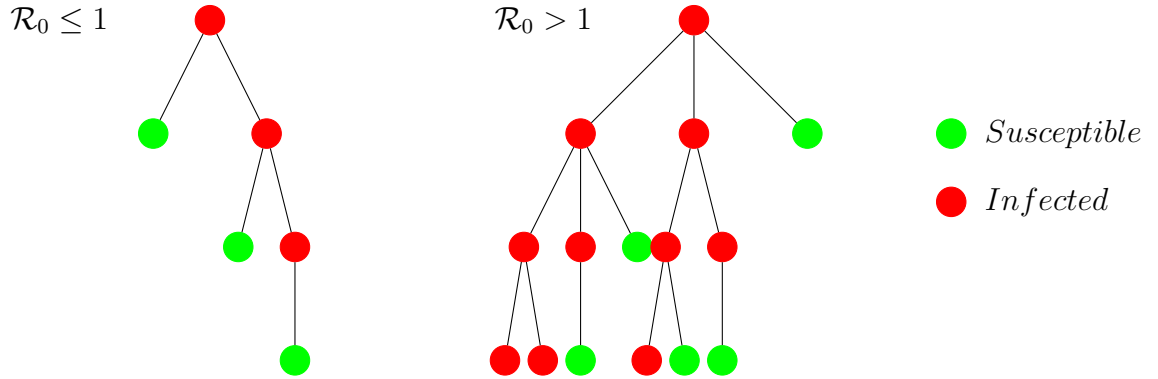


Figure 1.5: Pattern of Spreading of infection for the cases $\mathcal{R}_0 \leq 1$ and $\mathcal{R}_0 > 1$.

Our main goal of interventions is keeping \mathcal{R}_0 less than 1. Therefore, we can prevent the spread of Ct within a population by reducing the rate of exposure to Ct, reducing the efficiency of transmission, or shortening the duration of infectiousness for Ct [21]. Targeting each of these factors by individuals or committees to control the epidemic of Ct ends up with different strategies to take [21].

For individual level, the only safe way to prevent Ct is to abstain from sexual act with others [4]. However, this way is not realistic and applicable. People can reduce their risk of catching or transmitting the infection by changing their behaviors such as using condoms during every sexual act, reducing the number of concurrent sex partners, and undergoing regular screenings.

For population level, the strategies to control Ct with emphasis on different components depends on the local pattern and distribution of Ct in the community and economical condition of the community. There are several principles to apply: prevention can be aimed at uninfected people in the community to prevent them from acquiring infection (reducing to exposure and transmission) or at infected people to prevent the transmission of the infection to their sexual partners (reducing infection period) [1, 22]. In this subsection, we explain each of the principles which was taken from [1].

1.3.1 Behavioral approach: reducing to exposure and transmission

A **behavioral intervention** is a set of interventions encouraged by public health to individuals for implementing in order to reduce Ct transmission. Individual, group, and community-level behavioral interventions seek to directly change so-called behavioral determinants of risky behaviors, such as sexual and drug use knowledge, attitudes, beliefs, perceptions of risk, barriers, social norms, motivation to change, behavioral intentions, self-efficacy (confidence) and a variety of skills (e.g., partner negotiation skills, correct condom use skills) as a route to behavior change [1].

A **sexual behavior** is commonly defined as behavior that effects one's risk of contracting Ct and generally STIs. Because sexual activity is typically initiated in adolescence or early adulthood and because that period for many young people is characterized by greater amounts of experimentation, partner change, and risk taking than in later years, research programs with a focus on the behaviors of adolescents and young adults are of particular importance [23]. Aral [24] reviewed the sexual and other behaviors that place individuals at a high risk of exposure to Ct. These behaviors are:

1. Initiation of sexual intercourse at an early age, because adolescents are biologically more susceptible to Ct than adults.
2. Taking lots of concurrent partners: the greater the number of partners an individual has, the greater is the risk of exposure to any STI, because this behavior increases the chance of having an infectious partner.
3. Having sex with a partner who is likely to have had many partners.
4. Increased frequency of intercourse: the greater is the frequency of intercourse with an infected partner, the greater are the chances of transmission.
5. Lack of circumcision of male partner: women with male partners who are circumcised are at lower risk of exposure compared to those with uncircumcised partners.
6. Lack of barrier contraceptive use such as condoms [24].

Condoms, if used correctly and consistently during every sexual intercourse, are the most effective method of preventing exposure to Ct [4]. Condoms are also highly effective against bacterial and viral STIs including HIV infection, however, failure to use a condom correctly and consistently, rather than potential defects of the condom itself, is considered to be the major barrier to condom effectiveness [25]. Data show that condom-use has increased in the United States in the last few decades: six in ten high school students in the United States, who are sexually active, reported they used condoms at their most recent sexual intercourse. Condom-use among this group increased from 46% in 1991, to 63% in 2003, and was 59% in 2013 [26]. Reece et al. [27] also studied rates of condom-use among sexually active individuals in the United States population. Based on their result, adolescents reported condom-use during 79.1% of the past 10 vaginal intercourse events.

1.3.2 Biomedical approach: reducing infection period

The goal of **Biomedical interventions** is to reduce the risk of infected individuals transmitting infection to their partners [1]. These approaches entail encouraging health seeking behavior and increasing screening and appropriate treatment of symptomatic and asymptomatic people and tracing, screening, and treating sexual partners of infected people, and presumptive treatment of people at high risk of infection [1]. Historically, most of the Ct programs aim to reduce infection period by treating infected people and their partners through screening and partner notification.

Screening: early diagnosis and treatment of Ct are valuable and inexpensive, because if Ct is well controlled other serious long term sequelae can be prevented [21]. In the United States specialized STI clinics provide screening and treatment for people with symptoms of, or who feel they are at risk of, STIs [21].

Partner Notification: partner notification has been a component of STI programs in the United States for many years [28], and has continued to be supported through current federally funded STI programs. For the infections which the incubation period is long like syphilis, partner notification is able to break the chain of transmission by identifying source of infection and their partners and or by identifying and treating partners exposed to infection [29]. For STIs with short incubation period like gonorrhea and Ct the rationale of partner notification has to be modified [29]. For example, emphasis can be placed on locating asymptomatic infected partners of symptomatic or asymptomatic screened individuals and on providing early treatment to prevent complications [29]. Partner notification prevents transmission to partners and directly benefit the exposed individual by preventing symptomatic infection and is considered to be a strategy that benefits the partner of individual index patient and the community and even index patients themselves because treatment of their partner causes that they do not become reinfected [1].

There are several approaches of implementing partner notification: one of the widespread techniques in partner notification is *provider referral*. This method relies on intensive interviews with patients about their sexual histories and partners, followed by active outreach by public health staff to identify and locate partners to ensure that they are examined and treated [21]. Although labor intensive and costly, provider referral is still carried out within most public health programs for some selected STIs including Ct [17].

In *Patient referral* the patients themselves notify their partners about Ct exposure which is time effective for public health staff.

If index patient undertakes to notify partners themselves in a given time frame *Contract referral* will be used, i.e if the partners are not notified in this period, the health adviser will attempt to notify them with the patients consent [1].

When the partner is notified through one of the above methods then he/she may be given medications without testing, *partner treatment*. This practice, although widespread, has several disadvantages for preventing infection including the small but real risk of adverse drug reactions in unseen patients, the inability to screen the partner for other STIs, and the lack of opportunity to examine and counsel the partner [1]. Partner may follow test first and then follow medication if infected, *partner screening*. The following diagram explains the process in partner notification.

1.4 Mathematical Approaches to Control Ct

Mathematical models create frameworks for understanding underlying epidemiology of diseases and how they are correlated to the social structure of the infected population [30–40]. Transmission-based models can help the medical/scientific community to understand and to anticipate the spread of diseases in different populations and help

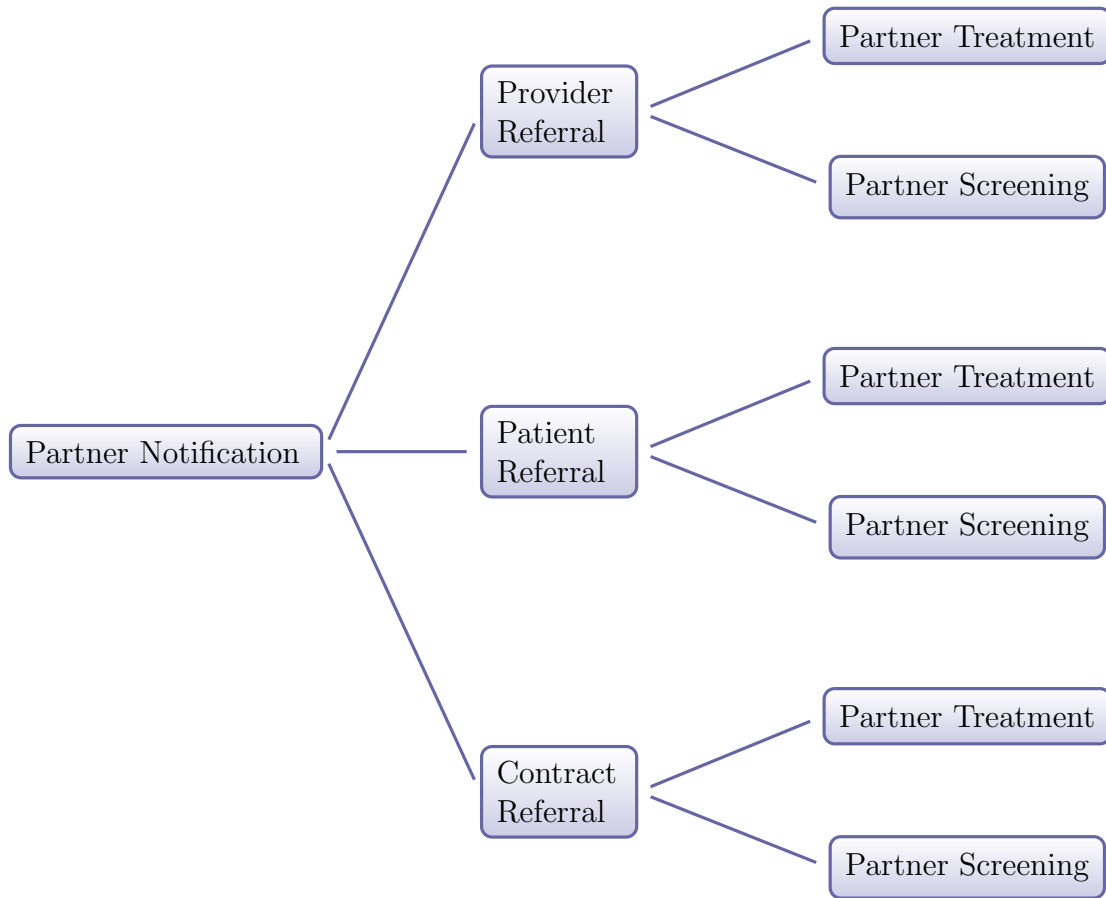


Figure 1.6: Components of Partner Notification.

them to evaluate the potential effectiveness of different approaches for bringing the epidemic under control. Therefore, primary goal of mathematical modeling effort is to create a detailed model that can be used understand the spread of infection and predict the impact of mitigation efforts to reduce the prevalence. In this Section we review some of the most important and recent mathematical models for Ct, and then we outline our project on mathematical model and mitigation efforts on controlling Ct in New Orleans.

The SEIRS Ct transmission model developed by Althaus et al. [41] captures the most essential transitions through an infection with Ct to assess the impact of Ct infection screening programs. Using sensitivity analysis they identified the time

to recovery from infection and the duration of the asymptomatic period as the two most important model parameters governing the disease prevalence. Longer recovery time diminishes the effect of screening, however longer duration of the asymptomatic period results in a more pronounced impact of program. They also used their model to improve the estimates for the duration of the asymptomatic period by reanalyzing previously published data on persistence of Ct in asymptotically infected women. This model did not divide the population into separate risk groups and assumed that all men and women had the same number of partners.

Clarke et al. [42] investigated how control plans can affect observable quantities and demonstrated that partner positivity (the probability that the partner of an infected person is infected) is insensitive to changes in screening coverage or partner notification efficiency. They also evaluated the cost-effectiveness of increasing partner notification versus screening and concluded that partner notification along with screening is the most cost-effective mitigation approach.

Kretzschmar et al. and Turner et al. [43, 44] evaluated different screening and partner referral methodologies in controlling Ct. They compared the RIVM model to evaluate the effectiveness of opportunistic Ct screening program in the Netherlands [44]; the ClaSS model to evaluate proactive, register-based Ct screening using home sampling in the UK [45]; and the HPA model to evaluate opportunistic national Ct screening program in UK [46].

A selective sexual mixing STI model was developed by Hyman et al. [34] to capture the heterogenous mixing among people with different number of partners. This model is well-described by Del Valle et al. [47] to investigate the impact of different mixing assumptions on spread of infectious diseases and how sensitivity analysis can be used to prioritize different possible mitigation efforts.

Our goal in this work is to create, to analyze, and to extend mathematical models for understanding and predicting the spread of Ct. These models can help guide public

health workers improve the effectiveness of intervention strategies for mitigating the impact of this infection. Our main focus will be to help optimize the interventions in an ongoing program for reducing the prevalence of Ct in the New Orleans adolescent and young adult AAs. We will design several compartment and agent-based network models within different Chapters:

Chapter 2 is about a multi-risk compartment model for Ct. In Chapter 3 we will extend this model to a continuous-risk compartment model. And finally in Chapter 4 we will provide a next generation of agent-based network models for the spread of Ct in New Orleans, and will test and will compare different mitigation method to control its epidemic.

In all proposed models the parameters will be estimated within a reasonable level of accuracy in order for results to give qualitative and quantitative understanding of how Ct is spreading [34]. We will use local sensitivity analysis to identify the relative importance of the model parameters and numerical examples to illustrate how we can prioritize mitigation strategies based on their predicted effectiveness.

Chapter 2

Multi-risk Compartment Model

In this chapter we develop and analyze our first and simplest model that is a multi-risk compartmental model that can be used to help understand the spread of Ct and to quantify the relative effectiveness of different mitigation efforts. Our model is closely related to the deterministic population-based model developed by Clarke et al. [42] to explore the short-term impacts of increasing screening and partner notification. Also, it is related to the STI models for the spread of the HIV/AIDS virus in a heterosexual network [38, 39].

The number of partners a person has (his/her risk), and the number of partners that their partners have (his/her partner's risk) both affect the spread of Ct. That is, different assumptions about the distribution of risk behavior of the population will result in different disease forecasts. We use the selective sexual mixing STI model developed by Hyman et al. [34] to capture the heterogenous mixing among people with different numbers of partners.

Although age, ethnicity, economic statues, and the spatial location of the individuals all influence the assortative mixing of sexual acts, the risk of contracting Ct is primarily a function of the number of partners a person has, the number of acts per partner, the probability that a partner is infected, and the use of prophylactics (e.g.

condoms).

In our ordinary differential equation model (ODE), we consider defining the risk categories based on the number of partners a person has. The relative importance of the number of partners and the number of acts per partner on the spread of an STI depends on the disease infectiousness. Ct is a very infectious disease and the probability of transmission per sexual act from an infected person to uninfected one is high; one act with an infected person is enough to catch the infection. Therefore, the number of people a person infects depends mostly upon the number of partners he/she has.

In this chapter we first formulate the mathematical model, then we derive the basic reproduction number, \mathcal{R}_0 , for two main risk groups (high-risk and low-risk) for men and women. We then use sensitivity analysis of \mathcal{R}_0 and the equilibrium points with respect to the model parameters to study how the heterogeneous mixing affects spread of Ct [48].

2.1 Ct Transmission Model Overview

In modeling the spread of Ct, the population is divided into the susceptible sexually active population (S), the exposed infected, but not infectious population (E) and the infectious population (I). Once a person has recovered from Ct infection, they are again susceptible to infection. Therefore, the models all have a $S \rightarrow E \rightarrow I \rightarrow S$ (SEIS) structure, or a SIS structure if the exposed state is combined with the infectious state.

Because the exposed (infected, but not infectious) time period is short compared to time in the infectious stage, we do not include a exposed stage in our model. We divide men and women into n risk groups based on the number of partners an individual has in a year. This SIS model can be written as the system of $2n$ ordinary

differential equations:

$$\begin{aligned}\frac{dS_k}{dt} &= \mu(N_k - S_k) - \lambda_k S_k + \gamma_k I_k, \\ \frac{dI_k}{dt} &= \lambda_k S_k - \gamma_k I_k - \mu I_k,\end{aligned}\tag{2.1}$$

where $k = 1, \dots, n$ denotes men with risk from 1 to n , and $k = n + 1, \dots, 2n$ denotes women with risk from 1 to n . The migration rate, μ , determines the rate at which people enter and leave the population, $N_k = S_k + I_k$ is the total population of group k , λ_k is the rate at which a susceptible person in risk group k is being infected, and γ_k is the rate that a person recovers either through screening, or natural recovery.

We model a population of 15–25 year-old individuals and assume that the primary mechanism for migration is by aging into, and out of, the population, where migration rate $\mu = 0.003 = [(25 - 15) \text{ years}]^{-1}$, with the assumption that death is negligible compared to the rate that people enter and leave the modeled population. We assume that, in the absence of infection, equilibrium population N_k^o for each risk group of men and women is given, and that everyone aging into the model population enters as a susceptible person.

The rate the infected population is treated, γ_k , depends upon the sex of the person and their risk level. The treatment can be initiated when infection is identified through screening, partner notification, or a medical check-up. Most infected people are asymptomatic and, when a significant fraction of a population is infected, then screening has been found to be a cost-effective approach to identify, and treat, infected people.

Natural recovery rate, γ_k^n , is determined by assuming an exponential distribution for the average time to recovery $1/\gamma_k^n$, and screening recovery rate, γ_k^s , is determined by assuming a log normal distribution for the average time to recovery through screening $1/\gamma_k^s$. We also define the probability that an infected individual is screened and treated each day, σ_d^k , in terms of the fraction of the population that will be screened at least

once within a year as σ_y^k . That is,

$$\sigma_d^k = 1 - (1 - \sigma_y^k)^{1/365}. \quad (2.2)$$

2.1.1 Transmission rate

We will derive the disease transmission rate for the heterosexual case where a susceptible person in group k can be infected by someone of the opposite sex in any of the infected groups j .

The force of infection, λ_k , is the rate that people in risk group k are infected through sexual acts. We define λ_k as the sum of the rate of disease transmission from each infected group, I_j , to the susceptible group, S_k :

$$\lambda_k = \sum_{j=1}^n \lambda_{kj}. \quad (2.3)$$

The rate of disease transmission from the infected people I_j in group j to the susceptible individuals S_k in group k , λ_{kj} , is defined as the product of three factors:

$$\begin{aligned} \lambda_{kj} &= \left(\begin{array}{c} \text{Number of partners} \\ \text{a susceptible in group } k \\ \text{has with someone in} \\ \text{group } j \text{ per unit time} \end{array} \right) \left(\begin{array}{c} \text{Probability of} \\ \text{disease transmission} \\ \text{per partner} \end{array} \right) \left(\begin{array}{c} \text{Probability that} \\ \text{partner in group } j \\ \text{is infectious} \end{array} \right) \\ &= p_{kj} \beta_k P_I(t, j), \end{aligned}$$

where

- p_{kj} is the number of sexual partners per unit time that each individual in group k has with someone in group j , and
- β_k is the probability of disease transmission per partner for a susceptible person

in group k , and

- $P_I(t, j)$ is the probability of that the person in group j is infected.

For this last factor, we assume that the partners in group j are all equally likely to be infected. That is, the probability the person in group j is infected is the same as the fraction of the people in group j that are infected, $\frac{I_j}{N_j}$.

2.1.2 Partnership formation

The extent that Ct spreads through a population is sensitive to the heterogeneous mixing (partnership selection) among the different risk groups. The model approximates the mixing through mixing probabilities p_{kj} that define how many partners a typical person in group k has with someone in group j . These mixing functions must dynamically change to account for variations in the size of the groups [33, 47, 49].

The force of infection, λ_k , depends on how many partners people in group k have, the number of acts they have per partner, and the probability that their partners are infected. The mixing is biased since people who only have a few sexual partners (low-risk) typically have partners who are also at low risk.

We define the model parameters so that someone in group k has, on average, p_{kj} partners who are in group j per day. Therefore, the total number of partnerships per day between people in group k and group j is $p_{kj}N_k = p_{jk}N_j$. Since each partnership may have more than one act, we define a_k as the average number of sexual acts per partner for people in group k .

To determine p_{kj} , we use a heterogeneous mixing algorithm developed in [33]. This approach starts by defining \bar{p}_k as the *desired* number of partnerships someone in group k wishes to have per unit time. Because there may not be sufficient available partners for everyone to have their desired number of partners, the actual number of partners could be different.

We define the *proportional* partnership (mixing) as the desired fraction ρ_{kj} of these partnerships that a person in group k wants to have with someone in group j . That is, a person in group k wants to have an average of $\rho_{kj}\bar{p}_k$ partnerships per unit time with someone in group j . Unfortunately, there is no guarantee that the total number of desired partnerships that people in group k want to have with people in group j will be the same as the total number of desired partnerships that people in group j want to have with people in group k . That is, in general $\rho_{kj}\bar{p}_k N_k \neq \rho_{jk}\bar{p}_j N_j$, and this must be reconciled.

Since not everyone can have their desired number of partners distributed exactly as they wish, the different heterogenous mixing algorithms represent different compromises to resolve these conflicts. All of the heterogenous mixing algorithms maintain the detailed balance for mixing where the total number of partnerships for people in group k with people in group j is the same as the total number of partnerships that people in group j have with people in group k . In our model, we use the heterogenous mixing algorithm based on the algorithm described in [33, 47] to determine p_{kj} .

The population in group k desires $\rho_{kj}\bar{p}_k N_k$ partners from group j , and the population in group j desires $\rho_{jk}\bar{p}_j N_j$ partners from group k . As a compromise, we set the total number of partners the people in group k have with people in group j , and vice versa, to be the harmonic mean

$$p_{kj}N_k = p_{jk}N_j = \frac{2(\rho_{kj}\bar{p}_k N_k)(\rho_{jk}\bar{p}_j N_j)}{(\rho_{kj}\bar{p}_k N_k) + (\rho_{jk}\bar{p}_j N_j)}. \quad (2.4)$$

Other possibilities include the geometric mean or minimum of $(\rho_{kj}\bar{p}_k N_k)$ and $(\rho_{jk}\bar{p}_j N_j)$. All of these averages satisfy the balance condition to have the property that if $\rho_{jk} = 0$ then $p_{kj} = p_{jk} = 0$, where if one group refuses to have a partnership with another group, then this partnership does not happen. In our model, we use the harmonic

mean and define

$$p_{kj} = \frac{1}{N_k} \frac{2(\rho_{kj}\bar{p}_k N_j)(\rho_{jk}\bar{p}_j N_k)}{(\rho_{kj}\bar{p}_k N_k) + (\rho_{jk}\bar{p}_j N_j)} . \quad (2.5)$$

Hence, $p_k = \sum_j p_{kj}$ is the actual average number of partners someone in group k has per day.

Note that this approach is only appropriate if the desired number of partners between any two groups is in close agreement, that is, $\rho_{kj}\bar{p}_k N_k \approx \rho_{jk}\bar{p}_j N_j$. This is because, the approach assumes that if the partners are not available from the desired group, then the individuals will not change their preferences to seek partners in other risk groups. The model can be extended to handle these situations where the people adjust their desires to be in closer alignment with the availability of partners through a simple iterative algorithm. However, we avoid this complication in our simulations and initialize the populations so the groups desires are close to the availability of partnerships.

2.1.3 Probability of transmission per partner

The probability of a susceptible person catches infection from their infected partner depends upon the number of sexual acts between the people. We allow the number of acts per partner for a person in group k , a_k , to depend upon the number of his/her actual partners and his/her total number of acts per unit time, $A_k = a_k p_k$, where A_k is total number of acts per unit time.

The probability of transmission per act, β , can be used to define the probability that a susceptible person will not be infected by a single act with an infected person, $1 - \beta$. Therefore, the probability of someone in group k not being infected after a_k acts with an infected person is $(1 - \beta)^{a_k}$. Hence, the probability of being infected per partner is [37]

$$\beta_k = 1 - (1 - \beta)^{a_k} . \quad (2.6)$$

Parameter	Description	Unit	Baseline
N	Total population.	people	20000
N_1	High-risk men population.	people	2400
N_2	Low-risk men population.	people	4600
N_3	High-risk women population.	people	2500
N_4	Low-risk women population.	people	10,500
μ	Migration rate.	1/days	0.00
β	Probability of transmission per act.	1/act	0.11
$1/\gamma_i^n$ ($i = 1, 2, 3, 4$)	Average time to recover without treatment.	days	365
$1/\gamma_i^s$ ($i = 1, 2, 3, 4$)	Average time to recover with treatment.	days	7
A_1	Total number of acts per time for a high-risk man.	1/days	0.14
A_2	Total number of acts per time for a low-risk man.	1/days	0.07
A_3	Total number of acts per time for a high-risk woman.	1/days	0.07
A_4	Total number of acts per time for a low-risk woman.	1/days	0.04
\bar{p}_1	Desired number of partners per time for a high-risk man.	people/days	0.14
\bar{p}_2	Desired number of partners per time for a low-risk man.	people/days	0.03
\bar{p}_3	Desired number of partners per time for a high-risk woman.	people/days	0.06
\bar{p}_4	Desired number of partners per time for a low-risk woman.	people/days	0.02
$\bar{\rho}_{13}$	Desired fraction of high-risk partner for a high-risk man.	–	0.75
$\bar{\rho}_{24}$	Desired fraction of low-risk partner for a low-risk man.	–	0.80
$\bar{\rho}_{31}$	Desired fraction of high-risk partner for a high-risk woman.	–	0.75
$\bar{\rho}_{42}$	Desired fraction of low-risk partner for a low-risk woman.	–	0.80
σ_y^i ($i = 1, 2, 3, 4$)	Fraction of people in group i randomly screened per year.	–	0.00

Table 2.1: Table for the variables and parameters in the model (2.1). All the parameter values are based on our assumption and are not estimated or taken from literature.

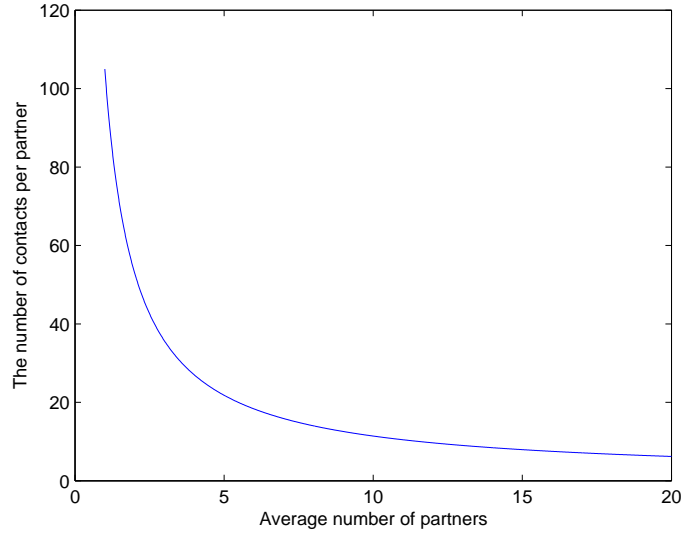


Figure 2.1: The number of acts per partnership per unit time (year), a_k , is a decreasing function of p_k , that is, people with more partners have fewer acts per partner per unit time than people with fewer partners. If A_k is total number of acts for a person in group k , a_k is defined as $a_k = \frac{A_k}{p_k} = \frac{A_k}{\sum_j p_{kj}}$.

2.2 Basic Reproduction Number

The basic reproduction number, \mathcal{R}_0 , is the number of new infections introduced if a newly infected person is introduced into a population at the $(S_k = N_k, I_k = 0)$. We will derive the basic reproduction number \mathcal{R}_0 using the next generation approach [50, 51] for situation with two risk levels for men and women labeled: 1 = high-risk men, 2 = low-risk men, 3 = high-risk women and 4 = low-risk women. We have differential equations

$$\frac{dI_k}{dt} = \sum_j \alpha_{kj} I_j - \tau_k^{-1} I_k, \quad (2.7)$$

where $\tau_k = 1/(\gamma_k + \mu)$ is the average time that an infected person stays in the k -th infection compartment. The force from infection, $\alpha_{kj} = \beta_k q_{kj} S_k$, is the rate (per day) that a typical infected person in group j infects a susceptible one in group k . Here the factor q_{kj} is defined as $q_{kj} = p_{kj}/N_j$ and because we had $p_{kj}N_k = p_{jk}N_j$, therefore, $p_{kj}/N_j = p_{jk}/N_k$, and that means $q_{kj} = q_{jk}$ is the fraction of people in

group j someone in group k has as a partner. The Equation (2.7) for the infected populations, $I = (I_1, I_2, I_3, I_4)^T$, can be written as a matrix equation for the rate of production of new infections, F , minus the removal rate of individuals from that population class, V ,

$$\frac{dI}{dt} = \mathbf{F}I - \mathbf{V}I, \quad (2.8)$$

where the kl -th element of the matrix \mathbf{F} is $\mathbf{F}_{kl} = \alpha_{kl}$, and V is diagonal matrix $V_{kk} = \tau_k^{-1}$, for $k, l = 1, \dots, 4$. At DFE, $\alpha_{kj} = \beta_k q_{kj} N_k$ and the Jacobian matrices, \mathbf{J}_F and \mathbf{J}_V^{-1} , of FI and VI are

$$J_F = \begin{pmatrix} 0 & 0 & \alpha_{13} & \alpha_{14} \\ 0 & 0 & \alpha_{23} & \alpha_{24} \\ \alpha_{31} & \alpha_{32} & 0 & 0 \\ \alpha_{41} & \alpha_{42} & 0 & 0 \end{pmatrix}, \quad J_V^{-1} = \begin{pmatrix} \tau_1 & 0 & 0 & 0 \\ 0 & \tau_2 & 0 & 0 \\ 0 & 0 & \tau_3 & 0 \\ 0 & 0 & 0 & \tau_4 \end{pmatrix}.$$

We define \mathcal{R}_0 as spectral radius of $J_F J_V^{-1}$ or (equivalently) $J_V^{-1} J_F$,

$$J_F J_V^{-1} = \begin{pmatrix} 0 & 0 & \alpha_{13}\tau_3 & \alpha_{14}\tau_4 \\ 0 & 0 & \alpha_{23}\tau_3 & \alpha_{24}\tau_4 \\ \alpha_{31}\tau_1 & \alpha_{32}\tau_2 & 0 & 0 \\ \alpha_{41}\tau_1 & \alpha_{42}\tau_2 & 0 & 0 \end{pmatrix}, \quad J_V^{-1} J_F = \begin{pmatrix} 0 & 0 & \alpha_{13}\tau_1 & \alpha_{14}\tau_1 \\ 0 & 0 & \alpha_{23}\tau_2 & \alpha_{24}\tau_2 \\ \alpha_{31}\tau_3 & \alpha_{32}\tau_3 & 0 & 0 \\ \alpha_{41}\tau_4 & \alpha_{42}\tau_4 & 0 & 0 \end{pmatrix}. \quad (2.9)$$

Note that jk -th element of $J_V^{-1} J_F$ is $\mathcal{R}_0^{j \rightarrow k} = \alpha_{jk} \tau_j$. Based on a result of Sylvester's inertia theorem [52]¹, if a matrix K can be factored into the product of a diagonal positive definite matrix A and a symmetric matrix B , then eigenvalues of K are the same as eigenvalues of $A^{\frac{1}{2}} B A^{\frac{1}{2}}$. To apply this result, we rewrite $J_V^{-1} J_F = AB$ where

¹ Let K be a hermittian matrix. We define $e^+(K)$ as the number of positive eigenvalues, $e^-(K)$ as the number of negative eigenvalues, and $e^0(K)$ as the number of zero eigenvalues. Inertia of K is a tuple $(e^+(K), e^-(K), e^0(K))$. If A is an invertible matrix then Sylvester inertia theorem states: $\text{inertia}(K) = \text{inertia}(A^{-1}KA)$.

A is a diagonal positive definite matrix and B is symmetric,

$$A = \begin{pmatrix} \beta_1 N_1 \tau_1 & 0 & 0 & 0 \\ 0 & \beta_2 N_2 \tau_2 & 0 & 0 \\ 0 & 0 & \beta_3 N_3 \tau_3 & 0 \\ 0 & 0 & 0 & \beta_4 N_4 \tau_4 \end{pmatrix}, \quad B = \begin{pmatrix} 0 & 0 & q_{13} & q_{14} \\ 0 & 0 & q_{23} & q_{24} \\ q_{31} & q_{32} & 0 & 0 \\ q_{41} & q_{42} & 0 & 0 \end{pmatrix}. \quad (2.10)$$

Therefore, eigenvalues of $J_V^{-1} J_F$ are the same as eigenvalues of symmetric block anti-diagonal generation matrix

$$A^{\frac{1}{2}} B A^{\frac{1}{2}} = \begin{pmatrix} 0 & 0 & \sqrt{\alpha_{13} \tau_1 \alpha_{31} \tau_3} & \sqrt{\alpha_{14} \tau_1 \alpha_{41} \tau_4} \\ 0 & 0 & \sqrt{\alpha_{23} \tau_2 \alpha_{32} \tau_3} & \sqrt{\alpha_{24} \tau_2 \alpha_{42} \tau_4} \\ \sqrt{\alpha_{31} \tau_3 \alpha_{13} \tau_1} & \sqrt{\alpha_{32} \tau_3 \alpha_{23} \tau_2} & 0 & 0 \\ \sqrt{\alpha_{41} \tau_4 \alpha_{14} \tau_1} & \sqrt{\alpha_{42} \tau_4 \alpha_{24} \tau_2} & 0 & 0 \end{pmatrix} = \begin{pmatrix} 0_{4 \times 4} & M \\ M^T & 0_{4 \times 4} \end{pmatrix}, \quad (2.11)$$

where M^T is transpose of M and

$$M = \begin{pmatrix} \sqrt{\alpha_{13} \tau_1 \alpha_{31} \tau_3} & \sqrt{\alpha_{14} \tau_1 \alpha_{41} \tau_4} \\ \sqrt{\alpha_{23} \tau_2 \alpha_{32} \tau_3} & \sqrt{\alpha_{24} \tau_2 \alpha_{42} \tau_4} \end{pmatrix} = \begin{pmatrix} r_{13} & r_{14} \\ r_{23} & r_{24} \end{pmatrix}, \quad (2.12)$$

where $r_{jk} = \sqrt{\mathbb{R}_0^{j \rightarrow k} \mathbb{R}_0^{k \rightarrow j}}$ is the geometric average of group j -to-group k and group k -to-group j reproduction numbers. The basic reproduction number is spectral radius of $J_V^{-1} J_F$, therefore, $\mathcal{R}_0 = \rho(A^{\frac{1}{2}} B A^{\frac{1}{2}}) = \sqrt{\rho(M^T M)}$ where

$$M^T M = \begin{pmatrix} r_{13}^2 + r_{23}^2 & r_{13} r_{14} + r_{23} r_{24} \\ r_{13} r_{14} + r_{23} r_{24} & r_{14}^2 + r_{24}^2 \end{pmatrix},$$

and

$$\mathcal{R}_0 = \frac{1}{2}((r_{13}^2 + r_{23}^2 + r_{14}^2 + r_{24}^2) + \sqrt{(r_{13}^2 + r_{23}^2 - r_{14}^2 - r_{24}^2)^2 + 4(r_{13}r_{14} + r_{23}r_{24})^2}). \quad (2.13)$$

2.3 Sensitivity Analysis

We use sensitivity analysis to quantify the change in model output quantities of interest (QOI), such as the basic reproduction number \mathcal{R}_0 and endemic equilibrium point, due to variations in the model input parameters of interest (POI), such as the average time to recovery after infection [53–55].

Consider the situation where the baseline value of the input POI is p_b and generates the baseline output QOI $q_b = q(p_b)$. Sensitivity analysis is used to address what happens if p_b is changed by the fraction θ_p , $p_{new} = p_b(1 + \theta_p)$. Our goal is to find resulting fractional change in the output variable $q_{new} = q_b(1 + \theta_p^q)$. That is, the normalized sensitivity index measures the relative change in the input variable p , with respect to the output variable q and can be estimated by the Taylor series

$$q_{new} = q(p_b + \theta_p p_b) \approx q_b + \theta_p p_b \left. \frac{\partial q}{\partial p} \right|_{p=p_b} = q_b(1 + \theta_p^q). \quad (2.14)$$

We define the normalized sensitivity index as

$$\mathbb{S}_p^q := \frac{p_b}{q_b} \left. \frac{\partial q}{\partial p} \right|_{p=p_b} = \frac{\theta_p^q}{\theta_p}. \quad (2.15)$$

That is, if the input p is changed by θ_p percent, then the output q will change by $\theta_p^q = \mathbb{S}_p^q \theta_p$ percent. The sign of \mathbb{S}_p^q determines the direction of changes, increasing (for positive \mathbb{S}_p^q) and decreasing (for negative \mathbb{S}_p^q). Note that this local sensitivity index is valid only in a small neighborhood of the baseline values.

2.3.1 Sensitivity indices of \mathcal{R}_0

The ability of Ct to become established in a population and its early growth rate is characterized by \mathcal{R}_0 , Equation (2.13). Sensitivity analysis of \mathcal{R}_0 can quantify the relative importance of the different social and epidemiological parameters in reducing the ability of the STI to become established in a new population.

Table (2.2) of the sensitivity indices of \mathcal{R}_0 shows that it is most sensitive to the probability of transmission per act β with $\mathbb{S}_\beta^{\mathcal{R}_0} = 1.95$. That is, if the probability of infection per act decreases- say by increasing the condom-use - by 15% then $\theta_\beta = -0.15$, then \mathcal{R}_0 will decrease by 30% from 4.01 to 2.84:

$$\mathcal{R}_{0_{new}} = \mathcal{R}_0(1 + \theta_\beta \mathbb{S}_\beta^{\mathcal{R}_0}) = 4.01(1 - 0.15 \times 1.95) = 2.84.$$

That is, sensitivity analysis can quantify the amount of behavior change that would be needed to keep an epidemic from becoming established in a new population.

A negative sensitivity index indicates that \mathcal{R}_0 is a decreasing function of correspondent parameter, while the positive ones show \mathcal{R}_0 increases when the parameter increases. The second most important model parameters for the early growth rate are the recovery rates of the high-risk men and women γ_1 and γ_3 . Since, $\mathbb{S}_{\gamma_1}^{\mathcal{R}_0} = \mathbb{S}_{\gamma_3}^{\mathcal{R}_0} = -0.95$, a 10% increase in the screening rate would result in a 9.5% decrease in \mathcal{R}_0 , which this supports the need to actively screen both men and women for Ct infection.

The number of acts for high-risk men, A_1 , is also an important parameter for controlling the early growth of the Ct. Because local-sensitivity analysis is valid in a small neighborhood of the baseline case, sometimes it is useful to plot the change in the QOI over a wide range of possible values. The sensitivity index is then the slope of the response curve at the baseline values. The Figure (2.2) shows how \mathcal{R}_0 changes as parameters β and A_1 are varied over a broad range.

Sensitivity index of \mathcal{R}_0 for all parameters in the model					
Parameter p	Baseline	$\mathbb{S}_p^{\mathcal{R}_0}$	Parameter p	Baseline	$\mathbb{S}_p^{\mathcal{R}_0}$
β	0.11	1.95	\bar{p}_1	0.14	0.05
A_1	0.14	0.76	\bar{p}_2	0.03	-0.06
A_2	0.07	0.15	\bar{p}_3	0.06	0.24
A_3	0.07	0.71	\bar{p}_4	0.02	-0.07
A_4	0.04	0.22	γ_1	0.003	-0.95
$\bar{\rho}_{13}$	0.75	0.35	γ_2	0.003	-0.48
$\bar{\rho}_{31}$	0.75	0.58	γ_3	0.003	-0.95
$\bar{\rho}_{24}$	0.8	0.04	γ_4	0.003	-0.48
$\bar{\rho}_{42}$	0.8	0.12	μ	0.00	-0.09

Table 2.2: The sensitivity index of \mathcal{R}_0 with respect to parameters of the model at the baseline parameter values where $\mathcal{R}_0 = 4.01$. The most sensitive parameter is the probability of transmission per act, β , followed by the recovery (screening) rates of the high-risk men and women γ_1 and γ_3 .

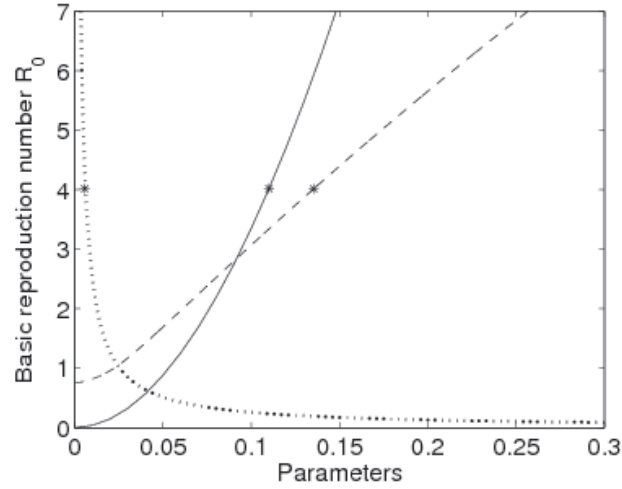


Figure 2.2: The sensitivity of \mathcal{R}_0 with respect to β (solid line), and A_1 (dashed line). The sensitivity index is then the slope of the response curve at the baseline values, indicated by *. The response is approximately linear near the baseline case and, therefore, the local sensitivity analysis is actually valid over a broad range of parameters.

2.3.2 Sensitivity indices of endemic equilibriums

The current Ct epidemic is established in many cities, therefore, to evaluate the relative impact of the model parameters in bringing it under control requires that the sensitivity analysis be performed about the current state of the system, the steady-state endemic equilibrium. We will investigate the impact the mitigation efforts on the relative change in the number of infected people as a function of the relative change in the model parameters. This is best done in terms of the nondimensional variables defined by dividing each variable by the steady-state zero-infection equilibrium total population for that sex. That is, $i_m = I_m/N_m^o$, $i_w = I_w/N_w^o$, $n_1 = N_1/N_m^o$, $n_2 = N_2/N_m^o$, $n_3 = N_3/N_w^o$, and $n_4 = N_4/N_w^o$, where, $N_m^o = N_1^o + N_2^o$, $N_w^o = N_3^o + N_4^o$. The Table (2.3) shows that the sensitivity indices for endemic (steady-state) equilibrium infected populations, i_j , as a function of the model parameters. Note that the magnitudes (relative importance) of sensitivity indices have the same order as they did for \mathcal{R}_0 , although the magnitudes are different.

Sensitivity of equilibriums for all parameters in the model					
Parameter p	Baseline	i_1	i_2	i_3	i_4
β	0.11	2.61	4.05	2.7	4.02
A_1	0.14	1.7	0.58	0.71	0.66
A_2	0.07	0.31	1.5	0.33	1
A_3	0.07	0.65	0.56	1.13	0.53
A_4	0.04	0.42	1.18	0.37	1.61
$\bar{\rho}_{13}$	0.75	0.36	-0.21	0.24	-0.36
$\bar{\rho}_{31}$	0.75	0.41	-0.15	0.56	0.03
$\bar{\rho}_{24}$	0.8	0.02	-0.13	0.08	-0.10
$\bar{\rho}_{42}$	0.8	0.15	-0.21	0.08	-0.33
\bar{p}_1	0.14	0.04	0.17	0.08	0.23
\bar{p}_2	0.03	0.27	0.31	0.21	0.26
\bar{p}_3	0.06	0.27	0.31	0.21	0.26
\bar{p}_4	0.02	-0.05	0.03	-0.03	0.04
γ_1	0.003	-1.10	-0.60	-0.73	-0.68
γ_2	0.003	-0.35	-1.66	-0.37	-1.11
γ_3	0.003	-0.66	-0.56	-1.13	-0.53
γ_4	0.003	-0.47	-1.31	-0.41	-1.78
μ	0.00	-0.13	-0.20	-0.13	-0.20

Table 2.3: Local sensitivity indices of the endemic equilibrium points. At this baseline $\mathcal{R}_0 \geq 1$, so this endemic point is a solution of model at steady state.

The prevalence of infection, i_j , is most sensitive to probability of transmission per act β , i.e increasing β increases i_j s more than other parameters. Then A_j s and γ_j s have the second most effect on i_j s in positive and negative direction, correspondingly.

Prevalence in high-risk men, i_1 , is sensitive to the total number of acts for the high-risk

men A_1 and γ_1 more than the other A_j s and γ_j s for $j \neq 1$. Prevalence in high-risk women, i_3 , is also sensitive to A_3 and γ_3 more than the other A_j s and γ_j s for $j \neq 3$. It means when high-risk people increase their number of acts, regardless of what others do, the fraction of infected people between high-risk people increases, because they have many partners. On the other hand, when infection period for high-risk people increases, the prevalence in high-risk population increases.

For low-risk men, the prevalence, i_2 , has the same sensitivity to A_2 and A_4 . It means when low-risk people increase their act, the prevalence in low-risk men increases, and we have the same story for low-risk women. It is reasonable, because low-risk people do not have many partner, therefore, more acts for them and their partners plays an important role. Prevalence in low-risk men, i_2 , has also the same sensitivity to γ_2 and γ_4 . It means when we decrease γ_2 and γ_4 -infected people in low-risk men stay in infection category for a longer time and also infected women in low-risk group stay in infection category for a longer time- we see increment in the value of i_2 more than the other parameters. There is a similar analysis for low-risk group i_4 : low-risk group i_4 is sensitive to γ_2 and γ_4 with the same magnitude and more than the other γ_j s.

Another interesting result is that the endemic equilibrium points are more sensitive, than \mathcal{R}_0 , to most of the parameters. This result says, controlling parameters to have a low fraction of infected population is easier than adjusting the parameters to have smaller \mathcal{R}_0 .

2.4 Screening Scenarios

The goal of this Section is to study the impact of different screening strategies on prevalence of Ct among different groups. In all the simulations, the parameters are fixed with the baseline values given in Table (2.1), unless specifically defined otherwise. In the first simulation, we assume that fraction of people who can be screened each year, σ_y , is limited by a budget, or other factors. We also assume that if an infected person is screened for Ct, then there is a 100% probability that infection will be detected.

We will compare the fraction of the population that is infected as a function of the

screening rate σ_y^k people from different subgroups k . We will also optimize the σ_y , for a fixed budget, that will minimize the fraction of infected people at steady state. That is, if $(i_1^*, i_2^*, i_3^*, i_4^*)$ are the fraction of infected people at steady state, we find the optimal screening rates that solve the optimization problem:

$$\begin{aligned} & \underset{\sigma_y^k}{\text{minimize}} && \sum_{j=1}^4 N_j i_j^*(\sigma_y^1, \sigma_y^2, \sigma_y^3, \sigma_y^4), \\ & \text{subject to} && \sum_{j=1}^4 N_j \sigma_y^j = N \sigma_y = 0.2N = 400, \end{aligned}$$

where $N_j i_j^*$ is the number of infected people in group j and in steady state. The Figure. (2.3) shows the result for six different scenarios defined in Table (2.4).

Scenario	\mathcal{R}_0	Scenario	\mathcal{R}_0
(1) No screening	4.01	(2) Screen high-risk men	0.86
(3) Screen high-risk women	0.91	(4) Screen low-risk men	1.26
(5) Screen low-risk women	1.22	(6) Optimized Screening	0.12

Table 2.4: Basic reproduction number, \mathcal{R}_0 , for different scenarios with respect to parameters of the model at the baseline parameter values. Implementing optimized screening decreases \mathcal{R}_0 to the order of -1 .

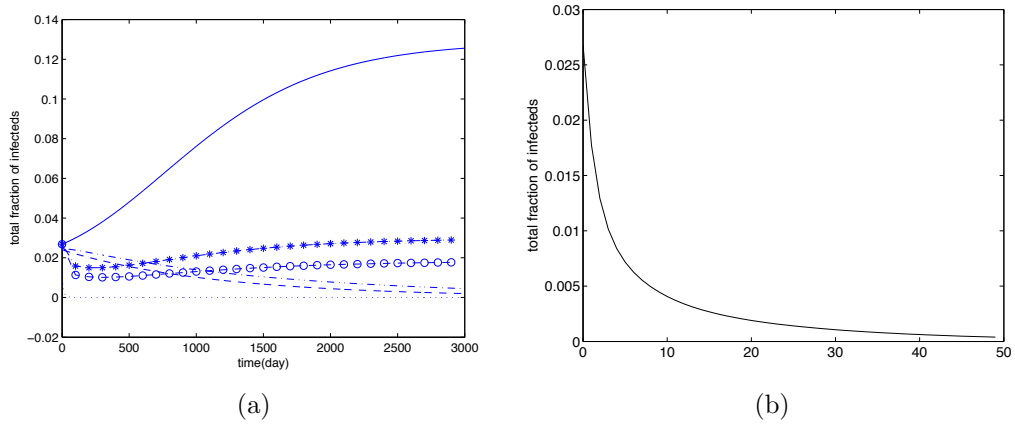


Figure 2.3: 2.3(a): the fraction of infected people after implementing different scenarios: no screening (solid line), screen $\sigma_y N$ people per year for: high-risk men(dash line), high-risk women(dash-dot line), low-risk men (dash-star), low-risk women (dash-circle), and optimized screening(dotted line). 2.3(b): zooms on the optimized screening, by optimized screening the infection dies out very fast.

We observe that in case of no screening the epidemic goes up to its original endemic equilibrium point. The effectiveness of screening is seen by the dramatic reduction in the

fraction of infected people. However, between all scenarios screening high-risk people and optimized screening cause that epidemic dies out and for optimal choice it dies out much faster than the other two cases.

We also list the value of \mathcal{R}_0 for different scenarios in Table (2.4). The Figure (2.3) and Table (2.4) show that $\mathcal{R}_0 > 1$ implies a persistent infection, though not a macroscopic outbreak in screening cases, and when $\mathcal{R}_0 < 1$ epidemic goes to DFE. Also, for the optimized scenario, which its \mathcal{R}_0 is the lowest one, the epidemic dies out faster than the other scenarios. Therefore, optimized screening was the most effective scenario among all six scenarios.

To push our understanding of the effects of optimized screening further, we do sensitivity analysis of equilibrium points with respect to screening rates at their optimized values. In this case sensitivity index become a matrix like:

$$\mathbb{S} = \begin{pmatrix} i_1^* & 0 & 0 & 0 \\ 0 & i_2^* & 0 & 0 \\ 0 & 0 & i_3^* & 0 \\ 0 & 0 & 0 & i_4^* \end{pmatrix}^{-1} \times J_{i^*}(\sigma_y) \times \begin{pmatrix} \sigma_y^1 & 0 & 0 \\ 0 & \sigma_y^2 & 0 \\ 0 & 0 & \sigma_y^3 \end{pmatrix},$$

where $J_{i^*}(\rho_y)$ is jacobian matrix. Each column k of \mathbb{S} represents sensitivity index of equilibrium points with respect to screening rate σ_y^k . Therefore, $(k, j)th$ element of \mathbb{S} is sensitivity index of i_k^* with respect to σ_y^j . Table (2.5) lists the elements of this matrix: all the values in table are negative, it means there is a inverse pattern between equilibrium points and screening rate: when we increase screening rates the fraction -therefore, the number- of infected people at steady state will decrease. Among all, i_1^* is the most sensitive one, it means changing screening rates affects the high-risk men more than the others.

	$i_1^* = 0.00$	$i_2^* = 0.00$	$i_3^* = 0.00$	$i_4^* = 0.00$
$\sigma_y^1 = 0.06$	-0.13	-0.00	-0.01	-0.13
$\sigma_y^2 = 0.20$	-0.56	-0.37	-0.27	-0.41
$\sigma_y^3 = 0.05$	-0.08	-0.09	-0.09	-0.09

Table 2.5: Sensitivity indices of equilibrium points with respect to screening rates at optimized baseline values. The most sensitive output parameter is fraction of infected high-risk men.

2.5 Discussion and Conclusion

In this Chapter we created a multi-risk heterosexual SIS transmission model for the spread of Ct with biased mixing partnership selection to investigate the impact that screening for the disease can have in controlling its spread. We derived the threshold conditions for the early spread of the disease and defined the basic reproductive number, \mathcal{R}_0 , using the next generation matrix approach. The analysis of \mathcal{R}_0 identified a new approach to reduce the size of the next generation matrix for a heterosexual Ct model with n risk groups from an $2n \times 2n$ nonsymmetric sparse matrix to an $n \times n$ symmetric full matrix. This approach can be used in similar heterosexual STI models to greatly simplify the threshold analysis.

We used the sensitivity analysis of \mathcal{R}_0 and endemic equilibrium steady-state solutions to quantify the relative effectiveness of different intervention strategies in mitigating the disease. The analysis identified the probability of transmission per act (related to condom-use) is the most sensitive parameter in controlling the epidemic. The second most effective control mechanism was the screening, and treating infections, of both high-risk men and women. Currently, most mitigation programs only target screening high-risk women. The model indicates that it is equally important to identify infections and treat high-risk men. We confirmed that in the model the higher-risk groups are driving the epidemic and that \mathcal{R}_0 is most sensitive to the behavior of these higher-risk people.

We implemented different screening scenarios consist of screening only high-risk men, only high-risk women, only low-risk men, only low-risk women, and optimized screening. We then solved for an optimal screening strategy for infection mitigation when there are limited resources and then determined the best screening approach to minimize the endemic steady state infection prevalence, optimized screening. Not surprisingly, we found that this same strategy also minimizes \mathcal{R}_0 . In the next Chapter, we generalize our multi-risk model to continuous-risk, when individuals can take as many number of partners as they want and we focus on impact of condom-use to control the epidemic of Ct.

Chapter 3

Continuous Risk-based Model

In this chapter, we extend the multi-risk group model in Chapter 2 to a continuous risk-based transmission model that can be used to understand the spread of Ct in the adolescents and young adult population. The model predicts the impact of people having different number of concurrent partners or using prophylactics, such as condoms, on the rate that infection spreads.

We use this risk-based integro-differential model [56] to study the impact of variations in number of partners, mixing patterns in selecting partners, and condom-use to determine optimal Ct prevention policies. We study how the number of partners that a person has, and how often they use condoms, will affect the spread of Ct. Here, the risk is defined based on the number of partners a person has per year. The distribution of risk behavior for a population, such as the fraction of the population having multiple partners and also, the number of partners that their partners have (their partner's risk) affects the spread of Ct and must be accounted for in the model. Our model accounts for a broad range of risk behavior, defined as the number of partners per year, that is captured as a continuous variable. This model could also be used to include separate core high-risk groups, such as sex workers. However, in the young adult population being modeled, sex-workers are not believed to be a major factor in the spread of highly infectious STIs like Ct.

The risk of contracting Ct is primarily a function of a person's risk, the probability that a partner is infected, and the use of prophylactics (e.g. condoms). We use the selective

mixing model developed by Busenberg et al. [49] to capture the heterogenous mixing among people with different number of partners. Our model is closely related to the models for the spread of the HIV/AIDS in heterosexual networks [38, 39] that distribute the population based on their risk, such as the number of partners [36–39].

We design the model with a complete explanation of its variables and parameters. For the parameters, we used two different data sources for population distribution and amount of condom-use by people with different risks. We use local sensitivity analysis to identify the relative importance of condom-use and illustrate how this analysis can be used to prioritize individual-level behavioral strategies based on their predicted effectiveness.

3.1 Ct Transmission Model Overview

We model a population of 15-25 year-old sexually active individuals and assume that the primary mechanism for migration is by aging into, and out of, the population. We assume a closed steady-state population $N(r) = S(t, r) + I(t, r)$ of people with risk $r \in [r_0, r_\infty]$ is divided into $S(t, r)$, and $I(t, r)$, where $S(t, r)$ ($I(t, r)$) is the number of susceptible (infected) people with risk r at time t . The susceptible population becomes infected at the rate of λ per year, and infected population recovers with constant rate γ to again become susceptible. We assume both susceptible and infected people leave the population at the migration rate μ per day and that people maintain the same risk r while in the modeled population. Our integro-differential equation model for the spread of Ct is

$$\begin{aligned} \frac{\partial S(t, r)}{\partial t} &= \mu(N(r) - S(t, r)) - \lambda(t, r)S(t, r) + \gamma I(t, r), \\ \frac{\partial I(t, r)}{\partial t} &= \lambda(t, r)S(t, r) - \gamma I(t, r) - \mu I(t, r), \\ S(0, r) &= S_0(r), \quad I(0, r) = N(r) - S_0(r), \end{aligned} \tag{3.1}$$

where initial distributions of the susceptible and infected population are given at time $t = 0$. Note that this model does not distinguish between men and women and is appropriate for homosexual STIs or infections when the distribution of risk and infection incidence in

men and women is approximately the same. This also requires that the probability of transmitting the infection from an infected man to a susceptible woman is approximately the same as the probability of transmission from an infected woman to a susceptible man. This is a reasonable assumption for some STIs including Ct. In the absence of symmetry in the transmission parameters or in the risk behavior in men and women, then the model would need to be extended to a two-sex bipartite model.

We model a population of 15-25 year-old sexually active individuals and assume that individuals enter and leave the modeled population only through aging, that is, migration rate is defined as $\mu = [(25 - 15) \text{ years}]^{-1} = 1/(10 \text{ years}) = 1/(3650 \text{ days})$. We also assume that everyone aging into the population is susceptible to infection, and that people do not change their risk while in the modeled population. To properly account for changes in risk behavior as the population ages would require adding an additional variable (age) and is beyond the scope of this model. The risk behavior is distributed in a way that number of people with risk r decreases as risk r increases, that is, there are fewer individuals with many partners. We also assume that there is an exponential distribution for the rate the infected population with an average infection period $1/\gamma$ days.

3.1.1 Transmission rate

The force of infection, or transmission rate, $\lambda(t, r)$, for susceptible person with risk r at time t , is the rate that susceptible people with risk r become infected through sexual act. The mixing among people with different risks determines if a susceptible person with risk r can be infected by someone infected with risk r' . We define $\lambda(t, r)$ as the integral of the rate of disease transmission at time t from each infected person with risk r' , $I(t, r')$, to the susceptible one by

$$\lambda(t, r) = \int_{r_0}^{r_\infty} \tilde{\lambda}(t, r, r') dr'. \quad (3.2)$$

The rate of disease transmission from the infected persons with risk r' to the susceptible individuals with risk r , $\tilde{\lambda}(t, r, r')$, is defined as the product of three factors:

$$\begin{aligned} \tilde{\lambda}(t, r, r') &= \left(\begin{array}{c} \text{Number of } r' \text{--risk} \\ \text{partners of susceptible} \\ \text{with risk } r, \text{ per year} \end{array} \right) \left(\begin{array}{c} \text{Probability of} \\ \text{disease transmission} \\ \text{per partner} \end{array} \right) \left(\begin{array}{c} \text{Probability that} \\ \text{partner with risk } r' \\ \text{is infected} \end{array} \right) \\ &= p(r, r') \quad \beta(r, r') \quad P_I(t, r') , \end{aligned}$$

where

- $p(r, r')$ is the partnership mixing function defined as the number of sexual partners per day that a person with risk r has with a person with risk r' , and
- $\beta(r, r')$ is the probability of disease transmission per partner to a susceptible person with risk r from their infected partner with risk r' , and
- $P_I(t, r')$ is the probability that a person of risk r' is infected. Here we assume that there is random mixing among individuals with the same risk, $P_I(t, r') = \frac{I(t, r')}{N(r')}$.

The Figure (3.1) shows a diagram of components of the transmission rate λ , and in the following sections, all components will be explained.

3.1.2 Partnership formation

The mixing distribution, $\rho(r, r')$, captures the mixing between people of different risks. This distribution is defined as the fraction of partners of a person with risk r who have risk r' . The distribution function $\rho(r, r')$ is the expected distribution of partners and is typically estimated based on inaccurate survey data or other assumptions. It cannot be as the actual mixing function $p(r, r')$ since it usually will not satisfy the balance condition:

$$N(r)p(r, r') = N(r')p(r', r),$$

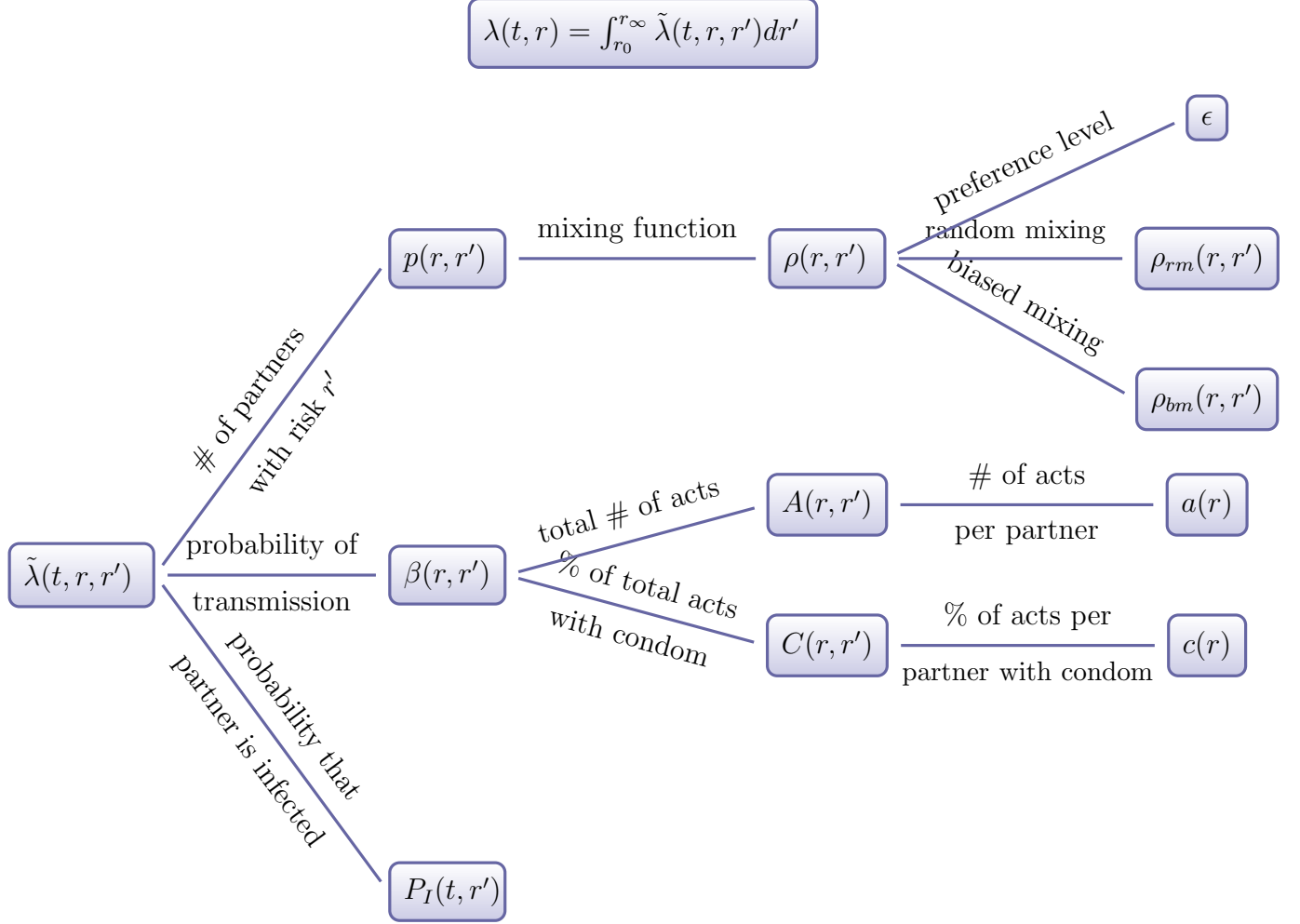


Figure 3.1: Components of the transmission rate $\lambda(t, r)$ for a susceptible person with risk r .

that means the total number of people with risk r with partners of risk r' must be equal to the total number of people with risk r' with partners of risk r .

We assume that $\rho(r, r')$ is a linear combination of randomly selected partners, with the random mixing distribution $\rho_{rm}(r, r')$, and partners based on their preference, with the biased mixing distribution $\rho_{bm}(r, r')$. These mixing distribution functions ρ_{rm} and ρ_{bm} are normalized to have unit integral. Feng et al. [57] used a similar model to account for multi-level mixing of people within a specified group and among the general population.

Random mixing distribution: When the mixing is random (sometimes called proportional mixing), then individuals with risk r do not show any preference for their partners based on risk. The random mixing function for the probability that a person of risk r picks

a partner with risk r' is defined by the ratio of total number of partners for all people with risk r' , $r'N(r')$, to total number of partnerships, $\int_{r_0}^{\infty} uN(u)du$. Thus, the random mixing distribution

$$\rho_{rm}(r, r') = \frac{r'N(r')}{\int_{r_0}^{\infty} uN(u)du} , \quad (3.3)$$

is independent of the risk r of the person seeking a partnership.

Biased mixing distribution: In our biased (associative or preferential) mixing model, we assume homophily (love of the same) where people with risk r prefer to have partners with similar risk. We also assume that people at high risk have partners with a broader range of risk than people at low risk. That is, the standard deviation, $\sigma(r)$, for the distribution of risk of partners of a person with risk r is an increasing function of r . This is in agreement with the study by Lescano et al. [58] that observed the partners of people with many partners are mostly casual partners with few acts (sexual acts) per partnership. They also observed that the partners of people with few partners are more often longer term partners with more acts per partnership.

We define the biased mixing distribution $\rho_{bm}(r, r')$ for the probability that a person with risk r prefers to have a partner with risk r' from the range $r' \in [r - \sigma(r), r + \sigma(r)]$ as

$$\rho_{bm}(r, r') = \begin{cases} \frac{-|r'-r|+\sigma(r)}{\sigma(r)^2} & |r' - r| \leq \sigma(r) \\ 0 & elsewhere, \end{cases} \quad (3.4)$$

which satisfies the condition $\int_{-\infty}^{\infty} \rho_{bm}(r, r')dr' = 1$. The Figure (3.2) shows how the biased function ρ_{bm} is wider for the higher risk groups.

Combination of random and biased mixing distributions: We assume people choose some of their partners based on their preference (biased mixing) and that they have other partners chosen randomly from the whole population (random mixing). We define the preference level ϵ as fraction of partners of a person with risk r are selected preferentially and the rest are selected randomly, then we can express the mixing distribution as a convex

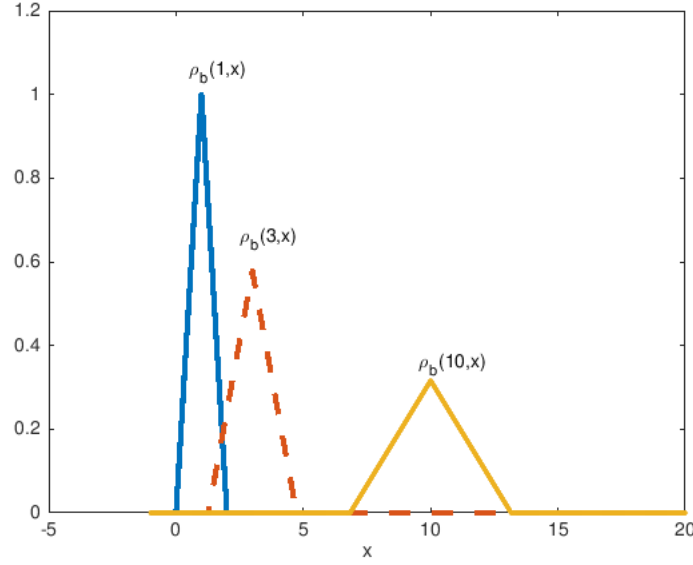


Figure 3.2: Plot of the triangle (hat) biased mixing function $\rho_{bm}(r, x)$ for $r = 1, 3, 10$. As the risk r increases, the mixing function becomes fatter and shorter to capture the effect that partners of higher-risk people have a broader range of risk than that of lower-risk people. This is similar to the mixing function used by Hyman et al. [38].

combination of ρ_{rm} and ρ_{bm} :

$$\rho(r, r') = \epsilon \rho_{bm}(r, r') + (1 - \epsilon) \rho_{rm}(r, r'). \quad (3.5)$$

When $\epsilon = 0$ the mixing is random, and when $\epsilon = 1$ it is purely biased mixing. Otherwise, a person with risk r chooses an ϵ fraction of his/her partners with a hat distribution of people with risk $r' \in [r - \sigma(r), r + \sigma(r)]$, and chooses the other partners randomly from all risk value groups.

Partnership mixing function: The partnership function $p(r, r')$ is the number of partners a person with risk r has with someone of risk r' per year. A person with risk r wants to have $r\rho(r, r')$ partners with risk r' , therefore, all individuals with risk r want to have $r\rho(r, r')N(r)$ partners with risk r' . On the other hand, all individuals with risk r' want to have $r'\rho(r', r)N(r')$ partners with risk r . The balance condition states that if people of risk r have $P(r, r')$ partners with risk r' , then the people with risk r' must have $P(r', r) = P(r, r')$ partners with risk r . Therefore, we define **actual** number of partnership

between people with risk r and people with risk r' as harmonic average of $r\rho(r, r')N(r)$ and $r'\rho(r', r)N(r')$:

$$P(r, r') \stackrel{\text{def}}{=} 2 \frac{r\rho(r, r')N(r) \times r'\rho(r', r)N(r')}{r\rho(r, r')N(r) + r'\rho(r', r)N(r')}. \quad (3.6)$$

The distribution $P(r, r')$ is a compromise for the actual number of partnerships between all people with risk r and all people with risk r' . Therefore, the actual number of partners that a person with risk r has with people of risk r' is

$$p(r, r') = \frac{P(r, r')}{N(r)}. \quad (3.7)$$

Remark: Harmonic average of two values is closer to the smaller one and this compromise weights the decision on forming a sexual partnership towards the person who is less interested in making partnership.

3.1.3 Probability of transmission per partner

The probability per partner, $\beta(r, r')$, that a susceptible person of risk r becomes infected by an infected partner of risk r' depends upon the number of acts (sexual acts) between the two risk groups, $A(r, r')$, and how often condoms are used in their acts, $C(r, r')$.

Sexual acts per partnership between risk groups: We define $A(r, r')$ as the total number of sexual acts per person per day between a person with risk r and a partner with risk r' . Since there must be the same as the number of sexual acts between person of risk r' with partner of risk r , the balance condition, $A(r', r) = A(r, r')$ must hold. Suppose a person with risk r desires to have, on average, $a(r)$ sexual acts per partner per day. We assume that $a(r)$ is a decreasing function of r :

$$a(r) = \frac{A}{r}, \quad (3.8)$$

where A is the total number of sexual acts per day. Because the number of desired sexual acts per partner for people of risk r is not necessarily the same as the number of desired sexual

acts per partnership for people of risk r' , $a(r) \neq a(r')$, then there must be a compromise for the balance condition to hold. We define the actual number $A(r, r')$ of sexual acts per person between the people in risk groups r and r' as

$$A(r, r') \stackrel{\text{def}}{=} 2 \frac{a(r)a(r')}{a(r) + a(r')} . \quad (3.9)$$

The Equation (3.9) satisfies the balance condition, and when there is a conflict, the harmonic average results in the actual number of sexual acts to be closer to the smaller number desired by the two individuals.

Condom-use as a function of risk: We assume that person with risk r desires to use a male-latex condom in $c(r)$ fraction of their sexual acts. We acknowledge that increased condom-use might have an effect on the risk behavior, however, this is not investigated in this work. We assume that higher-risk people are more likely to use condoms than the lower-risk people [58,59]. Therefore, we define $c(r)$ as increasing function of r . We observed that the function

$$c(r) \stackrel{\text{def}}{=} \alpha \left(\frac{r}{c_0 + r} \right) , \quad (3.10)$$

is a good approximation to survey data and interpolates between the case where people have no partners (hence no condom-use), $\lim_{r \rightarrow 0} c(r) = c(0) = 0$, and the limit where people have many partners and use condoms $\alpha = \lim_{r \rightarrow \infty} c(r)$ fraction of acts.

In Section 3.1.3, we described how the actual number of sexual acts between people of different risk groups had to be compromised to satisfy a balance condition. The same is true for condom-use. We define the actual fraction of times that a person of risk r uses a condom when having sex with a person of risk r' as $C(r, r') = C(r', r)$ and define this by an appropriate average of $c(r)$ and $c(r')$. The average will depend if the preference (final decision) is closer to the desired condom-use of the person who prefers to use condoms fewer times, or the person who prefers to use condoms more often.

Preference to low condom-use: In this case, we assume that a person who is less likely to use condom is more likely to convince the other not to use condom. We approximate

this situation for partners with risk r and r' to use a condom in

$$C_l(r, r') = \frac{2c(r)c(r')}{c(r) + c(r')}, \quad (3.11)$$

fraction of their acts.

Preference to high condom-use: In this case, a person who is more likely to use condom is more probable to convince the other one to use condom. We approximate this situation by taking the harmonic average of the fraction of acts people do not use condom ($1 - c(r)$ and $1 - c(r')$), and therefore, they use condoms in

$$C_h(r, r') = 1 - \frac{2(1 - c(r))(1 - c(r'))}{2 - c(r) - c(r')}, \quad (3.12)$$

fraction of their acts.

The probability of transmission with condom-use: We define β_{nc} and β_c as the probabilities of transmission per act for not using and using a condom, and we assume these probabilities are gender-independent, because unlike the heterosexual transmission of HIV/AIDS, the probability of highly infectious STIs (like chlamydia and gonorrhea) transmission from an infected man to a woman is approximately the same as from an infected woman to a man [7, 60, 61]. If the condom is 90% effective in preventing the infection from being transmitted, then probability of transmission when using a condom-use is $\beta_c = 0.1\beta_{nc}$.

To determine the probability of a susceptible person with risk r being infected by their infected partner with risk r' depends on the number of acts, $A(r, r')$, and how often they use condoms. If someone uses a condom in $C(r, r')$ fraction of acts, then they have a total of $C(r, r')A(r, r')$ acts with condoms and $(1 - C(r, r'))A(r, r')$ acts without condom per unit time. The person with risk r does not catch infection from their partner during a condom act with probability $(1 - \beta_c)^{C(r, r')A(r, r')}$, and for when not using a condom this probability is $(1 - \beta_{nc})^{(1 - C(r, r'))A(r, r')}$. Combining these, the probability of a susceptible being infected

after one act by infected partner with risk r' is

$$\beta(r, r') = 1 - (1 - \beta_c)^{C(r, r')A(r, r')} (1 - \beta_{nc})^{(1 - C(r, r'))A(r, r')}. \quad (3.13)$$

3.2 Parameter Estimation

The model parameters in Table (3.1), the distribution of risk in the population, and the condom-use were estimated from recent studies on sexual behavior.

Parameter	Description	Unit	Baseline	Ref.
$\int N(r)dr$	Total population.	people	10000	Assumed
A	Total (max) number of acts per time.	1/day	0.57	Assumed
$1/\gamma$	Average time to recover without treatment.	days	365	[44]
μ	Migration rate.	1/days	0.00	Assumed
β_{nc}	Probability of transmission per no-condom act.	1/act	0.11	[44]
α	Fraction of acts condom used by risky people.	–	0.70	Estimated
β_c	Probability of transmission per condom act.	1/act	0.01	Assumed
$r_0(r_\infty)$	Minimum(maximum) number of partners per time.	people/days	0.00(0.14)	Assumed
ϵ	Preference level.	–	0.60	Assumed

Table 3.1: Model parameters: parameter values are chosen for all simulations unless indicated otherwise.

3.2.1 Population distribution

A sample of 616 people ages 15-25 years old resident in Orleans Parish were asked about their number of concurrent partners [62]¹. This data was in agreement with other recent studies [63], that show that the partner distortion often follows an inverse cubic power law, $N(r) \propto r^{-3}$, for $r > r_0$. The value of $N(r)$ is chosen for the function to agree with the total population size, $\int N(r)dr$, being modeled.

3.2.2 Condom-use

The distribution of risk and condom-use were estimated based on surveys for the sexually active adolescents and young adult populations [27, 58, 59]. Reece et al. [27] studied rates

¹ We will explain these data in Chapter. (4)

15 – 16 years old		16 – 17 years old		17 – 18 years old	
Risk r	Fraction of condom-use	Risk r	Fraction of condom-use	Risk r	Fraction of condom-use
1.2	0.42	1	0.42	1	0.39
5.4	0.58	2	0.42	2	0.38
		7.4	0.60	4.7	0.50

Table 3.2: The average fraction of condom-use by high school students with different risks and different ages, the result of survey conducted in a large urban northwest high school [59].

of condom-use among sexually active individuals in the U.S. population and observed that adolescents reported condom-use during 79.1% of the past 10 vaginal intercourse events. Similar studies [26] in sexually active high school students in the U.S. reported that during 1991, 46%, during 2003, 63%, and in 2013, 59% of the students used condoms at their most recent sexual intercourse.

Beadnell et al. [59] surveyed 8 – 12th grade students in a large urban northwest school district annually for seven years. They observed that the younger students were more likely to use condoms and also the students with more partners were more likely to use condoms: the students with many partners used condoms, on average, in 68% of their sexual acts, while the students with few partners used condoms in 49% of their sexual acts. The condom-use function, Equation 3.10, is in close agreement with their observations (Table (3.2)) with the parameters $\alpha = 0.69$ and $c_0 = 1.35$:

$$c(r) = 0.69 \frac{r}{1.35 + r} . \quad (3.14)$$

A simple check shows this function is in close agreement with the survey data: $c(2) = 0.41$, $c(4.7) = 0.50$, $c(5.4) = 0.58$, and $c(7.4) = 0.60$.

3.3 Numerical Simulations

Because the equations are homogeneous in the total population, our results scale with the total population size. We display our numerical simulations in terms of the nondimensional variables defined by dividing each variable by the steady-state zero-infection equilibrium the total population of individuals with the risk r , $N(r)$. That is, we present the numerical

simulations in terms of the fraction of the population at risk r , i.e susceptible $s(t, r) \stackrel{\text{def}}{=} \frac{S(t, r)}{N(r)}$ or infected $i(t, r) \stackrel{\text{def}}{=} \frac{I(t, r)}{N(r)}$. We define $I^*(r)$ as the number of and $i^*(r)$ as the fraction of the population that is infected at the endemic steady state. In the numerical simulations, all the parameters are fixed with the baseline values given in Table (3.1), unless specifically defined otherwise.

3.3.1 Basic reproduction number \mathcal{R}_0

When the population is distributed as a function of risk, then it is possible to define a basic reproduction number for each value of risk, or a single \mathcal{R}_0 for the entire population based on the dominant eigenvalue of next generation operator. Using a single \mathcal{R}_0 is useful when studying the impact that changes in the biased mixing and condom-use parameters have on the early growth of an epidemic.

We follow Diekmann et al. [64] and define \mathcal{R}_0 as the spectral radius of the next generation operator defined as

$$K(r) = S(t, r) \int_{r_0}^{r_\infty} \tau p(r, r') \beta(r, r') I(t, r') dr', \quad (3.15)$$

where $\tau = \frac{1}{\mu + \gamma}$ is average time that a person is infected and $\tau p(r, r') \beta(r, r')$ is the expected number of people with risk r will be infected by a single infected person with risk r' . Thus, the next generation operator, $K(r)$, is number of secondary cases for over all the infected people with risk r' , $I(t, r')$, and is found by integrating over all possible risk groups. That is, $K(r)$ is the number of secondary cases with risk r that arises from all the infected people $I(t, r')$. The basic reproduction number \mathcal{R}_0 is the dominant eigenvalue of $K(r)$.

We first partition our integro-differential equation model (3.1) into subdomains for different risk groups, $[r_0, r_\infty] = \cup_{i=1}^n [r_{i-1}, r_i]$, where $r_n = r_\infty$ and define the populations on for each risk group as $I_i(t) = \int_{r_{i-1}}^{r_i} I(t, r') dr'$ and $S_i(t) = \int_{r_{i-1}}^{r_i} S(t, r) dr$. The equations can

then be expressed as

$$\begin{aligned}\frac{\partial S_i(t)}{\partial t} &= \mu(N_i - S_i(t)) - \lambda_i(t)S_i(t) + \gamma I_i(t), \\ \frac{\partial I_i(t)}{\partial t} &= \lambda_i(t)S_i(t) - \gamma I_i(t) - \mu I_i(t),\end{aligned}$$

where $\lambda_i = \sum_j \int_{r_{i-1}}^{r_i} p(r_i, r_j) \beta(r_i, r_j) I_j dr_j$.

We divide the equations by $N(r)$ and approximate the next generation operator $K(r)$ with the n -by- n next generation matrix \mathcal{K} based on assuming the populations are approximately constant within each risk group and that the population is at the zero-infection equilibrium, $s_i = 1$. The entries of \mathcal{K} are defined by

$$k_{ij} = \int_{r_{i-1}}^{r_i} \tau p(r_i, r_j) \beta(r_i, r_j) dr_j. \quad (3.16)$$

The basic reproduction number \mathcal{R}_0 defined as the dominant eigenvalue of \mathcal{K} , is calculated numerically.

The Figure (3.3) illustrates how \mathcal{R}_0 increases as the amount of biased mixing ϵ increases. When a new infection is introduced into the population, if there is even a slight amount of random mixing, someone in the high-risk population will quickly become infected [38]. Once this happens, then if the mixing is highly-biased (large ϵ) these infected high-risk people will infect other high-risk people and the epidemic will grow rapidly (large \mathcal{R}_0). If the mixing is close to random mixing (small ϵ), then many of the secondary infections from the early high-risk infected people will have low-risk and the epidemic will grow slower (smaller \mathcal{R}_0). The extreme sensitivity of \mathcal{R}_0 to α also is an indication of the importance of educating high-risk individuals in consistent condom-use to prevent infecting others, and the need of the low-risk population in using condoms to protect themselves from infection.

3.3.2 Endemic equilibrium

The fraction of the population that are infected at the endemic equilibrium infection, i^* , depends upon the distribution of risk, $N(r)$, the mixing between people of different risk

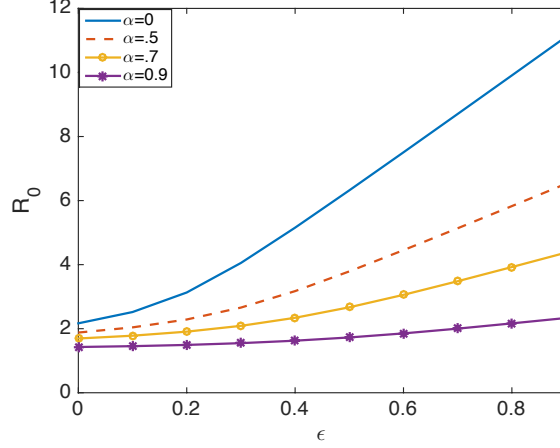


Figure 3.3: Basic reproduction \mathcal{R}_0 versus preference level ϵ for different condom-uses: the impact of α on \mathcal{R}_0 depends on mixing, for more biased mixing α has more impact on preventing the infection, however for less biased mixing, the impact of α decreases. As α decreases \mathcal{R}_0 increases much faster at bigger ϵ s than smaller ones.

behaviors, as measured by ϵ in Equation (3.5), and the fraction of the acts condom used by high-risk people, as measured by α in Equation (3.10).

The Figures 3.4(a) - 3.4(f) plot the endemic infection distribution as a function of risk r for

1. Random mixing where 90% of the partners are chosen randomly from the population, i.e $\epsilon = 0.1$,
2. Balanced mixing where all but 60% of the partners have similar risk behavior, i.e $\epsilon = 0.6$, and
3. Highly biased mixing where all but 90% of the partners have similar risk behavior, i.e $\epsilon = 0.9$.

For all values of risk, the fraction of infected population at steady state, i^* , decreases as condom-use, α , increases. In the Figures 3.4(a), 3.4(c), and 3.4(e), the α axis is between $\alpha = 1$ where the high-risk population uses condoms all the time, to $\alpha = 0$ where condoms are never used. The fitted value $\alpha = 0.69$ agrees with Beadnell et al. [59] studies. For low condom-use (small values of α), i^* increases with r indicating that a higher percentage of the high-risk people are infected than the low-risk people. For most values of condom-use,

$\alpha < 0.95$, having more partners (increase one's risk r), increases the likelihood of being infected.

When the high-risk people use condoms most of the time, $\alpha \geq 0.95$, while the lower-risk population only uses condoms occasionally, this trend is reversed. This effect is strongest when the mixing is highly biased ($\epsilon = 0.9$) i.e when most of a person's partners have very similar risk. We note that although this is mathematically consistent with our model, it is in an unrealistic parameter range for the population.

To quantify the effectiveness of condoms at reducing the prevalence, in Figure (3.5) we show fraction of the total infected population as a function of α , $i_T^* = \int I^*(r)dr / \int N(r)dr$ for different preference levels ϵ . There is a threshold for α to drops the epidemic down, and this threshold increases as mixing level ϵ increases. For example when level of mixing is $\epsilon = 0.1$ (Random mixing), to drop the prevalence drastically, α needs to be around 70%, however, for when $\epsilon = 0.6$ (Balanced mixing) this threshold is $\alpha = 0.9$, but for $\epsilon = 0.9$ (Highly biased mixing) threshold disappears which means condom-use by high-risk individuals does not have impact on controlling the prevalence. The reason is when people mix more randomly, then high-risk people have many partners with different risks, therefore, using more condom by them save this many partners with different risks, however, when mixing tends to be more biased, $\epsilon = 0.9$, most of the partners of high-risk people are themselves high-risk, which this case this group does not take heavy toll on the prevalence, no matter what fraction of their acts they use condom.

3.3.3 Condom-use scenarios

We compare three condom-use scenarios—explained in Table (3.3)—to quantify their impact on reducing the prevalence of the STI at the endemic equilibrium.

To study the influence of different scenarios on the total prevalence, we recorded prevalence at time t for each scenario. In Figure (3.6), the prevalence for all scenarios are shown as a function of time t for $\hat{c} = \bar{c} = 0.37$. When condoms are never used (NCU), the prevalence tends to $i(t) \rightarrow i_T^* = 0.18$. The prevalence is reduced the most for SCU when $\hat{c} = 37\%$

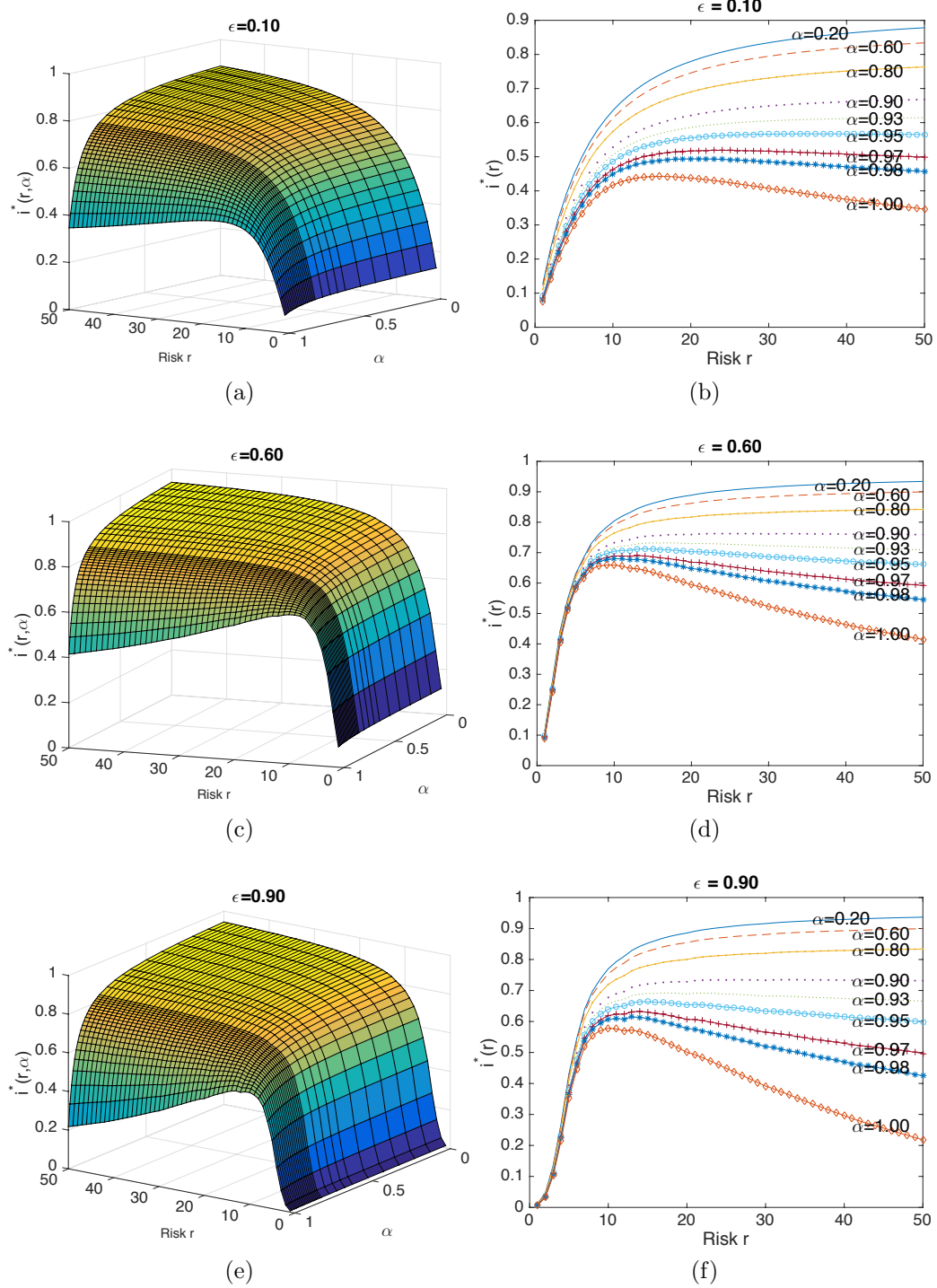


Figure 3.4: Surface plots of fraction of the infected population, $i^*(r, \alpha)$, at steady state versus r and α , for preference levels (a) $\epsilon = 0.1$, (c) $\epsilon = 0.6$, and (e) $\epsilon = 0.9$, and slices of the 3D surfaces versus r , $i^*(r)$, for different α values and preference levels (b) $\epsilon = 0.1$, (d), $\epsilon = 0.6$, and (f) $\epsilon = 0.9$: when $\alpha < 0.95$, the i^* increases with risk r , when high-risk people use condoms most of the time, $\alpha > 0.95$, then i^* decreases in the higher-risk groups as a function of r .

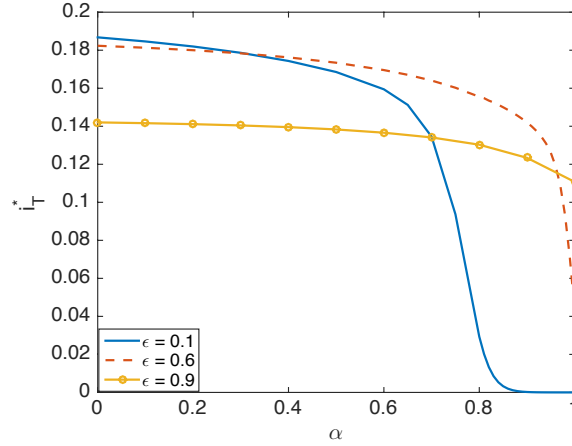


Figure 3.5: Total fraction of the population that is infection $i_T^* = \int I^*(r)dr / \int N(r)dr$ decreases as condom-use α increases for random mixing $\epsilon = 0.1$, combined mixing $\epsilon = 0.6$, and highly biased mixing $\epsilon = 0.9$ in partnership selection. Note that when people tend to pick partners randomly, $\epsilon = 0.1$, and the population uses condoms most of the time, $\alpha > 0.8$, then condom-use is an effective way to control the epidemic.

of population uses condoms all times. In this case, we observe a reduction of 7% of prevalence at steady state. The reason is that condom-use comes by act, and when $\hat{c} = 37\%$ of population use condoms in all their acts, then 37% of population are rarely infected. On the other hand, for scenario FCU, i.e when all people use condom $\bar{c} = 0.37$ of the acts, the reduction of prevalence is very weak, almost 0.5%, and this is because the model is applied for Ct as a highly infectious STI, that is the chance of catching or transmitting the infection by one act is high, therefore, even if all people use condom partially, there is a high chance of infection transmission in the acts which condom is not used.

In the scenario RCU, i.e using Equation (3.10) as a condom-use function for when $\bar{c} = 0.37$ which results $\alpha = 0.75$, the prevalence at steady state reduces by 2%. In this scenario, people on average use a condom in 37% of their acts, however, high-risk people are more likely to use a condom. As we observe, for this scenario, the growth of infection is slower than the other scenarios and it takes more time (around 10 years) to reach steady state. This is because, high-risk individuals, who are mostly responsible of spreading infection, use condom more and then transmit or catch infection less than the other scenarios, therefore, it takes time for them to transmit or catch infection.

Scenario	Description
NCU	No Condom-Use: the unrealistic case where condoms are never used is included as a reference case.
SCU	Some Condom User: the population is divided into condom users and non-users where in each risk group, \hat{c} fraction of $N(r)$ of the people use condom all the time, while $(1 - \hat{c})$ fraction of them never use a condom.
FCU	Fraction Condom Users: everyone uses a condom with probability \bar{c} in each act, that is, $c(r) = \bar{c}$ is constant.
RCU	Risk-based Condom-Use: the condom-use is a function of risk based on the function $c(r, \alpha)$ in Equation (3.10) and the scaling parameter α is chosen so the average condom-use $\langle c(r, \alpha) \rangle = \bar{c}$.

Table 3.3: Different condom-use scenarios.

3.4 Discussion and Conclusions

In this chapter we created a continuous-risk SIS transmission model for the spread of Ct with biased mixing partnership selection to investigate the impact that condoms can have in controlling their spread. The model incorporates functions describing mixing patterns as well as condom-use by individuals based on their risk. The mixing between people of different risks was modeled as a combination of random mixing and biased mixing, where people prefer partners of similar risk [39]. Our model includes the observed correlation between condom-use and the number of partners among adolescents and young adults [58, 59, 65] where people with higher number of partners are more likely to use condoms. Based on that, we fitted an increasing function of risk for condom-use to the information provided in [59]. We assumed that people with more partners (higher risk r) were less picky about the risk of their partners than people with fewer partners. We modeled this increased acceptance of the risk of the partners by increasing the standard deviation of risk of the partners as the square root of risk.

The endemic infection equilibrium is more sensitive to the rate that the people with bigger risk r -where there are fewer acts per partnership- use condoms than it is for people with smaller risk r -where there are more acts per partnership. When the probability of infection is high for a single act, as it is in our simulations, then the number of people

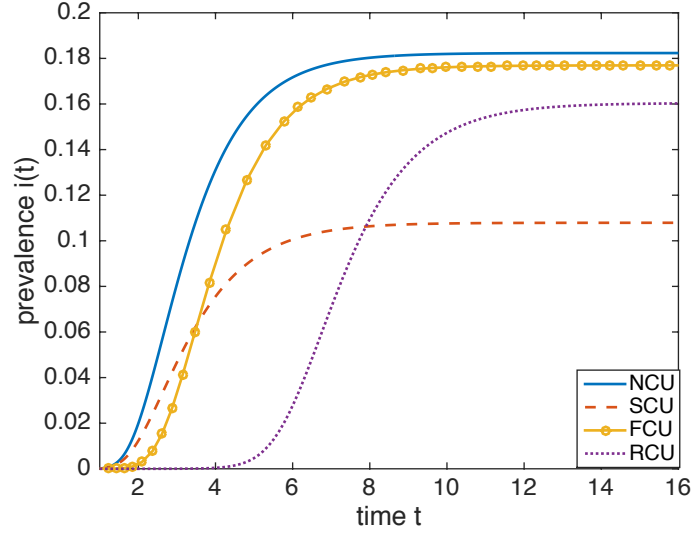


Figure 3.6: The prevalence of Ct as a function of time for different Scenarios: NCU=no condom-use, SCU=sometime condom user, FCU=fraction condom user, RCU = risk-based condom-use where $\hat{c} = \bar{c} = 0.37$ and $\alpha = 0.74$ and $\epsilon = 0.8$.

an infected person infects is more correlated to the number of partners that he/she has unprotected sex with, than the number of acts they have. Our model assumes that people with fewer partners have more acts per partnership than people with more partners. The risk of infection is high for a single act where condoms are not used, then even failing to use condoms a few times in a partnership is enough to pass on the infection. That is, the model indicates increasing the fraction of times that people with many partners use condoms could be an effective strategy in mitigating Ct.

The simulations quantified the rate that Ct spreads through a population based on different distributions of condom-use as a function of the population risk. We estimated the impact of condom-use by higher risk individuals on the distribution of endemic equilibrium. We found that for almost all amount of condom-use, having more partner increases the likelihood of being infected, the infection prevalence is greatest in the higher risk populations and it is always a good mitigation strategy to increase condom-use in these populations to mitigate an epidemic. This effect is stronger for when people select most of their partners preferentially.

We also observed that the total prevalence does on drop drastically unless the mixing tends to more random and high-risk individuals use condom in at least 70% of their acts.

However, when the mixing tends more toward biased mixing, prevalence at steady state loses its sensitivity to condom-use. Our simulations, also, demonstrate that when level of biased mixing is low, then it is also an effective mitigation strategy to increase condom-use in the the lower risk populations, as shown in Figure (3.5).

We derived the basic reproduction number \mathcal{R}_0 using the next generation approach [64] and used simulations to show the early growth of the epidemic depends on mixing pattern and condom-use. For very biased mixing, when people pick their partners to have similar risk, condoms are an effective approach to mitigate the spread of Ct. However, when the population mixed more randomly, then condom-use is less effective in controlling the epidemic.

The model investigates the role of the risk-structure and importance of homophily in the mixing between people with different risk on the spread of the epidemic. We formulated this simplified model because it is easier to analyze and can provide insight into the dynamics of the more complex models that also account situations where these assumptions do not hold.

The current model does not distinguish between men and women. In heterosexual populations, this approximation is only appropriate when the mixing between men and women is symmetric and the infection prevalence is approximately the same in both men and women. We are extending the model to a heterosexual mixing model, similar to our previous model in Chapter. 2 where we only included two risk groups . The heterosexual model can be used to more closely match partnership studies that show, on average, a sexually active man will have more partners than the sexually active women in the adolescents and young adult population. It can also be used to study the relative effectiveness of increasing the screening for men, women, or both sexes for Ct when there are limited resources.

We recognize that a more realistic approach is needed for guiding public health policy. This realistic model would track behavior change and mixing based on a person's age. For example, when an individual is infected and treated, then they are more likely to change their behavior to prevent being infected again. Behavior change is an important assumption which could be added in this model by including risk-based partial derivative terms in the

model. This extension would make the model significantly more complex and would not be a good model as using an agent-based model that can follow the infection status of each individual.

The analysis and simulations of our continuous-risk model has led us in creating a more appropriate model for studying the impact of screening, partner notification, partner treatment, condom-use, and behavior change in controlling the spread of Ct. In Chapter. 4 we will formulate a stochastic Monte Carlo - Markov Chain (MCMC) agent-based bipartite disease-transmission network-model where the men and women are the network nodes and sexual acts are represented by edges between the nodes. The network captures the distributions for number of partners that men and women have, and the correlations between the number of partners that a person has and the number of partners their partners have. These partnership distributions, and the transmission parameters, are based on survey data for the 15 – 25 year-old AA community in New Orleans.

Unlike the continuous-risk model, the network model can track an individual's behavior change, such as condom-use after being treated for infection, the affect of aging on number of partners a person has, or the differences in condom-use between primary and casual partners.

Chapter 4

Network Model

Up to now we have introduced an ordinary differential equation Ct transmission model that captures the most essential transitions through an infection with Ct to assess the impact of Ct infection screening programs, Chapter 2. We also have provided a selective sexual mixing hybrid differential/integral equation Ct model to capture the heterogeneous mixing among people with different number of partners, Chapter 3. An alternative, and more realistic model, is to represent the sexual network by a graph where each individual within a population is a node. The connecting edges between the nodes denote sexual relationships that could lead to the transmission of infection. These sexual mixing networks can capture the heterogeneity of whom an infected person can, or cannot, infect.

In this Chapter we create an agent-based heterosexual network model of Ct transmission to evaluate potential intervention strategies for reducing the Ct prevalence in urban cities, such as New Orleans [66]. We construct a network model that mimics the heterosexual behavior obtained from a sexual behavior survey of the young adult AA population in New Orleans and model Ct transmission as a discrete time Monte Carlo stochastic event on this network. The model is initialized to agree with the current New Orleans Ct prevalence. We use sensitivity analysis to quantify the effectiveness of different prevention and intervention scenarios, including screening, partner notification -which includes partner treatment, and partner screening (contact tracing)- and social friend notification, and rescreening [34, 66]. This model structure allows the sexual partnership dynamics, such as partner concurrency,

sexual histories of each person, and complex sexual networks, to be governed at the individual level.

In this Chapter we first review the data used for generating network, then we explain how we generated our networks, and the last Section would be transmission model on the networks and testing different interventions.

4.1 The New Orleans Sexual Activity Survey Data

Two types of studies were conducted to estimate the Ct infection among local people and to assess the effectiveness of biomedical and behavioral intervention programs in the general heterosexual population reside in New Orleans.

A community-based pilot study, called "Check-it", was performed among African American, AA, men ages 15 – 25 years old in a typical three-month period. The overall $n = 202$ men participant were asked about their age, number partners in the past three months, history of Ct test results, as well as living habits. Meanwhile, their partners information have been collected by asking questions referring to the status of each relationship such as, the partner's age, strength of relationship, first and last time of intercourse, and the possibility that their partner have intercourse with others [67].

An internet pregnancy/STI prevention study, called "You Geaux Girl", was conducted among AA women ages 18 – 21 years old. A total $n = 414$ participants have been asked the similar questions. Additionally, more partners information such as total number of sexual act for each relationship and number of partners their partner might have were asked from the participants [68].

4.1.1 Distributions for number of partners

The first and most vital information for constructing network is distribution of number of partners for men and women. Therefore, individuals were asked about how many partners they have had during the past three months. The Figure (4.1) shows the result for both men and women participants.

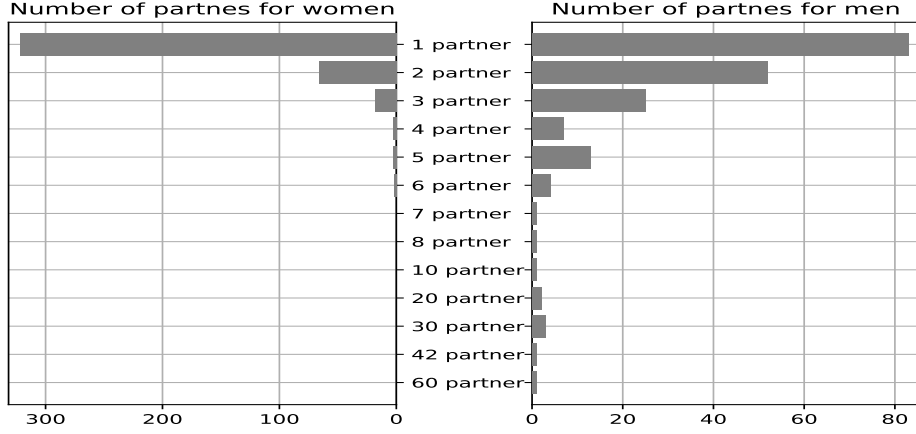


Figure 4.1: Bar plot of number of partners for men and women for the last three months.

We fitted a Generalized Pareto distribution to the data and fill the gaps in data. The Figure (4.2) shows the probability of having x partners for men and women and also their fitted distributions.

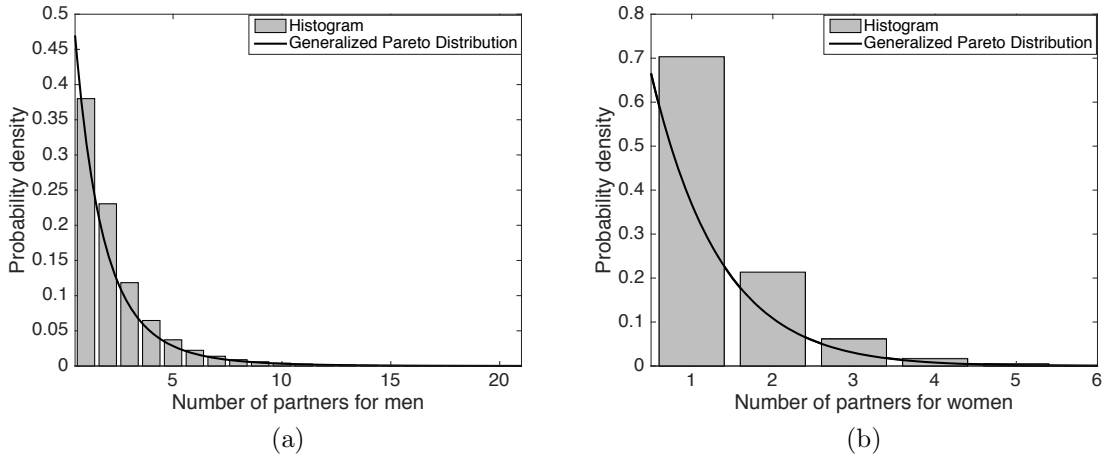


Figure 4.2: Reference number of partners for men (4.2(a)) and women (4.2(b)) participant with the probability of having x partners.

To generate a consistent network, the number of men and women should be selected properly: if N_m men in the population have an average \bar{p}_m partnerships with women, and N_w women have an average \bar{p}_w partnerships with men, then for consistency, we should have a total of $N_m \bar{p}_m = N_w \bar{p}_w$ partnerships in the population. In other word the number of men

	Number of Partners for Partners of Women Participants															
		1	2	3	4	5	6	7	8	9	10	11	12	13	16	21
Number	1	197	56	28	9	2	3	0	1	0	0	0	0	0	1	0
of	2	46	34	23	3	2	5	2	0	1	1	0	0	1	0	0
Partners	3	16	11	3	10	2	1	1	0	0	0	0	0	0	0	1
for	4	4	2	4	0	0	1	0	0	0	0	1	0	0	0	0
Women	5	0	2	3	0	0	4	0	0	0	0	0	1	0	0	0
Participants	6	3	0	5	1	0	0	1	0	0	0	0	1	0	1	0

Table 4.1: Joint-degree Table of sample data for women participant in the last three months.

and women in the network should follow consistency condition

$$\frac{N_m}{N_w} = \frac{\bar{p}_w}{\bar{p}_m} = \rho.$$

Using the fitted distribution shown in Figure (4.2) we can find the data f_i as the fraction of individuals having i partners for both men and women and also expected values \bar{p}_m and \bar{p}_w , and then we can find the fraction of active men and women in population with arbitrary size.

4.1.2 Distribution for number of partners of partners

In the "You Geaux Girl" survey, women participants were asked about the number of partners their partners have. The Table (4.1) is the extracted result from survey: each element (i, j) in the Table is the number of men with j partners which women with i partners have. In network terminology each element (i, j) counts the number of edges between women with degree i and men with degree j , therefore, it is trivial to see that for a consistent Table, if men with degree j were asked about the number of their partners with degree i , all of them would provide the same answer (i, j) . However, this is not always true for sample data, thus we have to implement this consistency condition for joint-degree Table for the population. To do that, at first we generate the joint-degree Table for the population, and then we make it consistent.

The Table (4.1) is an sparse table, for most of women we have no high-degree partners,

which is not correct, because from degree distribution for men in the previous subsection we have men with more than 10 partners. This can happen because of lack of data or information. Therefore, we have to fill the incorrect zeros in the table. In order to do that, we divide each row of table to sum of its elements, that is, we divide row i by $\sum_j(i, j)$. The new elements are fraction of edges between women with i partners and men with j partners. Then we fit these fractions to Generalized Pareto distribution to find probability of an edge between a woman with i partners and a man with j partners, Table (4.2).

Probability of Partner's Partner for Women Participants					
	1	2	...	n	
Probability	1	p_{11}	p_{12}	...	p_{1n}
of Partners	2	p_{21}	p_{22}	...	p_{2n}
for	\vdots	\vdots	\vdots	\vdots	\vdots
Women	m	p_{m1}	p_{m2}	...	p_{mn}

Table 4.2: Joint-degree probability for women participant in the last three months.

Now our goal is to find the number of edges between women with i partners and men with j partners: we have $f_i^w N_w$ women with i partners, where f_i^w is Generalized Pareto probability of having i partners for women and was computed in the previous subsection, and N_w is the population size of women. These women make total $i f_i^w N_w$ edges which p_{ij} fraction of these edges are between them and men with j partners. Therefore, we will have total $i f_i^w N_w p_{ij}$ edges between women with i partners and men with j partners. The value $i f_i^w N_w p_{ij}$ defines the (i, j) th element of this fitted joint-degree Table.

If men were asked about this question, we should have consistent table, but it is not consistent, therefore, we are using constrained optimization to refine elements p_{ij} to make the table consistent. In fact, we solve minimization problem

$$\begin{aligned}
& \text{minimize} && \|P - \tilde{P}\|^2, \\
& \text{subject to} && \sum_j i f_i^w N_w \tilde{p}_{ij} = i f_i^w N_w, \quad i = 1, \dots, m, \\
& && \text{and } \sum_i i f_i^w N_w \tilde{p}_{ij} = j f_j^m N_m, \quad j = 1, \dots, n.
\end{aligned}$$

where $P = (p_{ij})$, $\tilde{P} = (\tilde{p}_{ij})$, f_j^m is Generalized Pareto probability of having j partners for men, and N_m is population size of men. By definition of $\rho = \frac{N_m}{N_w}$ we can simplify the above optimization problem to

$$\begin{aligned} & \text{minimize} && \|P - \tilde{P}\|^2, \\ & \text{subject to} && \sum_j \tilde{p}_{ij} = 1, \quad i = 1, \dots, m, \\ & && \text{and } \sum_i i f_i^w \tilde{p}_{ij} = \rho j f_j^m, \quad j = 1, \dots, n. \end{aligned}$$

Using least square method we come up with the new Table of consistent probability of existing edge between women with i partners and men with j partners, Table (4.3).

Degree of men \ Degree of women	1	2	3	4	5	6
1	0.3775	0	0	0	0	0
2	0.1880	0.0205	0	0	0	0
3	0.0988	0.0396	0.0162	0.0033	0	0
4	0.0833	0.0734	0.0285	0.0087	0.0034	0.0010
5	0.0313	0.0264	0.0162	0.0083	0.0037	0.0014
6	0.0207	0.0209	0.0134	0.0066	0.0025	0.0003
7	0.0150	0.0167	0.0107	0.0046	0.0008	0
8	0.0116	0.0135	0.0082	0.0026	0	0
9	0.0093	0.0110	0.0061	0.0008	0	0
10	0.0075	0.0090	0.0043	0	0	0
11	0.0061	0.0074	0.0027	0	0	0
12	0.0050	0.0062	0.0014	0	0	0
13	0.0042	0.0053	0.0005	0	0	0
14	0.0034	0.0045	0	0	0	0
15	0.0027	0.0037	0	0	0	0
16	0.0021	0.0031	0	0	0	0
17	0.0016	0.0027	0	0	0	0
18	0.0012	0.0023	0	0	0	0
19	0.0009	0.0020	0	0	0	0
20	0.0007	0.0017	0	0	0	0
21	0.0059	0.0070	0.020	0	0	0

Table 4.3: Joint-degree probability distribution for heterosexual partnerships used in the computer simulations. Men and women are assumed to have fewer than 21 and 6 partners respectively. The entry in the i^{th} row and j^{th} column is the fraction of partnership (edges) between men who have i partners (degree i) and women who have j partners (degree j).

4.1.3 The number of sexual acts per partner

To better understand and predict the spread of Ct, we need to know the number of acts per unit time between two typical partners. In the "You Geaux Girl" survey data women were asked about their total number of acts per partner during the last three months. Each one reported two numbers which refer to their number of acts per primary and casual partners.

The Table (4.4) shows the number of women with k partners who engaged in n sexual acts with their primary and casual partners in the last three months.

Number of acts	1	2	3	4	5	6	7	8	9	10	11
# of degree 1 women	53(23)	27(6)	24(0)	19(0)	18(3)	10(1)	8(0)	12(0)	5(0)	20(0)	68(0)
# of degree 2 women	18(25)	7(10)	8(2)	3(7)	4(5)	1(1)	2(1)	3(0)	2(0)	3(0)	9(3)
# of degree 3 women	2(13)	1(8)	3(1)	1(2)	2(0)	4(1)	1(1)	1(0)	1(0)	2(1)	1(0)
# of degree 4 women	1(5)	2(1)	0(1)	0(1)	0(0)	0(0)	0(1)	0(0)	0(0)	0(0)	0(0)
# of degree 5 women	1(4)	2(0)	0(0)	0(0)	0(1)	0(0)	0(0)	0(0)	0(0)	1(1)	0(0)
# of degree 6 women	1(3)	2(1)	0(1)	0(1)	0(0)	0(0)	0(0)	0(0)	0(0)	0(0)	0(0)

Table 4.4: Element (k, n) in the table is the number of women with k partners who have n sexual act per primary (casual) partners within three months.

Using this Tables, we can find average number of acts per primary (casual) partner for women with k partners as

$$a_{wp}^k = \frac{\sum_{i=1}^{11} i(k, i)}{\sum_{i=1}^{11} (k, i)} \quad (a_{wc}^k = \frac{\sum_{i=1}^{11} i(k, i)}{\sum_{i=1}^{11} (k, i)}).$$

Our goal is to find one common value for sexual acts for women with k partners defined as a weighted average of a_{wp}^k and a_{wc}^k i.e

$$a_w^k = \alpha a_{wp}^k + (1 - \alpha) a_{wc}^k, \quad (4.1)$$

where α is fraction of primary partners for women with degree k .

If men were asked the same question about the number of their acts with different partners, then we would have similar information: for a man with k' partners, we can find

$a_m^{k'}$ with the same manner. Then, if a k – degree woman is partner of a k' – degree man, so the numbers a_w^k and $a_m^{k'}$ should be the same, but usually this does not happen, therefore, we use the average idea: our compromise, or resolution, function will be an average of a_w^k and $a_m^{k'}$. As in resolving conflicts in the partnership data, we choose the harmonic average that weights the smaller number more:

$$a_{kk'} = \frac{2a_w^k a_m^{k'}}{a_w^k + a_m^{k'}}. \quad (4.2)$$

By these definitions we have a consistent definition for our weighted network or symmetric adjacency matrix of network. However, we do not have any information about the number of acts reported by men. Therefore, we only use one-sided sexual act number: for any edge that its relevant woman node has degree k , we put weight a_w^k defined in (4.1) on the correspondent edge. The Table (4.5) shows the number of acts per day per partner for a women with different number of partners.

Number i of partners for women	1	2	3	4	5	6
Number of act per partners per day $a(i)$	0.1104	0.0563	0.0442	0.0241	0.0503	0.0222

Table 4.5: The average number of sexual act per partne per day for women with different number of partners.

4.1.4 Age distribution

Another factor in generating a sexual network is the age of individuals. Therefore, in Check-it survey men participants were asked about their age. The Figure (4.3) shows the frequencies of each age in the survey data.

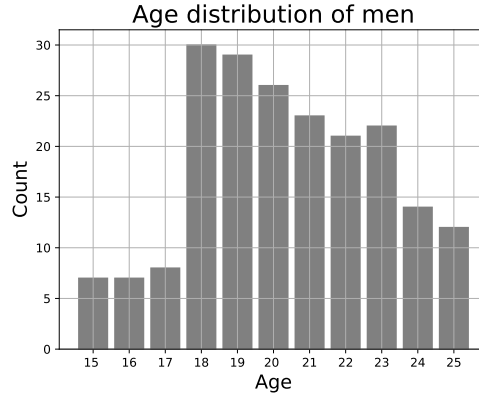


Figure 4.3: Bar plot of age distribution for men.

Because in Check-it survey, population under study was men ages 15 – 25 (people younger than 15 or older than 25 years old were not eligible in taking survey) we did not fit any distribution to this data, instead, we used empirical distribution to define probability distribution function for age of men. The Table (4.6) shows this function.

Age of men	15	16	17	18	19	20	21	22	23	24	25
pdf of age for men	0.035	0.035	0.04	0.15	0.15	0.13	0.115	0.105	0.11	0.07	0.06

Table 4.6: Probability distribution for men's age.

Men also were asked about their partners's age. The Figure 4.4(a) is the box plot of partners age versus men's age, and Figure 4.4(b) is the scatter plot of primary partners age versus men's age. These plots show, age is one factor in selecting primary partners for men: there is a strong linear trend with slope 1 between men's age and the average age of their primary partners. However, there is no strong age bias for selecting casual partners, though partners age is close to men's age.

4.2 The New Orleans Social Activity Data

For social activity of people in New Orleans we used the synthetic data produced using Simfrastructure [69,70] which is a high-performance, service-oriented, agent-based modeling and simulation system for representing and analyzing interdependent infrastructures. This

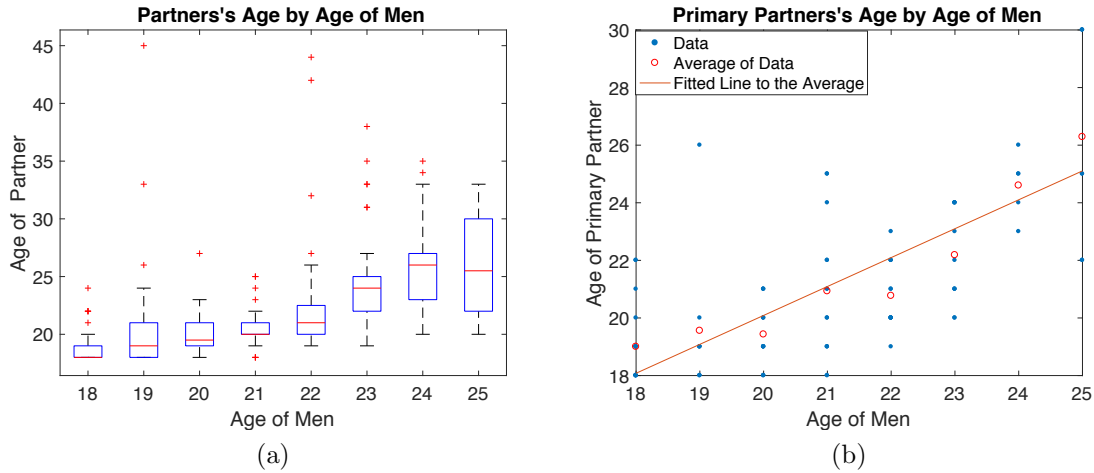


Figure 4.4: Box plot of age for all partners of men with different age: partners age is close to men's age 4.4(a). Scatter plot of age for primary partners: there is perfect linear correlation between men's age and average age of their primary partners, that is primary partners of men have the same age as them 4.4(b).

data is shown as two tables: first includes people information including their age and gender and second is a contact file such as¹

PID	FID	A	T
43722	16981	H	0.3
	11462	W	0.2
	37790	Sh	0.01
	⋮	⋮	⋮
51981	23476	Sc	0.16
	18462	O	0.02
	10790	H	0.5
	⋮	⋮	⋮
⋮	⋮	⋮	⋮

Table 4.7: This table is another representation of social contact network of 130,000 synthetic people reside in New Orleans.

In Table (4.7) **PID** is personal ID and **FID** is their social friend ID, **A** is activity in

¹ We should mention we did not use Simdemic software to generate Table. (4.7), but providing information about New Orleans population demographics we asked Network Dynamics and Simulation and Science Laboratory (NDSSL) to generate social contact file for synthetic population of New Orleans [70].

which PID meet FID, and \mathbf{T} is fraction of time in day that two friends meet with each other through activity \mathbf{A} . We have 5 different activities including H as home, W as work, Sc as school, Sh as shopping, and O as others. For example person 43722 lives with person 16981 at the same home for 8 hours a day.

4.3 Network Generation

Our goal of this Section is to generate a sexual network that represents the sexual activity of adolescent and young adult AAs reside in New Orleans. In this heterosexual network, each person is a distinct identity represented by a node in the network. Each node \mathbf{i} in the network -representing a person- is denoted by the index \mathbf{i} , and each edge \mathbf{ij} represents sexual partnership between two nodes \mathbf{i} and \mathbf{j} . The network is weighted, where the weight $0 < w_{\mathbf{ij}} \leq 1$ for edge \mathbf{ij} is the probability that there will be a sexual act between two partners \mathbf{i} and \mathbf{j} on an average day. In the model, each day and through a stochastic process, the edge \mathbf{ij} will exist (turn on) with probability $w_{\mathbf{ij}}$, the probability that two nodes \mathbf{i} and \mathbf{j} have sexual act in that day, or not exist (turn off) with probability of $1 - w_{\mathbf{ij}}$, which is equivalent to not having an edge (sexual act) between partners \mathbf{i} and \mathbf{j} on that day. To generate such a network we have sexual activity and social activity data and the tools (algorithms) defined in Appendices. (A) and (B).

The survey results explained in the previous Sections were used to construct the joint-degree distribution or BJD matrix (explained in appendix A) of a heterosexual network of individuals in New Orleans. For a population $P = 15,000$ sexually active adolescent and young adult men and their women partners (5250 men and 9750 women) residing in New Orleans we have

$$BJD = \begin{pmatrix} 1663 & 1588 & 1225 & 896 & \cdots & 14 \\ 474 & 452 & 350 & 255 & \cdots & 4 \\ & & \vdots & & & \\ 3 & \cdots & 2 & 1 & 1 & 0 \end{pmatrix}.$$

The dimension of this *BJD* matrix is 6×21 , that is, the maximum number of partners for women is 6 and for men is 21. We used this *BJD* matrix and algorithm explained in Appendices (A) and (B) to construct the bipartite heterosexual network. These generated networks statistically agree with the distribution for the number of partners men and women have had in the past three months, and the distribution for the number of partners of their partners (the joint-degree distribution).

4.3.1 Analysis of generated networks

We generated 150 sexual networks of 15000 people, 30 of them 20%, 30 others 40%, 30 60%, 30 80%, and the last 30 are 100% subgraph of social network. We then compared some descriptive measures of this ensemble of random networks such as *Sg*, *Nc*, and *Rc* that were not imposed when generating the networks. These measurements are defined in Appendix (A).

First, we evaluated and compared the *Sg* for giant component and bi-component (the first and second biggest connected components of network) for each group of the networks. The Figure (4.5) shows the box plot of these sizes: there is an increment in the size of giant components when people select most of their sexual partners from their social friends. Because in that case, sexually active people are more tight together within the social contact network. However, there is not a significant difference in the size of giant bi-component.

The number of connected components, *Nc*, is another measure characterizing network toughness. This measure can be, but not necessarily, correlated to size of components of network. The Figure (4.6) display descriptive statistics for *Nc* in each network group. Note that data distributions are approximately symmetrical, and measures of *Nc* are similar across groups, but, they change by changing the way of selecting sexual partners.

We also compare *Rc* for the networks in Figure (4.7): each data point $Rc(k)$ for degree k is obtained by averaging redundancy coefficient over the group of people with k partners. In most of the networks these values decrease with k [71]. Redundancy coefficient *Rc* is affected by social network: when people select more partners from their social friends the

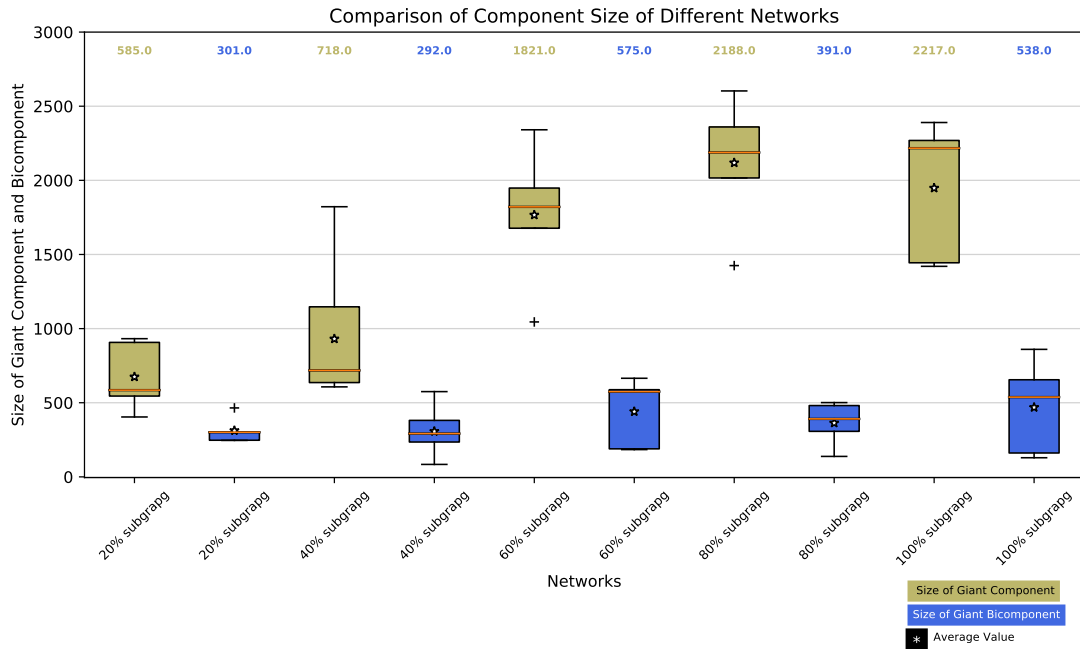


Figure 4.5: Box plot representing size of giant component and bi-component for each group of networks: the size of giant component becomes bigger when being subgraph of social network becomes stronger, however, social network does not have impact on the size of giant bi-component.

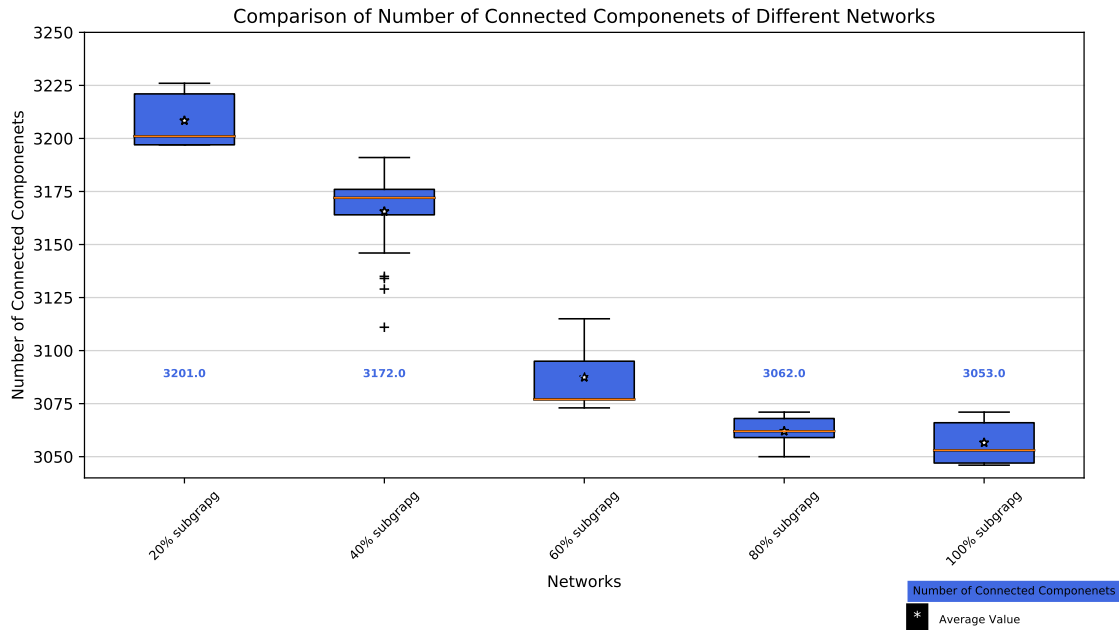


Figure 4.6: Box plot representing number of connected components, N_c , for each group of networks: a significant difference is observed in N_c between each group, N_c is lower in subgraph of social networks.

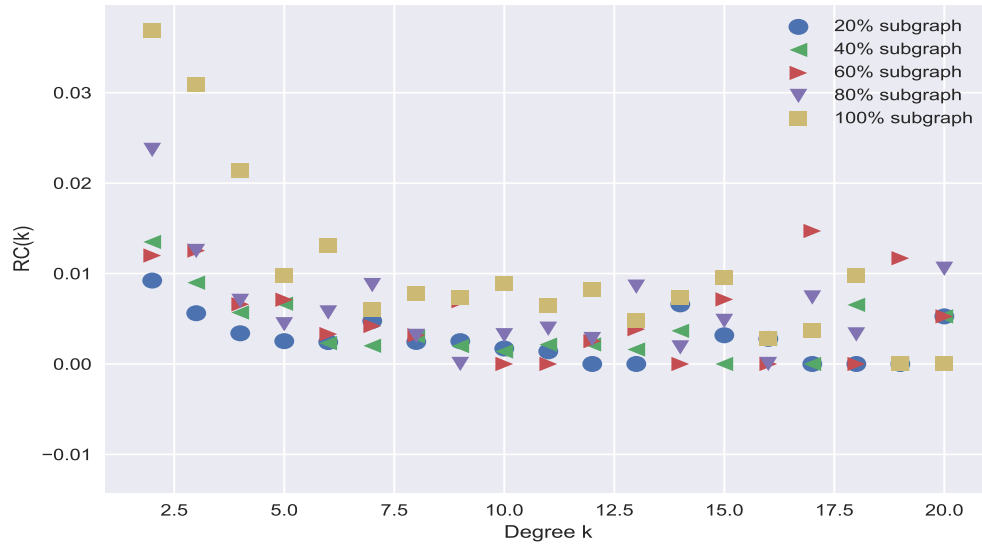


Figure 4.7: Scatter plot of R_c versus degree for five different networks: R_c for sexual network which is strong subgraph of social network is higher, because clustering coefficient for social network is high and therefore, sexual network inherits this property by having higher R_c than the ones which are weak subgraph of social network.

value for R_c increases which this fact is because of Phase. 1 of the algorithm in Appendix (B)- the extension of social network- when we connect friends of a person in social network it means we increase its clustering coefficient. Therefore, when sexual network is subgraph of social network it carries this property by increasing R_c of the network.

4.3.2 Age distribution of the network

When generating sexual network, we tried to select the partners for each person related to his/her age such that we can capture age data reported in Figure (4.4). The left panel of Figure (4.8) is the box plot of age for all social friends of men with different age and right panel is the box plot for the sexual partners. As it is observed while the age distribution for social friends is uniformly distributed, the age of sexual partners is correlated to the age of index men.

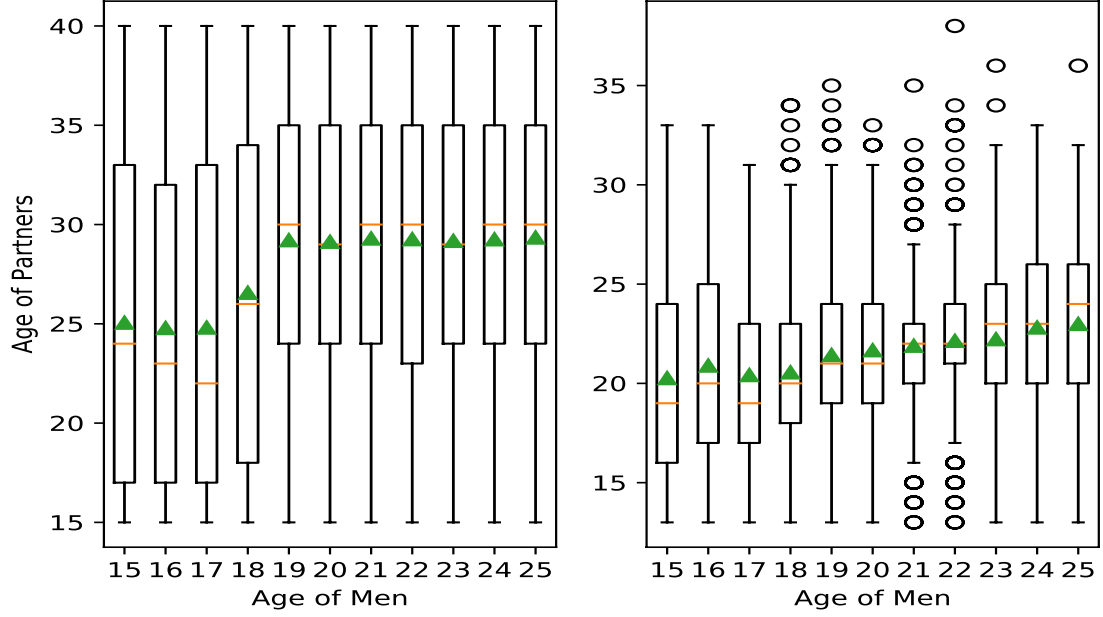


Figure 4.8: Box plot of age for all social friends (left panel) and sexual partners (right panel) of men with different age: though in social activities partner's age are distributed uniformly, in the generated sexual network 100% embedded in social contact one age of partners are correlated to age of men.

4.4 Ct Transmission Model Overview

In our heterosexual network model, each person is a distinct identity represented by a node in the network. This model structure allows the sexual partnership dynamics, such as partner concurrency, sexual histories of each person, and complex sexual networks, to be governed at the individual level.

Each node \mathbf{i} in the network represents a person, denoted by the index \mathbf{i} , and each edge \mathbf{ij} represents sexual partnership between two nodes \mathbf{i} and \mathbf{j} . The network is weighted, where the weight $0 < w_{\mathbf{ij}} \leq 1$ for edge \mathbf{ij} is the probability that there will be a sexual act between two partners \mathbf{i} and \mathbf{j} on an average day. In the model, each day and through a stochastic process, the edge \mathbf{ij} will exist (turn on) with probability $w_{\mathbf{ij}}$, the probability that two nodes \mathbf{i} and \mathbf{j} have sexual act in that day, or not exist (turn off) with probability of $1 - w_{\mathbf{ij}}$, which is equivalent to not having an edge (sexual act) between individuals \mathbf{i} and \mathbf{j} on that day. For the values for $w_{\mathbf{ij}}$ we use the values in Table (4.5) in which if \mathbf{i} is woman then $w_{\mathbf{ij}} = a(\deg(\mathbf{i}))$ otherwise $w_{\mathbf{ij}} = a(\deg(\mathbf{j}))$

In our stochastic Susceptible–Infectious–Susceptible (SIS) model, a person \mathbf{i} is either infected with Ct, $I_{\mathbf{i}}(t)$, or susceptible to being infected, $S_{\mathbf{i}}(t)$. During the day t , an infected person, $I_{\mathbf{j}}(t)$, can infect any of the susceptible partners, $S_{\mathbf{i}}(t)$, they have sexual act with. We define λ_{ij} as the probability that $S_{\mathbf{i}}(t)$ will be infected by $I_{\mathbf{j}}(t)$ by the end of the day, $S_{\mathbf{i}}(t) \xrightarrow{\lambda_{ij}} I_{\mathbf{i}}(t+1)$. Similarly, we define γ_j as the probability that an infected person, $I_{\mathbf{j}}(t)$, will recover by the end of the day, $I_{\mathbf{j}}(t) \xrightarrow{\gamma_j} S_{\mathbf{j}}(t+1)$.

4.4.1 The force of infection

The force of infection, $\lambda_{ij}(t)$, is the probability that a susceptible person S_i is infected on day t by infected partner I_j . This depends on probability of a sexual act between persons i and j on a typical day, as defined by edge weight, w_{ij} , in the model. We define β_{nc} as the probability of transmission per act when a condom is not used, and β_c as the reduced probability of transmission per act when a condom is used. The forces of infection between \mathbf{i} and \mathbf{j} for when condom is not used, λ_{ij}^{nc} , and for when condom is used, λ_{ij}^c , are defined by

$$\lambda_{ij}^{nc} = \begin{cases} \beta_{nc} & \text{with probability } w_{ij} \\ 0 & \text{with probability } 1 - w_{ij} \end{cases}, \quad \lambda_{ij}^c = \begin{cases} \beta_c & \text{with probability } w_{ij} \\ 0 & \text{with probability } 1 - w_{ij} \end{cases}. \quad (4.3)$$

We assume that couples use a condom in κ fraction of their acts correctly and that condom is 90% effective in preventing the infection from being transmitted, that is, $\beta_c = 0.1\beta_{nc}$.

4.4.2 Recovery from infection

The model accounts for infected people recovering through natural recovery or after being treated with antibiotics. We assume that a fraction of the people treated for infection will return later to be retested for infection.

Natural recovery: We assume that all infected people will eventually recover and return to susceptible status, even if they are not treated for infection. In the model, the time for natural (untreated) recovery has an exponential distribution with an average time

of infection of $\frac{1}{\gamma^n}$ days, and the duration of infection for an individual is a random number from this distribution.

Recovery through treatment: We assume that the time for infected person to recover after treatment is a log-normal distribution with an average of $\frac{1}{\gamma^t}$ days. That is, the duration of infection for a treated infected person \mathbf{k} would be set to a random number that follows log-normal distribution, $\log \mathcal{N}(\frac{1}{\gamma^t}, 0.25)$, rounded to the nearest day. In the model, if that number of days is smaller than the duration remaining for naturally clearing the disease, then the shorter time is use for the recovery period.

Each year, a fraction of the population is tested for Ct infection, e.g. through a routine medical exam (random screening) or after being notified that one of their previous partners or social friends was infected. Here we define all biomedical interventions implemented on the network.

Random Screening: We define random screening as testing for infection when there are no compelling reasons to suspect a person is infected. For example, random screening might be part of a routine physical exam and is an effective mitigation policy to identify asymptomatic infections. In our model, we assume that the fraction $\sigma_y\%$ of people are randomly screened each year, and an individual is screened with probability $\sigma_d = 1 - (1 - \sigma_y)^{\frac{1}{365}}\%$ each day.

Partner Notification : We assume that an infected person notifies θ_n^p fraction of their partners about their exposure to infection. Some of the notified partners will do nothing, some will test for Ct infection, and some will seek treatment for Ct without first testing because it is simpler. The notified partners of a tested and treated person are divided into three classes:

1. Partner treatment: θ_t^p fraction of the notified partners are treated, without first testing for infection.
2. Partner screening: θ_s^p fraction of the notified partners engage in screening test and then start treatment if infected.
3. Do nothing: $(1 - \theta_t^p - \theta_s^p)$ fraction are not tested or treated.

For simplicity, we assume notified partners are the ones who are notified and do something, that is, we assume $1 - \theta_t^p - \theta_s^p = 0$. Then we define $\theta_n^p \theta_t^p$ as fraction of partners of an infected person who are treated without first testing for infection (Partner treatment), and $\theta_n^p \theta_s^p$ as fraction of the partners follow screening test (Partner screening).

Partner notification spreads across the same network that originally spread the disease. The partner screening approach is more effective since every time the partner of an infected person is found to be infected, then the cycle repeats itself and their partners are notified.

Social Friends Notification²: We also assume that an infected person notifies θ_n^f fraction of their social friends about screening test. Some of the notified friends will do nothing, and some will test for Ct infection. The notified friends of a treated person are divided into two classes:

1. Social Friend Screening: θ_s^f fraction of the notified friends engage in screening test and then start treatment if infected.
2. Do nothing: $(1 - \theta_s^f)$ fraction are not tested or treated.

For simplicity, we assume notified friends are the ones who are notified and do screening test, that is, we assume $1 - \theta_s^f = 0$. Then we define $\theta_n^f \theta_s^f$ as fraction of the friends follow screening test (Social friend screening).

The model includes a time-lag of τ_N days between the day a person is found to be infected and the day their partners or friends are notified.

Rescreening: A common practice in disease control is rescreening. People found to be infected are given a treatment and asked to return after a short period to be tested again. In our model, we assume that a fraction, σ_r , of the treated people return for retesting τ_R days after treatment.

The Figure (4.9) shows the diagram of above explained biomedical interventions.

² When we say social friends we mean friends who are not sexual partners that is, if a person is both partner and social friend of an index case, we consider him/her as sexual partner not social friend.

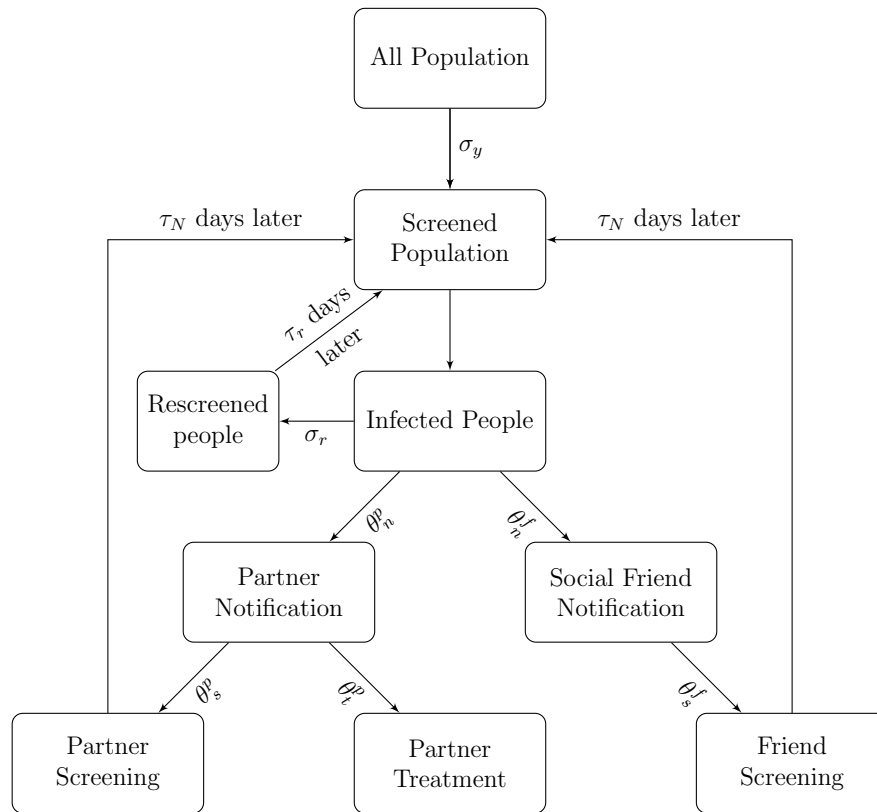


Figure 4.9: Biomedical intervention flow diagram.

4.4.3 Model initialization

Our goal is to model the current Ct epidemic in New Orleans with an initial prevalence of i_0 . Infected people are not dropped into an otherwise susceptible population, instead they are distributed as they would be as part of an emerging epidemic, one that started some time in the past. We call these initial conditions *balanced* because when the simulation starts the infected and susceptible populations, along with durations of infection, are in balance as an emerging epidemic would on average have. When the initial conditions are not balanced, then there is usually a rapid (nonphysical) initial transient of infections that quickly dies out as the infected and susceptible populations relax to a realistic infection network.

To define the balanced initial conditions, we start an epidemic in the past by randomly infecting a few high degree individuals. We then advance the simulation until the epidemic grows to the prevalence i_0 . We then reset the time clock to zero and use this distribution of infected people, complete with their current infection timetable, as our initial conditions. Because these are stochastic simulations, when doing an ensemble of runs we reinitialize each simulation by seeding different initial infected individuals. The Figure (4.10) illustrates the typical progression of the epidemic to reach the current Ct prevalence of 9% in men and 14% women in the 15–25 year-old New Orleans AA community. The numerical simulations comparing the different mitigation strategies all start at this endemic stochastic equilibrium.

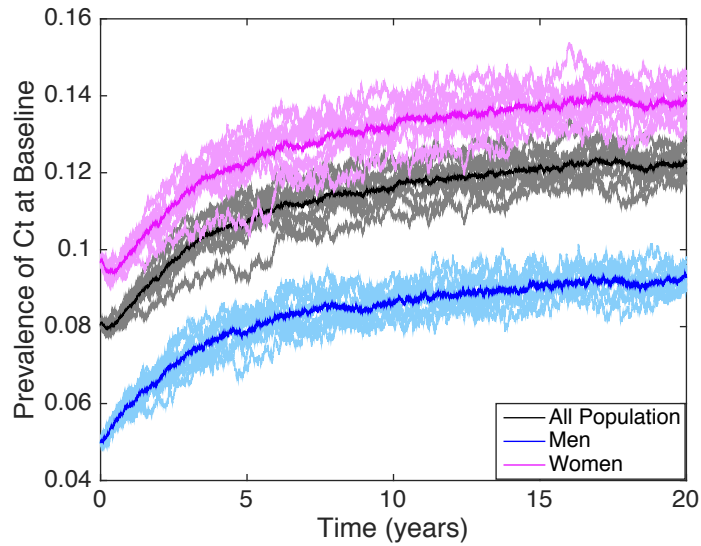


Figure 4.10: Prevalence increases to reach the current quasi-steady state. About 9% of men (blue lower curve) and 14% of women (pink upper curve) are infected at the equilibrium for the baseline model parameters. This is approximately the current prevalence in New Orleans 15-25 year-old AA population. The light areas around the dark mean values show the range of the solutions after 10 simulations.

4.5 Numerical Simulations

We compare the model-projected impact of increased random screening, partner notification- which includes partner screening and partner treatment- social friend notification and re-screening on the prevalence of Ct infection. All of the simulations start at a balanced equilibrium obtained with the model baseline parameters in Table (4.8). For probability of transmission per act, there is a wide range of reported values from 0.04 to 0.16 in different studies [45, 72–76]. We calibrated this parameter to the current prevalence of Ct among adolescents and young adult AAs in New Orleans [67], and found out our estimated value is close to corresponding parameter in [45, 77]- in which probability of transmission from man to woman is 0.16 and from woman to man is 0.12 and prevalence is 12%.

	Parameter	Description	Unit	Baseline
Network	P	Number of nodes in SexNet .	people	15000
Parameters	α_m	Sexually active age range for men.	years	[15, 25]
	α_w	Sexually active age range for women.	years	[15, 40]
Disease	β^{m2w}	Probability of transmission per act from men to women.	–	0.16
Parameters	β^{w2m}	Probability of transmission per act from women to men.	–	0.16
	$1/\gamma^n$	Average time to recover without treatment.	days	365
	$1/\gamma^s$	Average time to recover with treatment.	days	7
Intervention	κ	Fraction of times that condoms are used during sex.	–	0.6
Parameters	ϵ	Condom effectiveness.	–	0.90
	$\sigma_y^m(\sigma_y^w)$	Fraction of men(women) randomly screened per year.	–	0.05(0.40)
	σ_r	Fraction of infected people return for rescreening.	-	0.10
	$\theta_n^p(\theta_n^f)$	Fraction of the partners (friends) of an infected person who are notified and do test or treated for infection.	-	0.26(0)
	θ_t^p	Fraction of notified partners of an infected person who are treated without testing.	-	0.75(0)
	$\theta_s^p(\theta_s^f)$	Fraction of notified partners (friends) of an infected person who are tested and treated for infection.	-	0.25(0)
	τ_N	Time lag of partner notification.	days	5
	τ_R	Time lag of rescreening.	days	100

Table 4.8: Parameters and their baseline values: the model parameters describing the transmission of Ct infection, as well as recovery associated with natural recovery, and interventions were obtained from the literature [41, 67, 78], but other parameters are calibrated to biological, behavioral, and epidemiological data from general heterosexual population resides in New Orleans.

4.5.1 Dynamic of Ct on networks

To determine the impact of social network in sexual partner selection on spread of Ct, we compared the prevalence versus time for networks with different structures: networks in which people select their sexual partners from different sources. We want to observe whether different network properties mentioned in Section 4.3.1 causes a drastic difference on prevalence of Ct, and we hope not. Otherwise, it means that we cannot predict Ct preva-

lence, because there exist some parameters in generating network that are not preserved but has key role in the spread of infection. Thus, we introduced infection over different networks and let them spread till they converge to quasi-steady state³. Figure 4.11(a) is Ct spread over time for five different sexual networks: 20%, 40%, 60%, 80% and 100% subgraph of social network. Each curve correspondent to different network is the average of 50 runs where each run initialized by seeding same initial balanced infected individuals. The progression of Ct over time for these networks is not exactly the same, however they are slightly close to each other, the maximum difference of prevalence at quasi-steady state is less than one percent. Therefore, we can conclude that Ct prevalence has a mild dependence on sexual partner source. For this work we can ignore this dependence, however to have a better estimation on network structure, the question about source of partner selection from participants is needed. From now on for all the simulations, we use the sexual network which is 80% subgraph of social network, unless stated otherwise.

To find probability of transmission per sexual act β , we calibrated it to current Ct prevalence of 9% in men and 14% women in the 15–25 year-old New Orleans AA community. The Figure 4.11(b) illustrates the typical progression of the epidemic to reach this current Ct prevalence.

4.5.2 Analysis of infected population at quasi-steady state

The structure of sexual network plays an important role on the spread of infection and the status of infected people at quasi-steady state. To implement a proper intervention strategy, we look at the properties of infected people at quasi-steady state. These properties tell us about the highest risk people in network. We compare degree, betweenness and closeness centrality⁴ of infected people at quasi-steady state.

Each panel of Figure (4.14) compares different centrality score of all people and infected

³ In stochastic SIS model the steady state is disease free equilibrium point i.e if we run the model we eventually reach zero infection point even if $\mathcal{R}_0 \geq 1$, the amount of \mathcal{R}_0 affect the time to reach 0 infection point. Here saying quasi-steady state we mean that we run the simulations for a big enough time and we stop it if the average of simulations for the next day after final time is relatively close to average of prevalence for the final day.

⁴ These centralities are defined in Appendix (A)

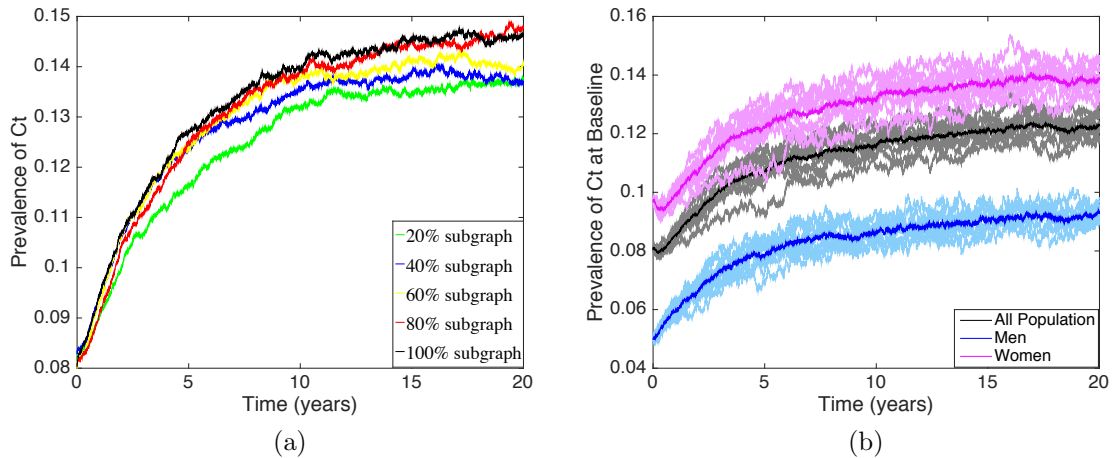
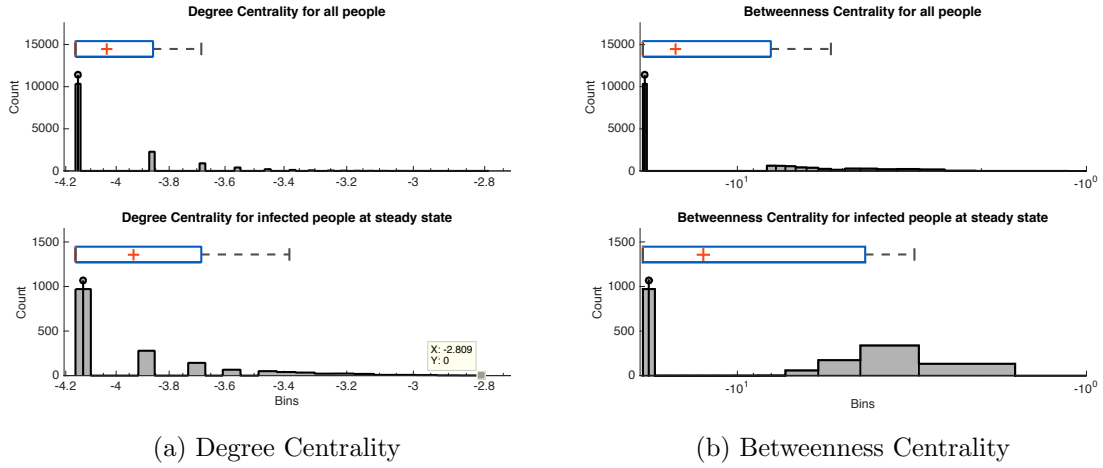


Figure 4.11: (a) Comparison of effect of different networks on Ct prevalence: Ct at quasi-steady state is mildly dependent on sexual partner source. There is less than one percent difference on Ct prevalence on different networks. (b) Ct prevalence at baseline values: about 9% of men (blue lower curve) and 14% of women (pink upper curve) are infected at the converging point for the baseline model parameters. The light areas around the dark mean values (mean is average of 50 different stochastic simulations) show the range of the solutions for only 10 simulations.

people at quasi-steady state. The panels 4.12(a) and 4.12(b) suggest that people with higher degree score (ones with many partners), or with higher betweenness score (people who are in the shortest path between many other people) are not necessarily at higher risk of infection, because the distribution of degree and betweenness centrality for all people and infected people are the same. In panel 4.12(c) we observe different distribution shape for all people and infected people at quasi-steady state: most of infected people at quasi-steady state are from people with higher closeness centrality scores (individuals who are reachable for many other people in network by a path).

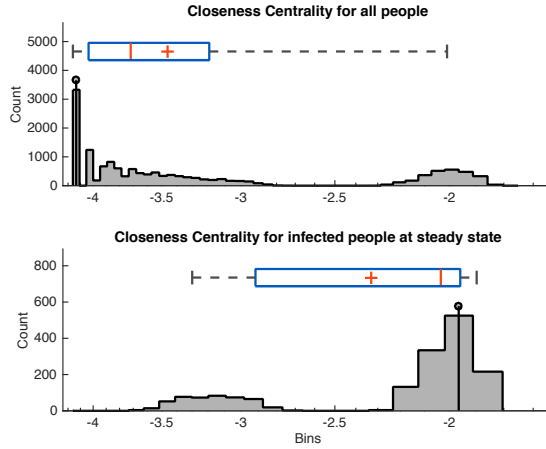
This information suggests us that people with higher and faster reachability are at higher risk of infection. We explain this result in schematic Figure (4.13): in this network node **i** has 5 neighbors and reaches total 5 nodes in the network, but node **j**, in spite of having fewer neighbors, reaches 9 other nodes in the network and therefore, is at higher risk for catching or transmitting the infection.

That means individuals who are close to too many other people in the network are good candidates to be tracked by public health staff. But there is no clue about reachability of



(a) Degree Centrality

(b) Betweenness Centrality



(c) Closeness Centrality

Figure 4.12: (a) **Degree Centrality**: the degree distribution for all people and infected ones have the same trend, thus, degree centrality score is not key parameter in infection spread. (b) **Betweenness Centrality**: the betweenness distribution for all people and infected ones have the same trend, thus, betweenness centrality score is not key parameter in infection spread. (c) **Closeness Centrality**: most of infection at quasi-steady state is clustered on people with high closeness score, that is, people with high reachability are at higher risk of infection.

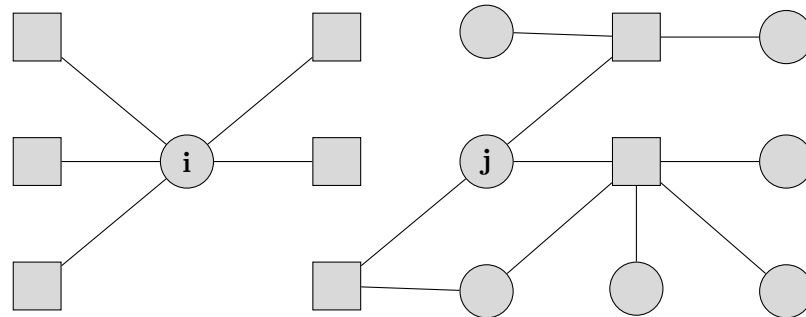


Figure 4.13: An example to compare degree and closeness scores for two typical nodes: node *i* has higher degree ($de(i) = 0.33$) than node *j* ($de(j) = 0.2$) but reaches fewer nodes (5) than *j* (9), therefore, *j* is at higher risk of infection than *i*.

a typical person. The only information we can ask individuals is about their number of partners (their degree) or the number of partners of partners. Thus, the first question may come in mind is that if there is any correlation between degree and closeness score of a node. The Figure 4.14(a) is the scatter plot of degree and closeness score of people in our sexual network. The Figure does not show any correlation between degree and closeness of people in sexual network.

To have a deeper look into relation between degree and closeness scores, we plot the distance-reachability cumulative distribution for each group of people with k partners in Figure 4.14(b): the point (x, y) in each curve shows the average probability of reaching y fraction of population within at most x steps. For example on average a person with 15 partners reaches to 12.5% of whole population within at most 20 steps or through people who are at most in distance 20 of him/her. For the networks with homophily in the degree, it is obvious that this distance-reachability cumulative distribution for higher degree individuals should move faster and reaches more people. In sexual network, for most of the degree groups we observe this pattern, however, for some high degree groups we see opposite pattern. For example curve for people with 15 partners grows faster and reaches more in compared with the curve for people with 16 partners.

This plot is for just one sexual network, but we should not fool ourselves based on one network. We generated 30 sexual networks and then for each of these networks we evaluated the fraction of population in each degree group can reach within 20 steps. The Figure 4.14(c) shows the result: each point (x, y) corresponds to one sexual network and tells that on average a person with x partners reaches y fraction of population within at most 20 steps. The red curve is smoothing spline fitted to the circle data. The large fluctuation for large degree x is because of paucity of people with high number of partners. The Figure tells that for lower risk people (people with few or moderate amount of partners) there is a linear correlation between degree and reachability, that is, when people increase their number of partners they can reach higher fraction of sexually active population. However, increasing the number of partners to 10 or more, the reachability fraction converges to a constant value 0.03 meaning that no matter how many partners a person has, he/she cannot

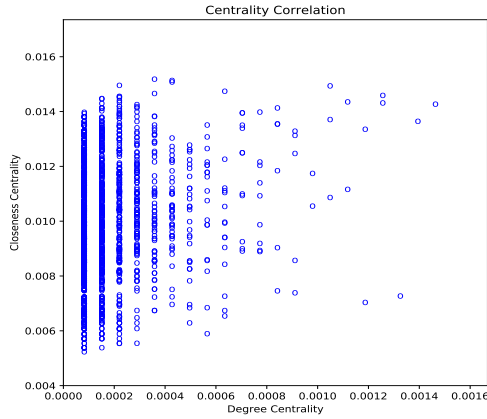
reach more than 3% of whole population within at most 20 steps. That is, to find proper person for screening- person with a high chance of carrying infection- the number of partner he/she may have matters if they have less than 10 partners. In other words, for people with degrees in range $[1, 10]$, more partner means reaching more people in the network which causes higher risk of catching Ct infection. But people with more than 10 partners reach the same fraction of population, therefore, there would not be any screening liability among them. This observation is similar to the result in Chapter (3) that studied the impact of condom-use in controlling Ct. In that works, we observed that there is a threshold for the impact of number of partners on risk of catching infection: individuals with number of partners more than a threshold value have the same risk of infection no matter how many times they use condom.

This result may not provide an intervention strategy by prioritizing individuals based on some criteria other number of partners for screening. However, it can be used in consulting individuals about their risky sexual behavior like number of partners: to reduce their risk of infection they have to keep their number of concurrent sexual partners less than some threshold value.

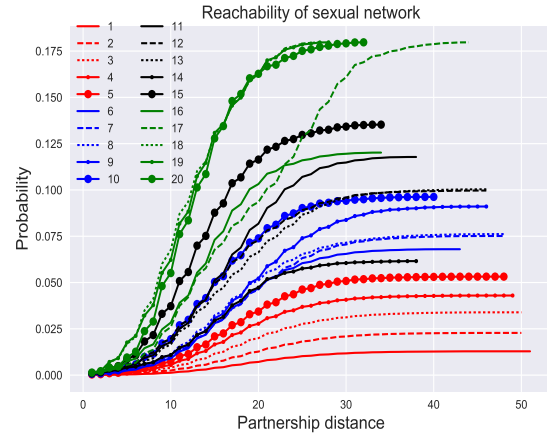
4.5.3 Mitigation efforts for controlling chlamydia

We compare the model-projected impact of increased random screening, partner notification – which includes partner screening and partner treatment – social friend notification, and rescreening on the prevalence of Ct infection. All of the simulations start at a balanced equilibrium obtained with the model baseline parameters in Table (4.8).

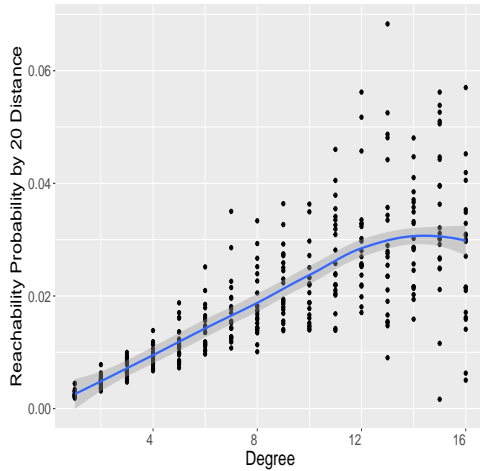
Random Screening: the fundamental component of our bundled intervention is screening men for Ct to reduce infections in population. An expert panel, convened in 2006 by the CDC, concluded that evidence is insufficient to recommend routine screening for Ct in sexually active young men because of several factors such as feasibility, efficacy, and cost-effectiveness, however, since then, evidence of the benefit of screening young men for Ct in high prevalence areas has been mounting including that it can be cost-effective and can



(a) Degree vs Closeness Centrality



(b) Distance-Reach Distribution



(c) Reachability probability within 20 distance

Figure 4.14: (a) Degree versus closeness centrality: the closeness score of people does not correlate with their degree. (b) **Distance-Reach distribution**: for degrees less than or equal to 10 the graph move faster and reaches more people as degree increases, for higher degrees we cannot see any trend which is because of paucity of people with that number of partners. (c) **Reachability probability within 20 distance**: for small and moderate degree individuals reach more people as they increase their number of partners, for high degree the fraction of reachable population tends to a constant value that is, when the degree is very high (10 or more for this set of data) that risk of Ct infection loses its dependence on the number of partners.

make an impact on rates among women [79,80]. Therefore, we consider screening the other part of the sexual network (i.e. men). Our model can provide information on how much of the intervention for men is needed for impact on Ct rates. To find men for screening we follow a venue-based screening approach: since most Ct infections are asymptomatic and young men are unlikely to seek traditional health care, a community rather than a clinic based approach is likely to reach more at risk AA men [67,81,82].

To determine the effectiveness of increasing the number of men screened for Ct per year, we compare the quasi-stationary state prevalence by varying the fraction of men who are screened randomly each year, σ_y^m . The current screening rate for young men for Ct in high prevalence areas, like New Orleans, is low. This scenario can estimate the cost effectiveness of increased screening of young men on the Ct prevalence in women [79,80]. The Figure 4.19(a) shows a reduction in the overall Ct prevalence and the Figure. 4.19(b) shows a reduction in Ct prevalence for different genders as the number of men randomly screened for Ct increases from 0 to 50%, $0 \leq \sigma_y^m \leq 0.5$. The filled circles are the mean of 50 different stochastic simulations and error bar are the 95% confidence intervals. The least-square linear fit suggests that the steady-state Ct prevalence will decrease by 0.01 for every additional 10% of the men screened during a year. Though a drop of five percent in prevalence is an admirable decrease, increased screening alone would not be sufficient to control Ct.

Rescreening: The rescreening scenario targets two goals: first finding the time-lag for rescreening, and second quantifying the impact of rescreening on prevalence of Ct:

1. Interval for rescreening

People who are found to be infected are more likely to be reinfected in the future. Repeated Ct infection can be the result of treatment failure, sexual activity with a new partner, or being reinfected from an existing infected partner. It makes sense to ask the infected people who were treated to return in a few months for retesting. We will use the model to compare the rates of reinfection to help optimize the time, τ_r , from treatment to rescreening.

The time τ_r for rescreening should be long enough so it is likely that the person will

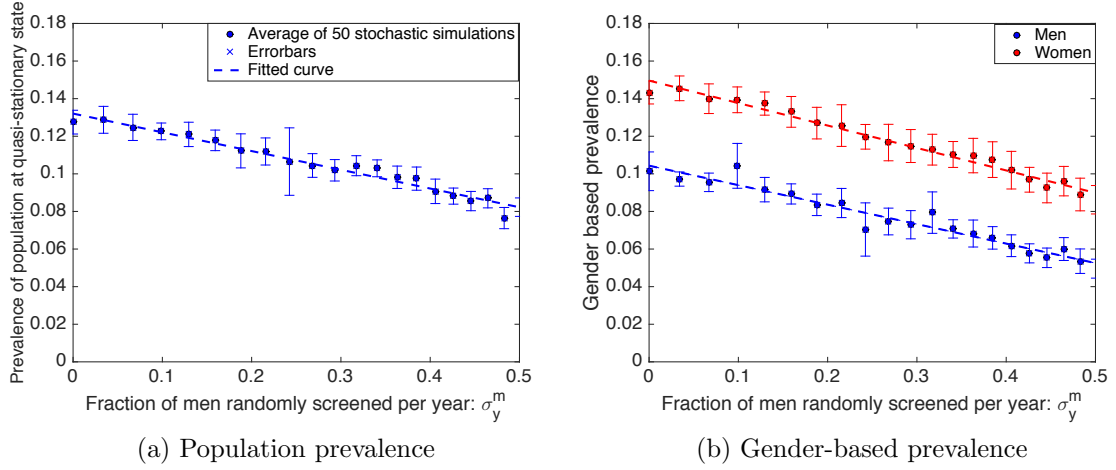


Figure 4.15: Quasi-stationary state prevalence decreases as more men are screened each year. σ_y^m : a low negative correlation, screening men randomly by 50% reduces prevalence by 5% which is not effective enough to implement as a sole intervention.

be reinfected, but not so long that such a reinfected person could infect significantly more people. We start by identifying the rescreening time when the prevalence for the treated population exceeds the prevalence for the whole population. That is, it becomes cost effective to rescreen when over 15% of previously screened people are again infected. To find this optimal time, we compute the time taken between screening time and next reinfection time for all individuals in the network assuming there is no rescreening i.e $\sigma_r = 0$. On average at baseline 12% of individuals are infected, therefore, through random screening, 12% of infected individuals are found. The current CDC guidelines recommend that people are rescreened for infection three months after treatment [83].

In our model, a person may be screened and be reinfected multiple times. Therefore, we count the number of tests and reinfection events rather than the number of individuals with a test and infection.

We plot cumulative distribution of time between screening and reinfection events in Figure (4.16). Past studies have observed that about 25% of the rescreened people are again found to be infected by three months. The Figure demonstrates that in our model also predicts that about 25% of treated individuals are again infected

after 100 days. Although the model supports the CDC guideline as reasonable, the time between treatment and rescreening could be shortened to two months with an improved impact.

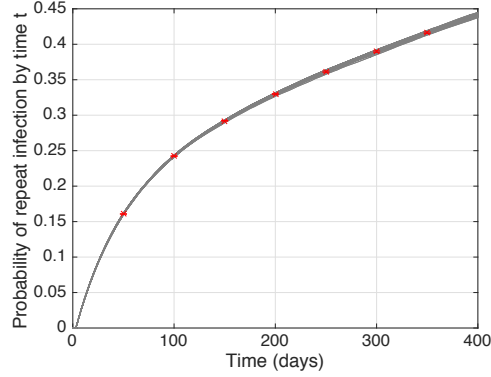


Figure 4.16: Truncated cumulative probability distribution of time between treatment and reinfection with Ct: fifty different curves from 50 stochastic simulations and 95% confidence interval are shown in this figure. About 25% of the treated people are again infected after 100 days. This increases to about 45% are reinfected after almost a year.

2. Rescreening rate

The secondary goal of rescreening scenario is to determine if rescreening for Ct infection at a larger rate would be successful in reducing its prevalence. At the baseline case only 10% of screened individuals return for rescreening. We assume a $0 \leq \sigma_r \leq 1$ fraction of screened individuals participate in a rescreening plan 100 days after their current screening day. The Figure (4.17) quantifies the prevalence of Ct at quasi-stationary state dependent on rescreening rate σ_r : there is a negative correlation between prevalence at quasi-stationary state and σ_r when σ_r fraction of screened individuals returns for rescreening, if σ_r fraction of screened individuals follow screening again then the prevalence reduces roughly by $0.02\sigma_r$.

Partner Notification: this scenario of partner notification quantifies the impact of giving an infected person's partners a chance to be tested and treated. We define θ_n^p as the fraction of infected person's partners who are notified that they might be infected. We then assume that only θ_t^p fraction of those notified partners are treated, without testing (partner treatment), and θ_s^p fraction are tested and if necessary, treated (partner screening). Note that the fraction $1 - \theta_n^p$ fraction of the partners are not notified.

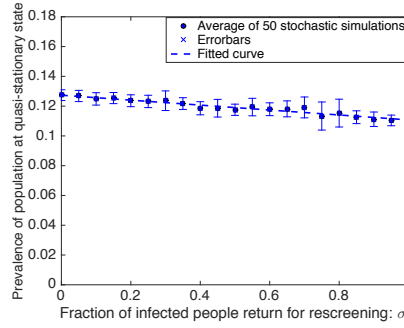


Figure 4.17: Quasi-stationary state prevalence of population versus the fraction of treated people who come back for screening, σ_r : the circles are the mean of 50 different stochastic simulations and error bars are 95% confidence intervals. Rescreening all the infected people reduces prevalence by 2%.

1. Partner treatment

In partner treatment we assume when someone is found to be infected the fraction θ_n^p of their partners are notified and then all of the notified partners will seek treatment without testing, in other words, we define $\theta_t^p = 1$. The Figure (4.18) shows the impact of partner treatment ranging from no notified partners treated, $\theta_n^p = 0$, to all notified partners treated, $\theta_n^p = 1$. The filled circles are the mean of 50 different stochastic simulations and error bars are 95% confidence intervals. The least-square linear fit suggests that the quasi-stationary state Ct prevalence will decrease by 0.07 for every 10% increment in the fraction of notified partners seeking treatment. This practice, although common in disease control today, is not as effective as partner screening as we will see.

2. Partner screening

To quantify the impact of screening the partners of an infected person, where partners are tested then treated if found to be infected, we assume that all notified partners of an infected person are screened, that is, we assume $\theta_s^p = 1$. The Figure (4.19) shows the impact as θ_n^p varies from 0 to 1. The filled circles are the mean of 50 different stochastic simulations and error bars are 95% confidence intervals. The logistic curve fit suggests that there is a threshold effect (tipping point) at $\theta_n^p \approx 0.4$, when the approach becomes extremely effective. This happens when the partner

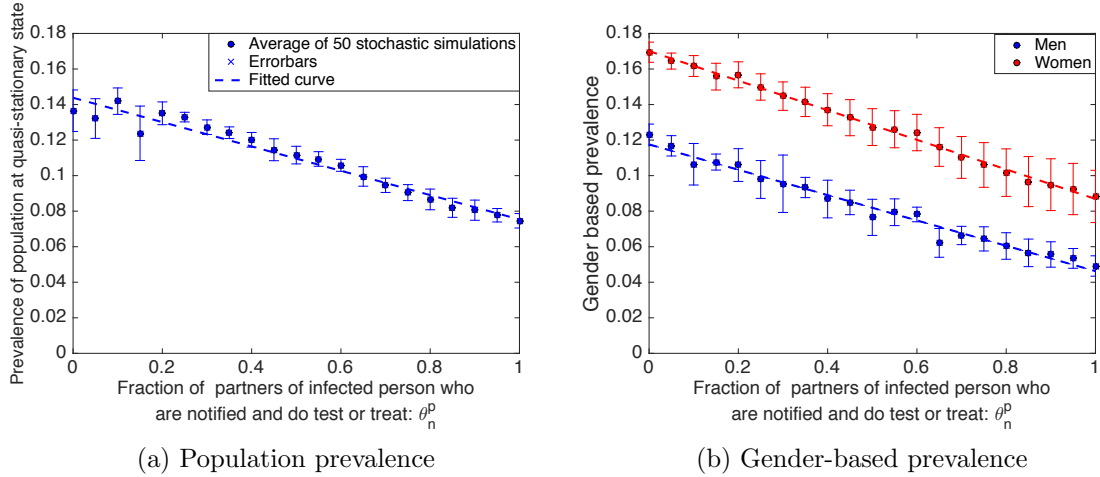


Figure 4.18: Prevalence decreases as the more partners are treated after being notified that they might be infected. In these simulations, we assume that all the notified partners are treated, without testing $\theta_t^p = 1$. This approach is only mildly effective and the prevalence remains high (8%), even when all the partners of treated people are treated.

screening percolates through the sexual network to identify the infected individuals.

Our model indicates that this is by far the most effective approach for bringing the epidemic under control.

3. Partner treatment and screening

In reality, some of the notified partners will seek treatment without testing, and some will allow themselves to be tested before being treated. We quantify the effectiveness of this mixture of the two previous scenarios by varying fraction of the partners taking action ($\theta_n^p = 0.10, 0.20, 0.50, 0.65$ and 0.80), along with the fraction of these notified partners that seek just treatment (θ_t^p) and the fraction being screened for infection ($\theta_s^p = 1 - \theta_t^p$).

When few partners are notified and take action (θ_n^p is small), then partner treatment and partner screening have almost the same impact on controlling the prevalence. For example, for $\theta_n^p = 0.10$, the prevalence versus $\theta_t^p = 1 - \theta_s^p$ is almost flat, that is, there is no difference between cases if partners follow treatment without testing or first test and then treat if infected.

As θ_n^p increases the partner screening becomes a highly successful mitigation policy.

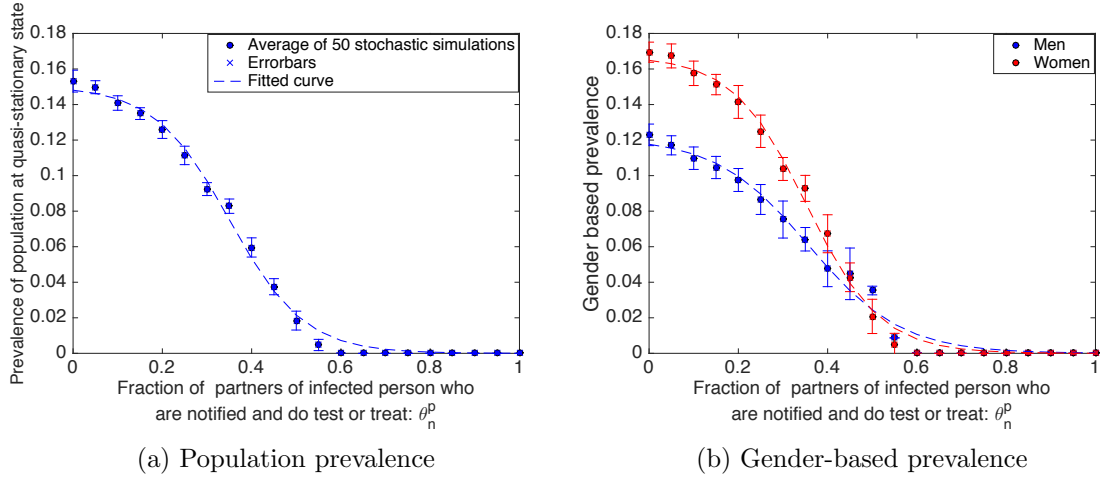


Figure 4.19: Prevalence drops to zero as the fraction of the partners of treated people are tested before possible treatment. In these simulations we assume that all of the notified partners are tested for infection, $\theta_s^p = 1$. This partner screening approach is highly effective if the fraction of tested partners, θ_n^p , exceeds its critical value $\theta_n^* = 0.4$. That is, when $\theta_n^p \geq \theta_n^*$ and $\theta_s^p = 1$, the Ct prevalence rapidly decays to zero.

Consider the case when half of the partners are notified and take action, $\theta_n^p = 0.5$, and half of them are screened for infection, $\theta_s^p = 0.5$, and the other half are treated without testing, $\theta_t^p = 0.5$. That is, half of an infected person's partners do nothing, the fraction $\theta_n^p \theta_t^p = 0.5 \times 0.5 = 0.25$ are treated without testing for infection, and the fraction $\theta_n^p \theta_s^p = 0.5 \times 0.5 = 0.25$ are tested and treated if found infected. If any of the tested notified partners of the infected person are found to be infected, their partners are then notified and the cycle repeats to spread out and identify more infected people. This conditional percolation of screening through the sexual network is why this policy is so effective. For this case, the prevalence reduction is 7%. Thus, compared with if all the notified partners follow treatment without testing, $\theta_t^p = 1$, which reduces the prevalence by only 1%, it works better. But compared with if all the notified partners follow test and treat if necessary, $\theta_s^p = 1$, which reduces the prevalence by 11%, this combined scenario is not the one to select, Figure (4.20).

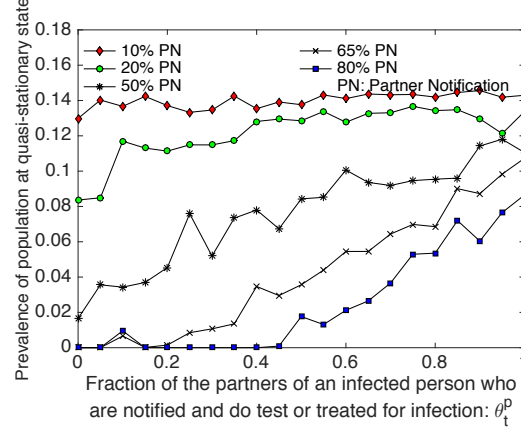
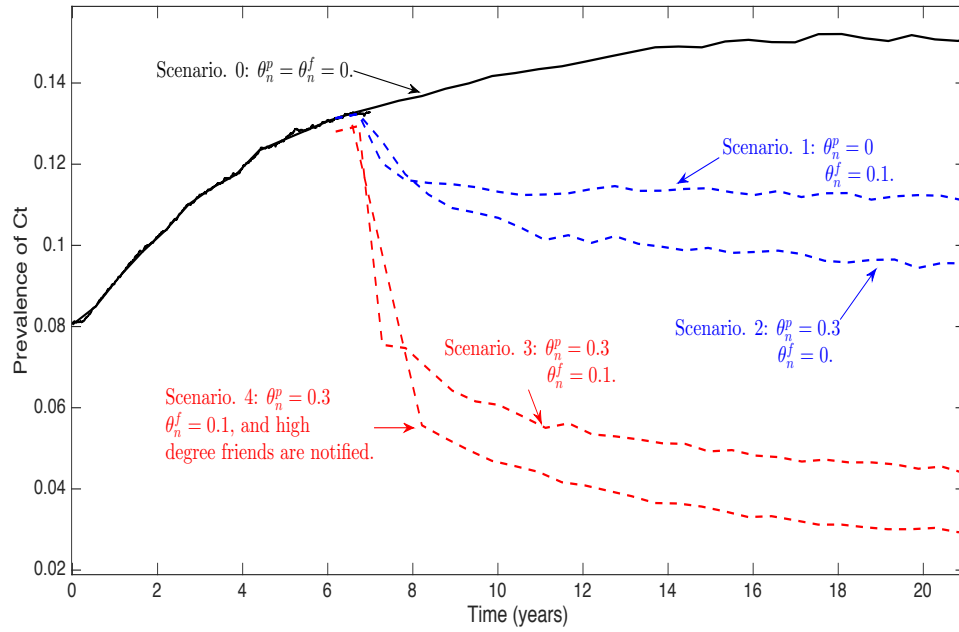


Figure 4.20: Prevalence at quasi-steady state increases when the fraction of partners notified are treated and not tested: when only a few partners of an infected person are notified, θ_n^p is small, then partner treatment and partner screening have similar small impact on Ct prevalence. When more partners of infected people take action, θ_n^p increases, then the partner screening strategy is more effective in controlling the infection.

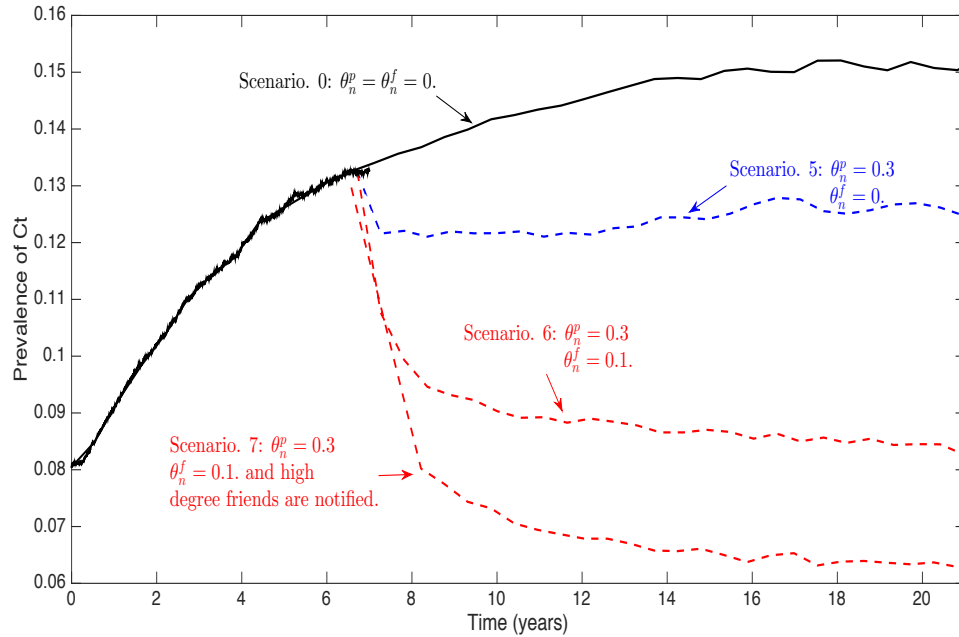
It is important to note that partner screening is more expensive than partner treatment. Given this last scenario, this suggests that when the fraction of partners we are able to notify, θ_n^p , is small then partner screening may not be a good strategy compared to partner treatment. However, if a large enough fraction of partners are notified then it is better to test and treat (partner screening) to control the spread of Ct effectively.

Social Friend Notification: up to now we have implemented several different Ct interventions and concluded that partner screening along with random screening was the effective approach in controlling Ct epidemic. Here we compare both their partner screening and partner treatment with Social Friend Screening and a combination of partner and social friend notification. We have several scenarios explained in Table (4.9).

The Figure 4.21(a) shows prevalence of Ct in time for scenarios 0-4, and the Figure 4.21(b) corresponds to scenarios 5-7. Currently at baseline case 26% of sexual partners of an screened infected person are notified, which some fraction of them do screening test and the rest treat themselves without testing [67]. However, in our first scenario, we assume nobody is notified, neither sexual partners nor social friends that is, $\theta_n^p = \theta_n^f = 0$, the black curve is the prevalence in absence of notification which end up with around 16% prevalence. Seven



(a) Partner screening



(b) Partner treatment

Figure 4.21: Prevalence of Ct v.s time for scenarios 1-7: (a) the impact of combination of sexual partner notification and social friend notification along with screening is the summation of impact of partner notification and friends notification when notified individuals follow screening. Revised scenario by notifying friends with high number of partners has 2% improvement in compare with non-modified version (red curves). (b) The impact of notification along with combination of sexual partner treatment and social friend screening is also the summation of impact of partner treatment and friends screening. Revised scenario by notifying friends with high number of partners has 2% improvement in compare with non-modified version (red curve)s.

Scenario	Description
Scenario. 0	There is no notification, i.e $\theta_n^p = \theta_n^f = 0$.
Scenario. 1	30% of sexual partners are notified and follow screening, i.e $\theta_n^p \times \theta_s^p = 0.3$ and $\theta_t^p = 0$.
Scenario. 2	10% of social friends are notified and follow screening, i.e $\theta_n^f \times \theta_s^f = 0.1$.
Scenario. 3	Scenario. 1 and Scenario. 2 .
Scenario. 4	Scenario. 1 and Scenario. 2 , such that the social friends who are notified and follow screening are from individuals with high number of sexual partners.
Scenario. 5	30% of sexual partners are notified and follow treatment, i.e $\theta_n^p \times \theta_t^p = 0.3$ and $\theta_s^p = 0$.
Scenario. 6	Scenario. 5 and 10% of social friends are notified and follow screening, i.e $\theta_n^f \times \theta_s^f = 0.1$.
Scenario. 7	Scenario. 6 , such that the social friends who are notified and follow screening are from individuals with high number of sexual partners.

Table 4.9: Different notification scenarios: in all these scenarios all other parameters are defined as in Table. (4.8), unless stated otherwise.

years after starting the infection epidemic, we implement different notification scenarios: first, infected individual found through screening notifies only some fraction of their sexual partners, and these notified partners follow screening, that is $\theta_n^p \theta_s^p = 0.3$. This scenario decreases the prevalence to the half which is highly effective. What if infected individual found through screening notifies their social friends instead. We assume they notify some fraction of their social friends and these social friends follow screening, that is $\theta_n^f \theta_s^f = 0.1$, which this reduces the prevalence to 10%. When we combine these two previous scenarios, that is, when infected individual found through screening notifies some of their sexual partners and some of social friends, the prevalence reduction becomes the summation of two sole notification scenarios, the red stard curve. The forth scenario is a modification of social friend notification: usually the sexual partners of infected person are more probable to follow screening than social friends, because their partner who had sex with is infected thus, they have a chance of carrying infection, the notified social friends may follow screening if they have too many sexual partners themselves. Therefore, in the forth scenario we assume notified social friends who follow screening are the ones with highest number of

sexual partners. Doing so the prevalence reduces to 3% which means there would be 13% improvement in compare with no notification or 9% improvement in compare with the current Ct prevalence in New Orleans.

Sexual partners of an infected individual are at a high risk of being infected, therefore, they may be advised to follow treatment without being tested. This is the reason behind the scenarios 5-7. In the fifth scenario we assume infected individual found through screening notifies only some fraction of their sexual partners, and these notified partners follow treatment that is, $\theta_n^p \theta_t^p = 0.3$. By this intervention prevalence at steady state becomes 12%. In scenario. 6 beside sexual partners, an infected person found through screening notifies his/her social friends i.e $\theta_n^f \theta_s^p = 0.1$ which reduces prevalence to 8%, and even by revised social friend notification we can reduce it 2 more percent, scenario. 7.

All these improvements in scenarios 1 – 7 can be seen after almost five years of implementing them.

4.6 Discussion and Conclusion

In this chapter after reviewing sexual activity data from a pilot study, we used the algorithms in Appendices (A) and (B) to generate an ensemble of heterosexual network with a prescribed degree and joint-degree distribution in and out of social context. We used heterosexual behavior survey and Ct prevalence data for adolescents and young adult AA population in New Orleans to create a stochastic, Monte Carlo - Markov Chain, agent-based bipartite sexually transmitted disease-transmission network model. In the model, men and women are represented by the network nodes and sexual partners are characterized by edges between the nodes. The edges between partners in the network dynamically appear and disappear each day depending if the individuals have sexual act on that day. The joint-degree distribution of the network captures the correlation of an individual's risk (their number of partners) with their partner's risk (number of partners of their partners). Our network model is updated each day to account for sexual acts as a dynamic variable. We use this model to quantify the impact of increasing screening of men for infection, partners

notification, social friend notification , and rescreening of treated individuals on reducing Ct prevalence.

In analysis of the properties of ensemble of generated heterosexual networks, we observed a tight distribution in the number of connected components and size of giant component and bi-component for all the networks which have the same joint-degree distribution and have the same percentage of edges in social network. Preserving joint-degree distribution, when the property of being subgraph of social network becomes stronger the size of giant component increases, and consequently the number of connected components decreases, which it is because of reducing the mixing in generating sexual network: when people select their sexual partners from their social friends they stand in a tight group within social network. Redundancy coefficients for networks increases as dependence of sexual network on social one rises, which is because of high clustering coefficient of social network. We studied these measures of networks because they may affect the spread of infection through network. However, none of the mentioned measures affects the spread of Ct over the network: the prevalence of Ct over networks in different groups are close to each other and therefore, ignorable.

Spreading infection over the network in absence of any type of intervention, we studied some properties of infected population at quasi-stationary state such as their degree, betweenness, and closeness scores. Our result show that people who are closer to more many other individuals in population are at higher risk of catching infection, even though he/she has a few number of partners. In network science terminology if there is a path between an individual and many other people in the network then shorter the path, higher his/her closeness score, and therefore, higher risk of Ct infection he/she has. This information can help us to identify more qualified people for random screening by relating individual's degree and closeness score. At the first glance, we did not observe any correlation between degree and closeness score, that means a person with high number of partners may not be necessarily at high risk of Ct infection. But, studying the relation between degree and reachability (how much they can reach other people in population) of individuals for an ensemble of heterosexual networks, we observed that reachability probability increases to a

fixed point as degree increases. That is, up to some degree value, increasing degree causes that reachability of a typical person and therefore, its closeness increases, which this puts him/her at higher risk of Ct infection. However, when this correlation converges to its fixed point, the impact of degree as a risk of Ct infection for a person disappears.

In intervention strategies the first approach was screening men. We observed that increasing Ct screening of men has a modest impact on reducing Ct prevalence in the young adult AAs in New Orleans, the Figure (4.15). Starting at a baseline of 13% prevalence under the assumption that 45% of the women are being screened each year for Ct, then increasing the screening of men from 0% to 50% would only reduce the overall Ct prevalence to 8%. Linking our result with [42] that found partner positivity is insensitive to screening, we found out that screening men alone cannot control epidemic in population and consequently among women drastically.

In evaluating the effectiveness of partner notification we assumed that a fraction of the partners of an infected person will seek treatment (without testing) or be screened (tested and treated) for infection. We observed that if most of the notified partners are treated, without testing, then this mitigation has only a modest impact on Ct prevalence. This practice, although common in disease control today, is not as effective as partner screening. When the partners of an infected person were tested before treatment, there was a tipping point where partner screening would bring the epidemic under control. That is, when over 40% of notified partners of all the infected people are screened for infection, then the Ct prevalence rapidly decreased to very low levels, the Figure (4.20). This critical threshold represents the partner screening level where a contact tracing tree can spread through the heterosexual network to identify and to treat most of the infected people. Our model indicates that this is by far the most effective approach for bringing the epidemic under control.

However, partner screening is more expensive than partner treatment. The partner treatment and screening suggests that when the fraction of partners took action (θ_n is small), then partner screening may not be a good strategy compared to partner treatment. But if a large enough fraction of partners are notified then it is better to test and treat

(partner screening) to control the spread of Ct effectively. These results of impact of partner notification are close to results from [43] who found for Ct, contact tracing is less effective at lower percentages when partners are treated, but with increasing levels of contact tracing it will be a highly effective intervention strategy.

Using social network in generating sexual networks and in studying the spread of STIs not only enable us to construct a more realistic sexual network but also helps us to improve interventions by spreading information through social network, social friend notification. Our result shows a combination of social friend notification and sexual partner notification has a significant reduction on prevalence of Ct compared with when there is no notification, or only sexual partner are notified. We studied two different approaches for notification. In the first case, infected person notifies some fraction of their sexual partners and social friends, and we assume both notified partners and social friends who take action test and treat if infected, partner and social friend screening. In the second case, infected person notifies some fraction of their sexual partners and social friends, and we assume notified social friends who take action test and treat if infected, social friend screening, and notified sexual partners who take action treat themselves without testing, partner treatment. In both cases, there is a relative 40% reduction on prevalence compared with the case only sexual partners receive notification and follow up test or treatment.

In rescreening, an infected individual returns for testing a few months after they are treated. We used the model to estimate the probability that a treated person would be reinfected as a function of the time since they were treated. The CDC guidelines recommend that treated people return for screening three months after treatment. We observed that for the baseline case of 13% infected population, about 25% of the treated population were reinfected three months after treatment. We observed that although the rescreening is a cost effective approach to identify infected people, it has only a small impact on the overall Ct prevalence. Even though there is a high chance of reinfection when the individual's behavior does not change, we do not observe an effective impact on prevalence of Ct by monitoring infected individuals. Rescreening program has a trend similar to screening, and none of them are effective as sole intervention because they are not able to find the chain of

infection like partner screening. On the other hand sensitivity of prevalence to rescreening is less than that of screening, indicating the fact that for a limited budget the idea of finding more people to screen, random screening, is more effective than frequent screening for less people.

The existence of heterosexual network with a prescribed joint-degree distribution in the context of social network is the first concern when generating the sexual network. One of our limitation is that we cannot test if a sexual network with a particular joint-degree distribution within a social network exist or not, therefore, we have to find it by trial and error. On the other hand, source of partner selection can be correlated to degree of individuals, but, in this work we ignored this correlation.

The uncertainty in the model parameters will require an extended sensitivity analysis to quantify the robustness of the predictions in the presence of uncertainty. Our future work will focus on validating the model predictions and identifying which trends and quantities can, and cannot, be predicted within limits of the model uncertainty.

Although our model includes-condom use, it does not account for behavior changes, such as increased condom-use after being treated for infection or the differences in condom-use between primary and casual partners. When we assign the type of partners for each individual in the network, we will change casual partners more frequently and will implement condom-use for contacting with casual partners. Also notification of partner strategy may be affected when people are biased about notifying partners. Collecting more data regarding partnership level will help us improve our model by distinguishing between partners. Our future research will improve the model so we can better quantify the impact of counseling and behavioral changes such as increasing condom-use or partner notification rates. We are also expanding our data analysis to include a cost-benefit analysis and estimate the averted PID cases in women.

Appendix A

Generating Bipartite Networks with a Prescribed Joint Degree Distribution

Bipartite networks can provide an insightful representation of the interactions between two disjoint groups, with applications ranging from ecological networks [84], social interactions, the spread of sexually transmitted infections, and citation/collaboration networks [85]. The accuracy of a mathematical model to understand the interactions of these networks depends on generating an ensemble of random graphs that faithfully captures the structure of the known real-world networks needed to reproduce the dynamics of the underlying problem.

When simulating a real-world problem on a network, the graph properties, such as the degree and joint-degree distributions, for the generated random graphs must be analyzed to see if they are consistent with the original problem. If any of these properties affect the questions being asked of the model, such as how fast a disease will spread among a population, then these properties must be preserved in the mathematical model. For example, social networks often exhibit homophily where there is a tendency of individuals to associate with others having similar characteristics.

This homophily is captured in the network by the joint-degree distribution, sometimes

called the degree correlation or degree-degree distribution. Although there are several methods, called 2K network generation algorithms, for generating simple graphs that preserve both a given degree and joint-degree distributions [86–91], there are few results for bipartite networks.

Typical network generation algorithms that preserve the degree distributions are based on *stochastic*, *rewiring*, or *reconfiguration* approaches. The Erdős-Rényi random graph generation algorithm [92] is an example of stochastic approach where every two nodes are connected with probability p defined by the average degree of nodes in the network divided by their size. This approach is easily generalized to match a given degree [93] or joint-degree distribution [86]. The rewiring approach rewires two random edges to preserve the average degree or degree distribution. The rewiring approach converges, although there is little analysis on the convergence rate [94]. The pseudograph reconfiguration algorithm [95] reproduces the given degree distribution exactly, however it may end up with self-loop or multiple edges between two nodes.

The joint-degree distribution is correlated with the structural and dynamical properties of networks [88–91]. This information is quantified in the symmetric joint-degree matrix (JDM) whose (i, j) element is the number of edges between nodes of degree i and nodes of degree j [96]. The necessary and sufficient condition for a simple network to exist for a given JDM is given by the Erdős–Gallai type theorem [96–98]:

Theorem A.0.1. (*Erdős–Gallai Type Theorem for JDM*) *Consider a network where M is the largest degree of the nodes in the network, then there is a simple network that has an $M \times M$ symmetric JDM if and only if*

1. $n_i = \frac{1}{i} \sum_{j=1}^M JDM(i, j)$ is the number of nodes with degree i for $i = 1 \cdots M$.
2. $JDM(i, i) \leq \binom{n_i}{2}$, for $i = 1 \cdots M$.
3. $JDM(i, j) \leq n_i n_j$, for $i \neq j$.

Mahavedan et al. [87] have extended the rewiring approach to generate random networks using joint-degree distribution. They use the term 2K-series to introduce joint-degree

distribution, and they compare stochastic, pseudograph, matching and rewiring and the extended pseudograph algorithms to construct networks using $2K$ -series. They compare the topology of networks made based on different algorithms and suggest that $2K$ -series or joint-degree distribution is enough to reproduce most metrics of interest for the network. They then use a configuration model to generate a $2K$ -network with the prescribed JDM , however their network may end up with multiple edges between two nodes.

A balanced degree invariant algorithm is provided by [96] for constructing simple networks from a given JDM , and a Monte Carlo Markov Chain method is used for sampling the networks. Gjoka et al. [99] design a new algorithm for constructing simple networks with a target JDM . Bassler et al. at [100] use JDM and develop an exact algorithm to find all pairwise degree correlations and the degree sequences.

We extend these methodologies for generating bipartite networks using prescribed joint-degree distribution. Note that the bipartite joint degree (BJD) [101] matrix of a bipartite network can be nonsymmetric and is not even a square matrix if the maximum degree in two groups are not the same. We find and prove a similar necessary and sufficient condition as Erdős–Gallai Type Theorem on BJD for constructing simple bipartite network and then use BJD matrix as an input to construct network. We then describe new bipartite algorithms for generating these random networks and investigating how well they reproduce other properties, such as the bipartite clustering, observed in real-world networks. This family of algorithms are called $B2K$ algorithms and they preserve a given degree and joint-degree distributions of the network.

A.1 Bipartite Network

A *bipartite network*, sometimes called *two-mode network* or *affiliation network*, is a network whose nodes can be divided into two disjoint sets \mathbf{v}^u and \mathbf{v}^l such that every edge connects a node in \mathbf{v}^u to one in \mathbf{v}^l , there is no edge between nodes in \mathbf{v}^u , and no edges between nodes in \mathbf{v}^l . This network is shown like $\mathbf{G} = (\mathbf{v}^u, \mathbf{v}^l, \mathbf{E})$ consisting of a set of $P^u = |\mathbf{v}^u|$ upper nodes, $\mathbf{v}^u = \{\mathbf{v}_i^u | i = 1, 2, 3, \dots, P^u\}$, a set of $P^l = |\mathbf{v}^l|$ lower nodes, $\mathbf{v}^l = \{\mathbf{v}_i^l | i =$

$1, 2, 3, \dots, P^l\}$, together with a binary adjacency relation defining the set of edges $\mathbf{E} = \{\mathbf{v}_i^u \mathbf{v}_j^l | i \in \{1, 2, 3, \dots, P^u\}, j \in \{1, 2, 3, \dots, P^l\}\}$, where $\mathbf{v}_i^u \mathbf{v}_j^l$ denotes the edge between node \mathbf{v}_i^u and node \mathbf{v}_j^l .

The *degree* of a node \mathbf{v}_i , $\mathbf{deg}(\mathbf{v}_i)$, is defined as the number of neighboring nodes connected to the node by an edge. The *degree distribution* d_k defines the number of nodes with degree k . The *joint-degree distribution* or sometimes called *degree-degree distribution* or *degree correlation* (k, j) is the number of nodes with degree j that are connected to nodes with degree k . A bipartite network \mathbf{G} can be represented by the *Bipartite Joint Degree* or *BJD* matrix:

$$BJD_G = \begin{pmatrix} e_{11} & e_{12} & e_{13} & \dots & e_{1l} \\ e_{21} & e_{22} & e_{23} & \dots & e_{2l} \\ \vdots & \vdots & \vdots & \ddots & \vdots \\ e_{u1} & e_{u2} & e_{u3} & \dots & e_{ul} \end{pmatrix},$$

where, u is the maximum degree in upper nodes, and l is the maximum degree in lower nodes, each element e_{ij} is the number of edges between upper nodes with degree i and lower nodes with degree j . The degree distribution of network \mathbf{G} is defined by the number of upper nodes, d_k^u , and lower nodes, d_k^l , with degree k :

$$d_k^u = \frac{\sum_{j=1}^l e_{kj}}{k}, \text{ and } d_k^l = \frac{\sum_{i=1}^u e_{ik}}{k}.$$

The number of nodes with degree k is $d_k = d_k^u + d_k^l$.

A *BJD* matrix is consistent with a bipartite network if there exist at least one bipartite network with this joint degree distribution. For an example, consider the *BJD* matrix

$$BJD = \begin{pmatrix} 2 & 2 \\ 4 & 0 \end{pmatrix},$$

each entry in the matrix, (i, j) , is an edge between an upper node with degree i and lower

node with degree j . There are $\frac{2+2}{1} = 4$ upper nodes with degree 1, and $\frac{4+0}{2} = 2$ upper node with degree 2, $\frac{2+4}{1} = 6$ lower nodes with degree 1, and $\frac{2+0}{2} = 1$ lower node with degree 2. On the other hand, $e_{21} = 4$ means that four of the edges of the graph will connect an upper node of degree 2 to a lower node of degree 1, or $e_{22} = 0$ means there is no edge between upper and lower nodes with degree 2.

Theorem A.1.1. *Let BJD be a matrix,*

$$BJD = \begin{pmatrix} e_{11} & e_{12} & e_{13} & \dots & e_{1l} \\ e_{21} & e_{22} & e_{23} & \dots & e_{2l} \\ \vdots & \vdots & \vdots & \ddots & \vdots \\ e_{u1} & e_{u2} & e_{u3} & \dots & e_{ul} \end{pmatrix},$$

where $d_i^u = \frac{\sum_j e_{ij}}{i}$ is the number of upper nodes with degree i , and $d_j^l = \frac{\sum_i e_{ij}}{j}$ is the number of lower nodes with degree j . If we have $e_{ij} \leq d_i^u d_j^l$ for $i = 1, \dots, u$ and $j = 1, \dots, l$, then, there exist at least one simple network, a network without self-loops or multiple edges, as defined by the BJD matrix.

Proof. Suppose the BJD matrix satisfies the assumption of theorem, and the network \mathbf{G} corresponding to BJD matrix has at most one edge between all nodes, except for two nodes, where there are two edges between the upper node \mathbf{u} of degree i and the lower node \mathbf{v} of degree j . There are d_i^u upper nodes with degree i and d_j^l lower nodes with degree j .

For the trivial case when $d_i^u = 1$ and $d_j^l = 1$, we have $e_{ij} \leq 1$ and there can not be a multiple edge between the sole node \mathbf{u} with degree i and sole node \mathbf{v} with degree j .

When either $d_i^u > 1$ or $d_j^l > 1$, then there is an upper node, \mathbf{u}' , with degree i and a lower node, \mathbf{v}' , with degree j that are not connected. This follows from the contradiction argument where if all nodes with degree i are connected to all nodes with degree j and \mathbf{u} is connected to \mathbf{v} with two edges, then $e_{ij} = d_i^u d_j^l + 1 \not\leq d_i^u d_j^l$, which contradicts the assumption of theorem. Therefore, such \mathbf{u}' and \mathbf{v}' exist. These \mathbf{u}' may be the same as \mathbf{u} or \mathbf{v}' may be the same as \mathbf{v} , but both can not happen:

- Case 1: we consider the case that \mathbf{u}' is different from \mathbf{u} and \mathbf{v}' is different from \mathbf{v} . Because \mathbf{u} is connected to \mathbf{v} within two edges, therefore, it has $i - 1$ disjoint neighbors, however, because all edges connected to \mathbf{u}' are simple, therefore, \mathbf{u}' has i disjoint neighbors, thus \mathbf{u}' has a neighbor, like \mathbf{w} , which is not a neighbor of \mathbf{u} . Also, for the same reason \mathbf{v} has $j - 1$ disjoint neighbors and \mathbf{v}' has j disjoint neighbors, thus \mathbf{v}' has a neighbor, like \mathbf{w}' , which is not a neighbor of \mathbf{v} . When this happens, then we rewire the network by first removing one of the the double edges \mathbf{uv} , as well as edges $\mathbf{u}'\mathbf{w}$ and $\mathbf{v}'\mathbf{w}'$, then adding the edges \mathbf{uw} , \mathbf{vw}' , and $\mathbf{u}'\mathbf{v}'$. Therefore, we have a simple network \mathbf{G} . The Figure (A.1) illustrates this rewiring process.

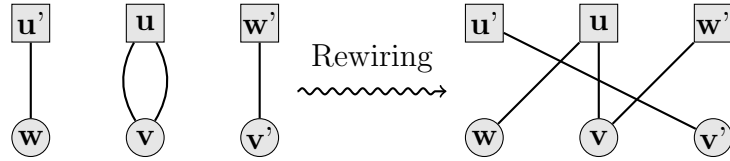


Figure A.1: Rewiring with 3 swaps: node \mathbf{u} is connected to node \mathbf{v} two times, there are nodes \mathbf{u}' with the same degree as \mathbf{u} , and \mathbf{v}' with the same degree as \mathbf{v} which are not connected. There are nodes \mathbf{w} (neighbor of \mathbf{u}' but not a neighbor of \mathbf{u}), and \mathbf{w}' (neighbor of \mathbf{v}' but not a neighbor of \mathbf{v}). We remove edges \mathbf{uv} , $\mathbf{u}'\mathbf{w}$ and $\mathbf{v}'\mathbf{w}'$, add edges \mathbf{uw} , \mathbf{vw}' , and $\mathbf{u}'\mathbf{v}'$.

- Case 2: If \mathbf{u}' is the same as \mathbf{u} , then \mathbf{v}' has to be different from \mathbf{v} , in that case, because \mathbf{v} has $j - 1$ disjoint neighbors and \mathbf{v}' has j disjoint neighbors, then \mathbf{v}' has a neighbor, \mathbf{w}' , which is not a neighbor of \mathbf{v} . Therefore, we rewire the network by removing edges \mathbf{uv} and $\mathbf{w}'\mathbf{v}'$ and adding the edges \mathbf{uv}' and $\mathbf{w}'\mathbf{v}$. The Figure (A.2) illustrates this process. For the case when \mathbf{v}' is the same as \mathbf{v} we have similar approach.

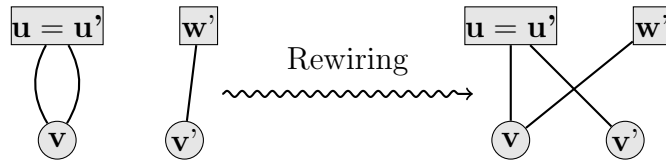


Figure A.2: Rewiring with 2 swaps: \mathbf{v}' is not neighbor of \mathbf{u} and has a neighbor like \mathbf{w}' which is not neighbor of \mathbf{v} , we remove edges \mathbf{uv} and $\mathbf{w}'\mathbf{v}'$ and add edges \mathbf{uv}' and $\mathbf{w}'\mathbf{v}$.

□

A.2 Some Definitions Related to Bipartite Network

Before designing algorithms to generate bipartite networks we define some properties for bipartite networks which are used in our network analysis.

Definition A.2.1. We define Nc as the number of connected components of the network.

Definition A.2.2. We define Sg as the size of giant component (the biggest connected component) of the network.

Definition A.2.3. The clustering coefficient for a network is the average of clustering coefficient for all nodes. The bipartite clustering coefficient for a node is a measure of local density of connections defined as [102]

$$cl(\mathbf{v}) = \frac{\sum_{\mathbf{u} \in N(N(\mathbf{v}))} c_{\mathbf{u}\mathbf{v}}}{|N(N(\mathbf{v}))|}$$

where $N(N(\mathbf{v}))$ are the second order neighbors of \mathbf{v} in network excluding \mathbf{v} , and $c_{\mathbf{u}\mathbf{v}}$ is the pairwise clustering coefficient between nodes \mathbf{u} and \mathbf{v} and defined by

$$c_{\mathbf{u}\mathbf{v}} = \frac{|N(\mathbf{u}) \cap N(\mathbf{v})|}{|N(\mathbf{u}) \cup N(\mathbf{v})|}.$$

Definition A.2.4. Redundancy coefficients Rc are measure of the degree to which nodes in a bipartite graph tend to cluster together. For a bipartite network, redundancy for a node is the ratio of its overlap to its maximum possible overlap according to its degree. The overlap of a node is the number of pairs of neighbors that have mutual neighbors themselves, other than that node [102]. For a typical node \mathbf{v} , the redundancy coefficient of \mathbf{v} is defined as

$$Rc(\mathbf{v}) = \frac{|\{\{\mathbf{u}, \mathbf{w}\} \subseteq N(\mathbf{v}), \exists \mathbf{v}' \neq \mathbf{v} \text{ s.t. } \mathbf{u}\mathbf{v}' \in \mathbf{E}, \mathbf{w}\mathbf{v}' \in \mathbf{E}\}|}{\frac{|N(\mathbf{v})|(|N(\mathbf{v})|-1)}{2}},$$

where, $N(\mathbf{v})$ is set of all neighbors of node \mathbf{v} , and \mathbf{E} is set of all edges in the network.

In graph theory and network analysis, we can identify the most important nodes within a network using centrality score of nodes. For example the most influential person(s) in a sexual network, such as super-spreaders of disease. Through centrality scores we can seek to quantify the influence of every node in the network. We define some of the most important centralities which are used widely in network analysis: degree, betweenness and closeness centrality scores.

Definition A.2.5. The first and conceptually simplest centrality is degree centrality which is defined by the number of links to a node: degree centrality of node \mathbf{v} is given by

$$de(\mathbf{v}) = \frac{\mathbf{deg}(\mathbf{v})}{N - 1},$$

where $\mathbf{deg}(\mathbf{v})$ is the number of neighbors of \mathbf{v} and N is the total number of nodes in the network. This centrality interprets the immediate risk of a node for catching or transmitting whatever is flowing through the network.

Definition A.2.6. Betweenness Centrality of a node \mathbf{v} is given by

$$bet(\mathbf{v}) = \frac{2}{(N - 1)(N - 2)} \sum_{\mathbf{u} \neq \mathbf{w} \neq \mathbf{v}} \frac{\sigma_{\mathbf{uw}}(\mathbf{v})}{\sigma_{\mathbf{uw}}},$$

where $\sigma_{\mathbf{uw}}$ is the total number of shortest paths from node \mathbf{u} to node \mathbf{w} , $\sigma_{\mathbf{uw}}(\mathbf{v})$ is the number of those paths that pass through \mathbf{v} , and N is the number of nodes in the graph. This centrality quantifies the number of times a node acts as a bridge along the shortest path between two other nodes. Therefore, the nodes that have a high probability to occur on a randomly chosen shortest path between two randomly chosen node have a high betweenness score [103].

Definition A.2.7. Closeness Centrality of a node \mathbf{v} -in a not necessarily connected network- is sum of the reciprocal of the shortest path distances from \mathbf{v} to all $N - 1$ other nodes. Since the sum of distances depends on the number of nodes in the graph, closeness is normalized

by the sum of minimum possible distances $N - 1$:

$$Clo(\mathbf{v}) = \frac{\sum_{\mathbf{u}=1}^{N-1} \frac{1}{d(\mathbf{v}, \mathbf{u})}}{N - 1},$$

where $d(\mathbf{v}, \mathbf{u})$ is the shortest-path distance between \mathbf{v} and \mathbf{u} , and N is the number of nodes in the graph [104]. In this concept the more central a node is, the closer it is to all other nodes.

A.3 Generating Bipartite Network

We introduce five *B2K* algorithms to construct simple bipartite networks for a given *BJD* matrix satisfying the assumptions of Theorem A.1.1. These algorithms are categorized as either an *edge* or *node* algorithm, depending on the network generation process. Both approaches can be used to generate an ensemble of B2K networks. However, as we will show, the statistical properties of the networks for different algorithms differ. That is, the different approaches have different biases in sampling the space of all feasible networks.

The algorithms begin by grouping nodes into upper and lower nodes and assigning each node a desired degree based on the *BJD* matrix. In the edge algorithms, we first choose an entry in the *BJD* matrix - a tuple of the desired degrees of the upper node and lower node. We find the list of pair of nodes that satisfies the conditions of the tuple. We choose one pair of nodes randomly from this list and attach the edge if one does not exist. If we cannot find a pair of nodes in the list that do not have an edge between them, we choose one at random and add a double-edge. We repeat adding edges until all edges are placed. If we attached a double-edge during the generation, we rewire the graph as described in subsection A.4. In practice, we found that the node based algorithms were more computationally expensive than the edge based algorithms.

The edge algorithms start with the unconnected list of upper and lower nodes and iteratively add new edges guided by the current state of the edges in the network:

- **Random Edge (RE):** Choose one (i,j) randomly from the *BJD*. We find a pair of

upper and lower nodes with degrees i, j respectively and add an edge between them, then update $(i, j) \rightarrow (i, j) - 1$. This process continues for each edge until the BJD becomes zero matrix.

Algorithm 1: Random Edge (**RE**)

```

while  $BJD > 0$  do
    Randomly select an element  $(i, j)$ ;
    Randomly select an upper node  $\mathbf{v}$  with degree  $i$  and  $stub(\mathbf{v}) > 0$ ;
    Randomly select a lower node  $\mathbf{v}$  with degree  $j$  and  $stub(\mathbf{v}) > 0$ ;
    Make edge  $\mathbf{uv}$ .  $stub(\mathbf{u}) \leftarrow stub(\mathbf{u}) - 1$ , and  $stub(\mathbf{v}) \leftarrow stub(\mathbf{v}) - 1$ ;
     $(i, j) \leftarrow (i, j) - 1$ .
end

```

- **Maximum Edge-Degree (ED_{\max}):** Of the remaining edges choose an edge to add from those with $max(d_{\max})$ where $d_{\max}(i, j) \stackrel{\text{def}}{=} \max(i, j)$ at random until there are no remaining edges.

Algorithm 2: Maximum Edge Degree (ED_{\max})

```

while  $BJD > 0$  do
    For remaining  $(i, j) > 0$ , find  $m$  where  $m \stackrel{\text{def}}{=} \max_{(i,j)>0} \{i, j\}$ ;
    Randomly select an element  $(i, j) > 0$  where  $i = m$  or  $j = m$ ;
    Randomly select an upper node  $\mathbf{u}$  with degree  $i$  and  $stub(\mathbf{u}) > 0$ ;
    Randomly select a lower node  $\mathbf{v}$  with degree  $j$  and  $stub(\mathbf{v}) > 0$ ;
    Make edge  $\mathbf{uv}$ ,  $stub(\mathbf{u}) \leftarrow stub(\mathbf{u}) - 1$ , and  $stub(\mathbf{v}) \leftarrow stub(\mathbf{v}) - 1$ ;
     $(i, j) \leftarrow (i, j) - 1$ .
end

```

- **Total Edge-Degree (TED):** Of the remaining edges choose an edge to add from those with $max(d_{\text{total}})$ where $d_{\text{total}}(i, j) \stackrel{\text{def}}{=} i + j$ at random until there are no remaining edges. (*Note:* we observed no statistical differences between the TED and ED_{\max}

approaches and will only present results for the ED_{\max} algorithm.)

Algorithm 3: Total Edge Degree (**TED**)

```

while  $BJD > 0$  do
    For remaining  $(i, j) > 0$ , find  $m$  where  $m \stackrel{\text{def}}{=} \max_{(i,j)} (i + j)$ ;
    Randomly select an element  $(i, j) > 0$  where  $i + j = m$ ;
    Randomly select an upper node  $\mathbf{u}$  with degree  $i$  and  $stub(\mathbf{u}) > 0$ ;
    Randomly select a lower node  $\mathbf{v}$  with degree  $j$  and  $stub(\mathbf{v}) > 0$ ;
    Make edge  $\mathbf{uv}$ ,  $stub(\mathbf{u}) \leftarrow stub(\mathbf{u}) - 1$ , and  $stub(\mathbf{v}) \leftarrow stub(\mathbf{v}) - 1$ ;
     $(i, j) \leftarrow (i, j) - 1$ .
end

```

The node algorithms start with the unconnected list of upper and lower nodes and iteratively add new edges based on current state of the nodes in the network:

- **Maximum Node-Degree (ND_{\max}):** Choose from the nodes with the highest desired degree. Choose possible edges that the chosen node could have and select appropriate neighbors. Select all of the neighbors for the chosen node, then choose another node from those with the highest desired degree. Repeat until all edges are added.

Algorithm 4: Maximum Node Degree (**ND+**)

```

while  $BJD > 0$  do
    From remaining nodes with positive stub, find the one with highest degree:
     $\mathbf{u} = \max_{deg(\mathbf{v})} \{\mathbf{v}\};$ 
    while  $stub(\mathbf{u}) > 0$  do
        if  $\mathbf{u}$  is upper node with degree  $i$  then
            From the row  $i$  of  $BJD$  matrix randomly select an element  $(i, j) > 0$ ;
            Randomly select a lower node  $\mathbf{v}$  with desired degree  $j$  and  $stub(\mathbf{v}) > 0$ ;
            Make edge  $\mathbf{uv}$ ,  $stub(\mathbf{u}) \leftarrow stub(\mathbf{u}) - 1$ , and  $stub(\mathbf{v}) \leftarrow stub(\mathbf{v}) - 1$ , and
             $(i, j) \leftarrow (i, j) - 1$ ;
        else
            From the column  $j$  of  $BJD$  matrix randomly select an element  $(i, j) > 0$ ;
            Randomly select an upper node  $\mathbf{v}$  with desired degree  $i$  and  $stub(\mathbf{v}) > 0$ ;
            Make edge  $\mathbf{uv}$ ,  $stub(\mathbf{u}) \leftarrow stub(\mathbf{u}) - 1$ , and  $stub(\mathbf{v}) \leftarrow stub(\mathbf{v}) - 1$ , and
             $(i, j) \leftarrow (i, j) - 1$ ;
        end
    end
end

```

- **Maximum Stub Minimum Node-Degree ($S_{\max}ND_{\min}$):** Find the nodes with the fewest placed edges – the most stubs – and sort them by their desired degree, and choose the one with the maximum desired degree. Choose possible edges that the chosen node could have and select appropriate neighbors and make the edge.

Continue until all edges are added.

Algorithm 5: Maximum Stub Minimum Degree ($S_{\max}ND_{\min}$)

```

while  $BJD > 0$  do
    From remaining nodes, find the node  $\mathbf{u}$  with  $\mathbf{u} = \min_{deg(\mathbf{v})} \{ \max_{stub(\mathbf{v})} \{\mathbf{v}\} \}$ ;
    if  $\mathbf{u}$  is upper node with degree  $i$  then
        From the row  $i$  of  $BJD$  matrix randomly select an element  $(i, j) > 0$ ;
        Randomly select a lower node  $\mathbf{v}$  with desired degree  $j$  and  $stub(\mathbf{v}) > 0$ ;
        Make edge  $\mathbf{uv}$ ,  $stub(\mathbf{u}) \leftarrow stub(\mathbf{u}) - 1$ , and  $stub(\mathbf{v}) \leftarrow stub(\mathbf{v}) - 1$ , and
         $(i, j) \leftarrow (i, j) - 1$ ;
    else
        From the column  $j$  of  $BJD$  matrix randomly select an element  $(i, j) > 0$ ;
        Randomly select an upper node  $\mathbf{v}$  with desired degree  $i$  and  $stub(\mathbf{v}) > 0$ ;
        Make edge  $\mathbf{uv}$ ,  $stub(\mathbf{u}) \leftarrow stub(\mathbf{u}) - 1$ , and  $stub(\mathbf{v}) \leftarrow stub(\mathbf{v}) - 1$ , and
         $(i, j) \leftarrow (i, j) - 1$ ;
    end
end

```

A.4 Rewiring Approach

During the construction of our network, it is possible that there is not two valid nodes, \mathbf{u} and \mathbf{v} , each of valid desired degrees, i and j that do not already have an edge between them. Our options are to increase a node beyond its desired degree, or attach a multiple edge. Because the final network satisfies a certain BJD, we choose to simplify the generation by allowing multiple edges between nodes \mathbf{u} and \mathbf{v} as long as the network still satisfies (i, j) . Once all of the edges are attached, we use rewiring to remove multiple edges, which maintains the proper edge count for each (i, j) .

Our approach follows the proof of theorem [A.1.1](#). Suppose \mathbf{G} is the bipartite network generated by one of the approaches defined in the last subsection, and suppose \mathbf{G} has at least

one multiple edge. We randomly start with one of the multiple edges, say edge attached to the nodes \mathbf{u} and \mathbf{v} and then we follow the rewiring process explained in the theorem A.1.1. Here is the algorithm of the rewiring process:

Algorithm 6: Rewiring Process

```

while Network  $\mathbf{G}$  is not simple do
    Select upper node  $\mathbf{u}$  and lower node  $\mathbf{v}$  with more than one edge between them;
    if There is lower node  $\mathbf{v}'$  with  $\deg(\mathbf{v}') = \deg(\mathbf{v})$  not connected to  $\mathbf{u}$  then
        Find a neighbor of  $\mathbf{v}'$  which is not neighbor of  $\mathbf{v}$ : upper node  $\mathbf{w}'$ ;
        Remove edges  $\mathbf{uv}$  and  $\mathbf{v'w'}$ ;
        Add edges  $\mathbf{uw'}$ ,  $\mathbf{vw'}$ .
    else if There is lower node  $\mathbf{u}'$  with  $\deg(\mathbf{u}') = \deg(\mathbf{u})$  not connected to  $\mathbf{v}$  then
        Find a neighbor of  $\mathbf{v}'$  which is not neighbor of  $\mathbf{v}$ : upper node  $\mathbf{w}'$ ;
        Remove edges  $\mathbf{uv}$  and  $\mathbf{v'w'}$ ;
        Add edges  $\mathbf{uw'}$ ,  $\mathbf{vw'}$ .
    else
        Find upper node  $\mathbf{u}'$  with  $\deg(\mathbf{u}') = \deg(\mathbf{u})$ , a lower node  $\mathbf{v}'$  disconnected to
             $\mathbf{u}'$  with  $\deg(\mathbf{v}') = \deg(\mathbf{v})$ ;
        Find a neighbor of  $\mathbf{u}'$  which is not neighbor of  $\mathbf{u}$ : upper node  $\mathbf{w}$ ;
        Find a neighbor of  $\mathbf{v}'$  which is not neighbor of  $\mathbf{v}$ : upper node  $\mathbf{w}'$ ;
        Remove edges  $\mathbf{uv}$ ,  $\mathbf{u'w}$ , and  $\mathbf{w'v'}$ ;
        Add edges  $\mathbf{uw}$ ,  $\mathbf{w'v}$ , and  $\mathbf{u'v'}$ .
    end
end

```

A.5 Romance Network

In order to verify the accuracy of presented *B2K* algorithms, we conduct some simulations by generating random bipartite networks, using RE, ED_{max}, ND_{max}, and S_{max}ND_{min} algorithms. We test the algorithms on an special real-world network called Romance network

by computing several properties of bipartite networks. We compare Nc , Sg , Cl , and Rc .

The network of sexual contact depicted in Figure (A.3) describes the structure of the adolescent romantic and sexual network in a population of 573 students at Jefferson High [105]. The original network is not a bipartite network: there are two edges that links two men and two women, representing homosexual relationships. We remove these two edges so that we have a bipartite network.

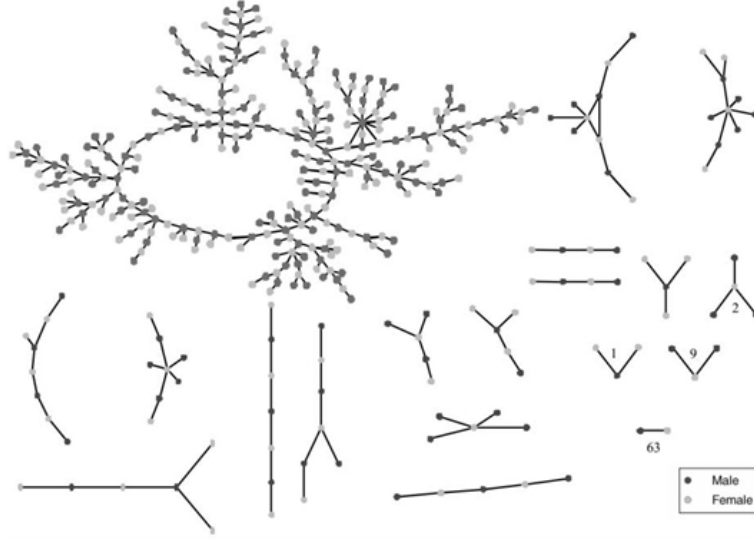


Figure A.3: The romance contact network at Jefferson High [105] consists of a single large connected component and several smaller romance groups.

We begin extracting the BJD matrix of this network, called BJD_R . The matrix has $k_w = 6$ rows, and $k_m = 8$ columns, where k_w is the maximum degree for women and k_m would be maximum degree for men.

Each element (i, j) is the number of edges between women with i partners and men with j partners. By BJD_R , we are able to find degree distribution for women and men: the number of women with i partners is summation of elements in i -th row divided by i , and the number of men with j partners is summation of elements in j -th column divided

by j . Here is the matrix extracted from the network:

$$BJD_R = \begin{pmatrix} 63 & 56 & 30 & 16 & 2 & 0 & 0 & 2 \\ 46 & 40 & 25 & 14 & 1 & 0 & 0 & 4 \\ 23 & 20 & 18 & 8 & 1 & 0 & 0 & 2 \\ 26 & 24 & 21 & 4 & 1 & 0 & 0 & 0 \\ 8 & 9 & 1 & 2 & 0 & 0 & 0 & 0 \\ 4 & 1 & 1 & 0 & 0 & 0 & 0 & 0 \end{pmatrix}.$$

As the matrix shows, we have big numbers for low degrees (upper left corner of matrix) and the rest are small or zero, making the average degree very low. Using our algorithms we compare the properties of BJD_R and the original romance network. In our numerical tests of generating an ensemble of 10000 networks for each algorithm, the algorithms succeeded in generating networks that preserved both the degree and joint-degree distributions in every simulation. We observed that the statistical properties of the networks for the $B2K$ algorithms were different, as shown in Table (A.1). This Table lists the Sg , Nc , Cl , and the Rc for the ensemble of generated networks. Note that the average size of giant component for the real network is noticeably above the mean size of giant components in the randomly generated networks, especially $S_{\max}ND_{\min}$.

	Real Network	RE	ED_{\max}	ND_{\max}	$S_{\max}ND_{\min}$
$\langle Cl \rangle$	0.3300	0.3338	0.3638	0.3617	0.3009
$SD(Cl)$	--	0.0052	0.0053	0.0058	0.0032
$\langle Rc \rangle$	0.0040	0.0039	0.0071	0.0117	0.0015
$SD(Rc)$	--	0.0057	0.0074	0.0091	0.0033
$\langle Sg \rangle$	287	217.57	256.35	244.79	87.0603
$SD(Sg)$	--	43.90	19.03	21.88	31.4488
$\langle Nc \rangle$	101	102.59	110.09	109.47	99.5267
$SD(Nc)$	--	1.7910	2.51	2.4992	0.7099

Table A.1: Properties of the real and randomly generated Romance networks. Note that the giant component size Sg of the real network is larger than the average size of the giant component in the randomly generated networks.

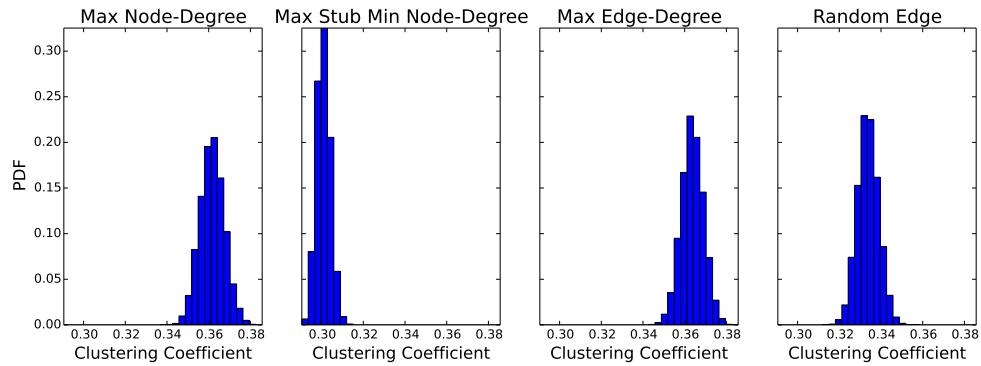
The Figure (A.4) plots the distribution of properties of the 10000 simulated networks from $B2K$ algorithms. For Cl , subfigure A.4(a), we observe all the algorithms have a normal trend with an small variance, however, for $S_{\max}ND_{\min}$ algorithm the mean value is smaller than the others, depicting the fact that joint-degree distribution may not be enough to capture clustering coefficient of the network. The subfigure A.4(b) is the distribution of Rc for the networks which all are right skewed. An interesting result from Sg is that $S_{\max}ND_{\min}$ underestimates this value compared to other algorithms and has a weak right skew unless the others which are almost normal, subfigure A.4(c). Finally for Nc , subfigure A.4(d), all the algorithms but $S_{\max}ND_{\min}$ follow a normal distribution, $S_{\max}ND_{\min}$.

We also compared ED_{\max} generating network algorithm with existing algorithms in NetworkX [106] using the degree distribution based on the configuration model [107] and Havel Hakimi graph [108]. Currently, there are no NetworkX algorithms to use joint-degree distribution for bipartite networks. The Table (A.2) lists some properties of real Romance network, ED_{\max} network and all other algorithms in NetworkX generated using Romance data.

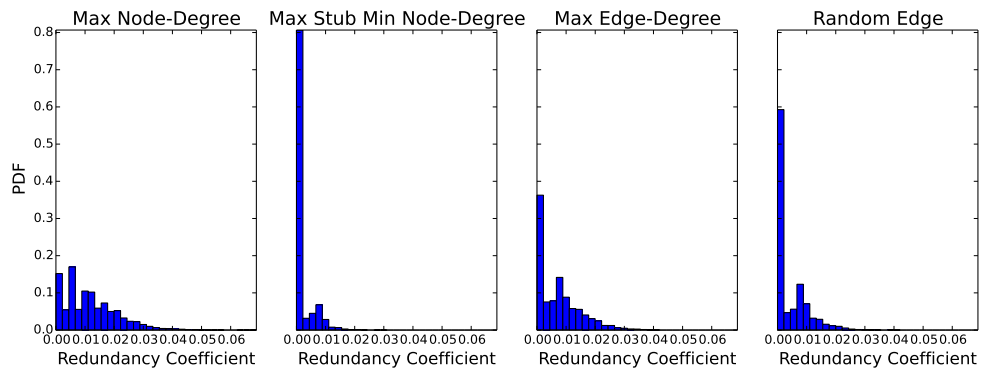
Network Model	Nc	Sg	Cl	Rc
Real Romance Network	101	287	0.3395	0.0044
ED_{\max}	100	259	0.3245	0.0049
Configuration Model	101	139	0.3693	0.0000
Havel-Hakimi Network	178	82	0.1827	0.5046
Alternative Havel-Hakimi	120	50	0.3834	0.0683
Reverse Havel-Hakimi	132	9	0.8210	0.5637

Table A.2: Properties of real Romance network and of the networks generated by the ED_{\max} algorithm, configuration model and Havel Hakimi algorithm. Note that the ED_{\max} accurately approximates the size of the giant component, the network clustering, and average redundancy coefficient in this low average degree network.

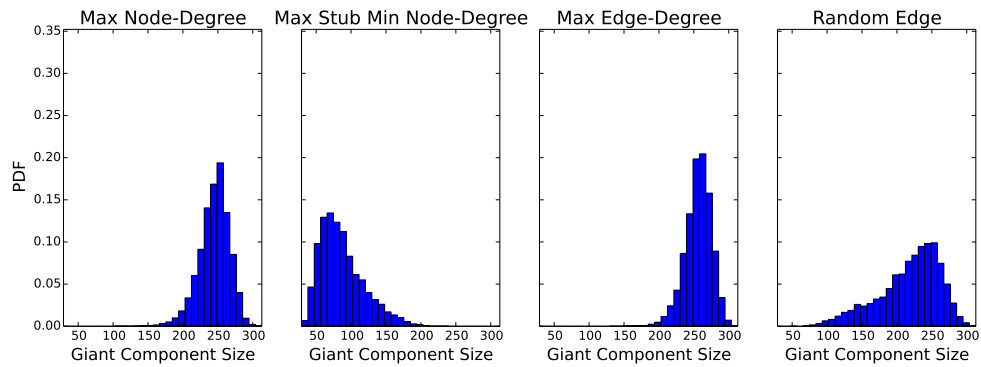
As we see in the Table (A.2), ED_{\max} algorithm is in better agreement with the real Romance network than other existing algorithms, though, it uses more information than these algorithms. The giant component of generated network using these algorithms are shown in Figure (A.5). This Figure shows the network generated by ED_{\max} is in agreement



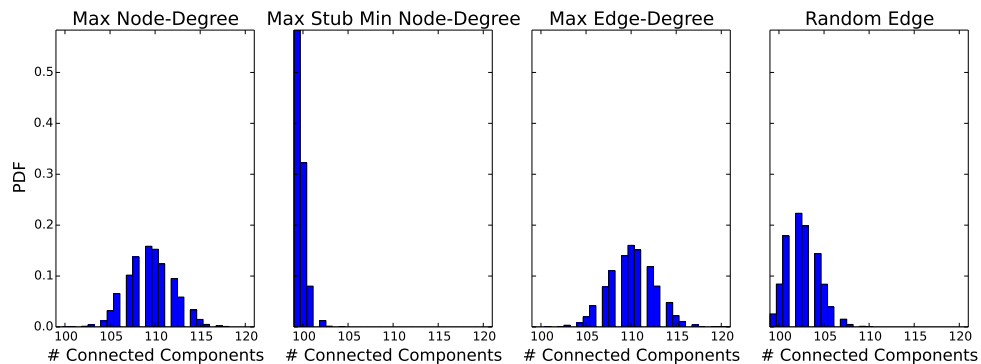
(a) Clustering Coefficient



(b) Redundancy Coefficient



(c) Size of Giant Component



(d) Number of Connected Components

Figure A.4: Bar plot of distribution of properties of 10,000 generated networks using *B2K* algorithms.

with the real network more than other existing networks in NetworkX. As expected, this example shows that the joint-degree distributions preserves more properties of the original network than the bipartite algorithms that just preserve the degree distribution.

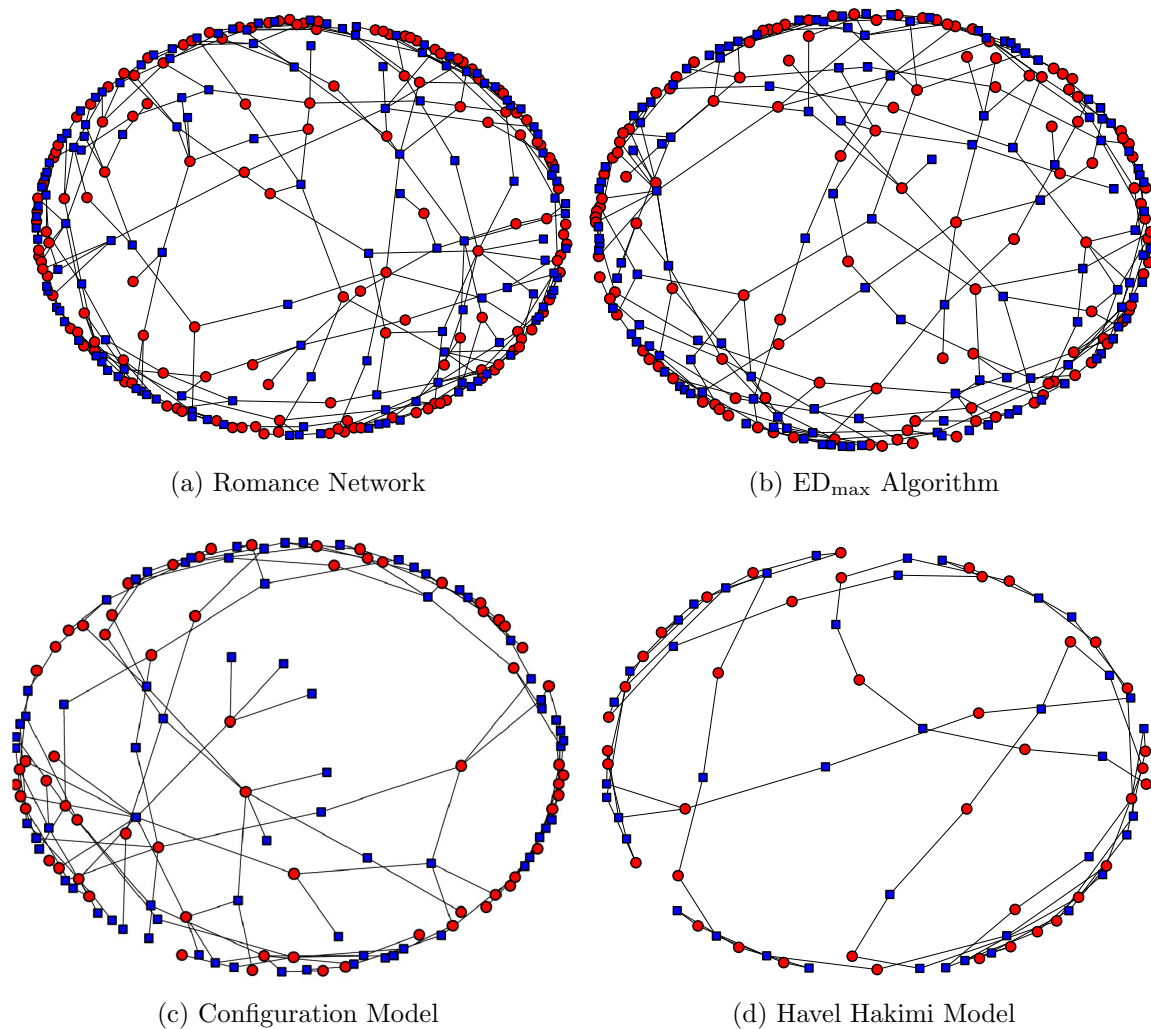


Figure A.5: The structure of the giant components of romance network and the $B2K$ generated network are similar. The configuration model and Havel Hakimi algorithms have the same degree distributions, but do not capture this property

Appendix B

Sexual Activities Hidden in Social Organization: A Preferential Attachment Mechanism for Human Sexual Network Formation in Social Network Context

The current appendix adds to our previous appendix on generating heterosexual networks with prescribed joint-degree distribution considering impact of people's social behavior (i.e., non-sexual partners) on their sexual partner selection. We generate a sexual network which has two properties: first property is that our sexual network is a subgraph of social network with a structure defined in [69], second it follows a joint-degree (degree-degree) distribution originated from sexual activity data.

B.1 Degree and joint-degree distribution and *BJD* matrix for a sexual network

A conventional heterosexual network \mathbf{G} , which is from bipartite family networks, is a sexual network of men and women, in which men only have partnership with women and vice versa, there is no partnership between two men or two women. Every edge \mathbf{ij} in this network means that two persons \mathbf{i} and \mathbf{j} are sexual partners. The *degree* of a person \mathbf{i} , is defined as the number of his/her sexual partners. The *degree distribution* d_k defines the number of people with degree k . The *joint-degree distribution* (k, j) is the number of men with degree j who are connected to women with degree k . This distribution can be represented by the *Bipartite Joint Degree* or *BJD* matrix:

$$BJD_G = \begin{pmatrix} e_{11} & e_{12} & e_{13} & \dots & e_{1m} \\ e_{21} & e_{22} & e_{23} & \dots & e_{2m} \\ \vdots & \vdots & \vdots & \ddots & \vdots \\ e_{w1} & e_{w2} & e_{w3} & \dots & e_{wm} \end{pmatrix},$$

where, w is the maximum degree in women nodes, and m is the maximum degree in men nodes, each element e_{ij} is the number of edges between women with i partners and men with j partners. The degree distribution of the number of women nodes, d_k^w , and men nodes, d_k^m , with k partners can be obtained from *BJD*_G:

$$d_k^w = \frac{\sum_{j=1}^m e_{kj}}{k}, \text{ and } d_k^m = \frac{\sum_{i=1}^w e_{ik}}{k}. \quad (\text{B.1})$$

B.2 Social network embedding sexual network

The Social Network called **SocNet** is a graph whose nodes are synthetic people, labeled by their demographics, and whose edges represent contacts determined in which each synthetic person is deemed to have made contact with a subset of other synthetic people through some

Activity types. We have five different activity locations: Home(H), Work(W), School(SC), Shopping(SH), and Others(O). Each edge is labeled with one of these activity locations and is weighted by the time spent on these contact per day. For example edge \mathbf{ij} labeled by W and weighted by T means two persons \mathbf{i} and \mathbf{j} have contact for T fraction of their total time spent at work [69].

B.3 Generating Bipartite Sexual Network

Our goal is to introduce an algorithm for generating a heterosexual network called **SexNet** that is a partial subgraph of social network **SocNet** and meets a particular joint-degree distribution represented by matrix BJD .

B.3.1 The algorithm

Now, we provide an algorithm that uses the sexual activity data (BJD matrix) and social network to generate the sexual network of individual called **SexNet**. This graph is partially embedded in **SocNet** -depends on what percentage of sexual partners of a typical person are selected from his/her social friends- and has a joint-degree distribution that meets BJD matrix. The algorithm includes three phases.

B.3.1.1 Phase 1: extension and revision of SocNet

This Phase is a procedure to extend **SocNet** and then to find its subgraph in a way that only consist the potensial edges for sexual activities:

1. The first step is to condense **SocNet** by making friendship between friends of an index case. For two persons \mathbf{i} and \mathbf{j} who are not currently connected, suppose the probability of their meet through a common social friend like \mathbf{k} within an activity A is p_{ij}^A . If they have $k(i, j)$ common social friends through a particular activity A , therefore, with probability of $1 - (1 - p_{ij}^A)^{k(i, j)}$ they meet each other and make friendship, that is, with probability of $1 - (1 - p_{ij}^A)^{k(i, j)}$ we make a new social edges

between **i** and **j**. We define $p_{ij}^A = p_i^A p_j^A$ where p_k^A for a person **k** is the average fraction of time spent per social friend for social friends within activity *A*, that is, if $N_A(k)$ is set of all social friends for person **k** through an activity location *A*, then

$$p_k^A = \frac{\sum_{l \in N_A(k)} T_{k,l}}{|N_A(k)|}. \quad (\text{B.2})$$

The Figure (B.1) represents an schematic of this approach: for the persons **i** and **j** who are not currently social friends but have three different common friends **k**₀, **k**₁, and **k**₂ though different activities. Suppose $A_{ik_0} = A_{jk_0} = A_{ik_1} = A_{jk_1} = A \neq A_{ik_2} \neq A_{jk_2}$, that is, **k**₀ meets **i** and **j** at the same location, similarly **k**₁ meets **i** and **j** at the same location to **k**₀'s, however, **k**₂ meets them in different places. To compute p_i^A and p_j^A we only count the friends who meet them at the same location *A*, therefore, $p_i^A = \frac{T_{ik_0} + T_{ik_1}}{2}$, and $p_j^A = \frac{T_{jk_0} + T_{jk_1}}{2}$.

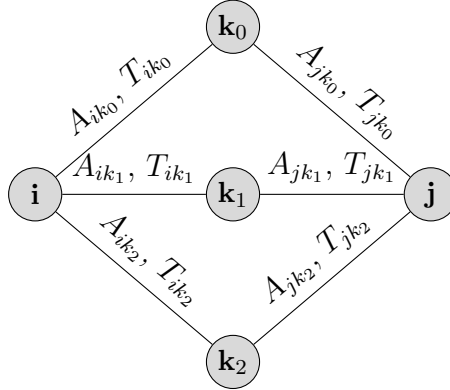


Figure B.1: An schematic of step 1, the only case that **i** and **j** have a chance to meet is when at least one of their common friends meet them within the same activity location.

2. If sexually active population under study has an age range $\alpha = [\alpha_1, \alpha_2]$, therefore people in **SocNet** but out of this age range cannot play a role in sexual network, for example a child with age six years old cannot be part of sexual network. Thus, the second step is to remove all people with ages $\notin \alpha$.
3. The sexual network we aim to extract from **SocNet** is heterosexual. That is, we do not have homosexual individuals in **SexNet**, therefore, the edges between two men

or two women in **SocNet** can not be a potential sexual edge, so we remove this edge from **SocNet**.

4. Our last assumption is that sexual partners are not living together, therefore household edges in **SocNet** (edges with label H) cannot be the proper edge ending up with sexual activity, so we remove household edges.

B.3.1.2 Phase 2: main algorithm

The main algorithm takes three inputs **SocNet**, BJD matrix corresponding to joint-degree distribution for **SexNet**, and $p \in [0, 1]$ the embedding percentage of **SocNet**, in fact the value p tells what percentage of edges in **SexNet** is in **SocNet**. The output would be heterosexual network **SexNet** which is a partially subgraph of **SocNet** and matrix BJD represents its joint-degree distribution. Starting with an empty set of nodes for **SexNet**, we select nodes in **SocNet** to add to **SexNet**: we sort nodes in **SocNet** based on their degree and as the first node in **SexNet** add the man node in **SocNet** with maximum degree to set of nodes in **SexNet** and assign its desired degree in **SexNet** equal to column size of BJD , and then select his first sexual partner with probability p from his social neighbors and with probability $1 - p$ from closest nodes in **SocNet** but not a social friend.

At any stage, we first find the partners for nodes in **SexNet** from their social friend, if the degree of all nodes in **SexNet** meet their desired degree, we add a new node to **SexNet**. We repeat adding edges until all edges are placed. Algorithms 7 and 8 explain this procedure, and table B.1 is the table of definition for symbols in the algorithms.

To keep or remove an edge we have to calculate the degree of nodes attached to it for each possible edge in the **SocNet**, thus, the full set of experiments run in $O(|E|P^mP^w)$ time, where $|E|$ is the number of edges in **SocNet**, P^m number of its men nodes and P^w number of its women nodes. This method is feasible if average degree $(\frac{2|E|}{P^m+P^w})$ of the network is not high.

$G.n$	$\stackrel{\text{def}}{=}$	set of nodes in G
$G.e$	$\stackrel{\text{def}}{=}$	set of edges in network G
$d_G(\mathbf{i})$	$\stackrel{\text{def}}{=}$	degree of node \mathbf{i} in network G
d_G	$\stackrel{\text{def}}{=}$	degree frequency list for network G
$G.N(\mathbf{i})$	$\stackrel{\text{def}}{=}$	set of neighbors of node \mathbf{i} in Network G
$dis(G, \mathbf{u}, \mathbf{v})$	$\stackrel{\text{def}}{=}$	distance between two nodes \mathbf{u} and \mathbf{v} in Network G
$M.col(M.row)$	$\stackrel{\text{def}}{=}$	column size (row size) of a matrix M
$M(i, :)(M(:, i))$	$\stackrel{\text{def}}{=}$	i^{th} row (column) of matrix M
$V(i)$	$\stackrel{\text{def}}{=}$	i^{th} element of vector V
$ S $	$\stackrel{\text{def}}{=}$	size (the number of elements) of a set S
$S.remove(m)$	$\stackrel{\text{def}}{=}$	remove member m from a set S
$S.sample(P)$	$\stackrel{\text{def}}{=}$	randomly select an element with property P (if $P=1$ there is no property) from set S
urn	$\stackrel{\text{def}}{=}$	uniform random number in $[0, 1]$

Table B.1: Table of notation for a conventional network G in algorithms.

Algorithm 7: Extracting sexual network from social network (**Soc2sex**)

```

SexNet. $n = \emptyset$ , SexNet. $n \leftarrow \mathbf{u} = \max_{d_{\text{SocNet}}(\mathbf{k})} \{\mathbf{k} \in \text{SocNet}.n\}$ ;
 $d_{\text{SexNet}}(\mathbf{u}) \triangleq \text{BJD.col}$ ,  $\text{stub}(\mathbf{u}) \triangleq d_{\text{SexNet}}(\mathbf{u})$ ;
 $E \triangleq \sum_i \sum_j \text{BJD}(i, j)$ ;
while  $|\text{SexNet}.e| \leq E$  do
     $NF \triangleq \{\mathbf{k} \in \text{SexNet}.n \text{ if } \text{stub}(\mathbf{k}) > 0\}$ ;
    while  $|NF| \geq 1$  do
         $\mathbf{u} = \max_{\text{stub}(\mathbf{k})} \{\mathbf{k} \in NF\}$ ;
         $(d', \mathbf{v}) = \text{FP}(\mathbf{u}, \text{SocNet}, \text{SexNet}, \text{BJD}, NF, p)$ ;
        if  $(d', \mathbf{v}) \neq \text{False}$  then
             $NF.\text{remove}(\mathbf{u})$ ;
        else
            Make edge  $(\mathbf{u}, \mathbf{v})$  in SexNet,  $\text{stub}(\mathbf{u}) \leftarrow \text{stub}(\mathbf{u}) - 1$ ,
             $\text{stub}(\mathbf{v}) \leftarrow \text{stub}(\mathbf{v}) - 1$ ;
            if  $\text{stub}(\mathbf{u})=0$  [ $\text{stub}(\mathbf{v})=0$ ] then
                 $d_{\text{SexNet}}.\text{remove}(d_{\text{SexNet}}(\mathbf{u}))$  [ $d_{\text{SexNet}}.\text{remove}(d_{\text{SexNet}}(\mathbf{v}))$ ];
            end
            if  $\mathbf{u}$  is woman then
                 $\text{BJD}(d, d') - 1$ 
            else
                 $\text{BJD}(d', d) - 1$ 
            end
        end
    end
    SexNet. $n \leftarrow \mathbf{u} = \max_{d_{\text{SocNet}}(k)} \{k \in \text{SocNet}.n - \text{SexNet}.n\}$ ;
     $d_{\text{SexNet}}(\mathbf{u}) \triangleq \max\{d_{\text{SexNet}}\}$ ,  $\text{stub}(\mathbf{u}) \triangleq d_{\text{SexNet}}(\mathbf{u})$ .
end

```

Algorithm 8: Finding partner with proper degree for a given node (**FP**)

```

 $d = d_{\text{SexNet}}(\mathbf{u});$ 
if  $\mathbf{u}$  is woman then  $R \triangleq \text{BJD}(d, :)$ , else  $R \triangleq \text{BJD}(:, d)$ ;
for  $\text{iter}$  in range( $|R|$ ) do
  if  $R \neq 0$  then
     $R.\text{sample}(d' : R(d') \neq 0);$ 
    if  $\text{urn} \leq p$  then
       $K1 \triangleq \{\mathbf{k} \in NF : \mathbf{k} \in \text{SocNet}.N(\mathbf{u}) - \text{SexNet}.N(\mathbf{u}), d_{\text{SexNet}}(\mathbf{k}) = d'\};$ 
       $K2 \triangleq \{\mathbf{k} \in \text{SocNet}.N(\mathbf{u}) - \text{SexNet}.n : d_{\text{SocNet}}(\mathbf{k}) \geq d'\};$ 
    else
       $K1 \triangleq \{\mathbf{k} \in NF : \mathbf{k} \notin \text{SocNet}.N(\mathbf{u}) \cup \text{SexNet}.N(\mathbf{u}), d_{\text{SexNet}}(\mathbf{k}) = d'\};$ 
       $K2 \triangleq \{\mathbf{k} \in \text{SocNet}.n - \text{SexNet}.n : d_{\text{SocNet}}(\mathbf{k}) \geq d'\};$ 
    end
    if  $K1 \neq \emptyset$  then
       $\mathbf{v} = K1.\text{sample}(\mathbf{w} : \text{dis}(\text{SocNet}, \mathbf{u}, \mathbf{w}) = \min\{\text{dis}(\text{SocNet}, \mathbf{u}, \mathbf{k}) \text{ for } \mathbf{k} \in K1\});$ 
      Break;
    else if  $K2 \neq \emptyset$  then
       $\mathbf{v} = K2.\text{sample}(\mathbf{w} : \text{dis}(\text{SocNet}, \mathbf{u}, \mathbf{w}) = \min\{\text{dis}(\text{SocNet}, \mathbf{u}, \mathbf{k}) \text{ for } \mathbf{k} \in K2\});$ 
       $d_{\text{SexNet}}(\mathbf{v}) \triangleq d', \text{stub}(\mathbf{v}) \triangleq d';$ 
      Break;
    else
       $R(d') \triangleq 0;$ 
    end
  else
     $(d', \mathbf{v}) = \text{False};$ 
    break;
  end
end
Return  $(d', \mathbf{v});$ 

```

B.3.1.3 Phase 3: correcting BJD

We intent to have a generated sexual network such that BJD matrix represents its joint-degree distribution. But, because in the main algorithm, we may not find a proper partner for some people, therefore, we may end up with a different joint-degree distribution for the network. The goal of third Phase is to correct joint-degree distribution of generated **SexNet** through some edge rewiring. We define \widetilde{BJD} as matrix representing joint-degree distribution of **SexNet** and $\mathcal{E} = BJD - \widetilde{BJD}$ as error matrix. Matrix \mathcal{E} may have nonzero elements:

1. If element (i, j) of \mathcal{E} for $i, j > 1$ is a positive value k , it means that **SexNet** needs k more edges between women with i partners and men with j partners. To make these edges we do the following process k times: In **SexNet** we find a woman with i partners like \mathbf{w}_i which has a degree-1 partner like \mathbf{m}_1 , then we find a man with j partners like \mathbf{m}_j which is social friend of \mathbf{w}_i but not her sexual partner and also has a degree-1 partner like \mathbf{w}_1 . Then we do a rewiring: remove edges $(\mathbf{w}_i, \mathbf{m}_1)$ and $(\mathbf{m}_j, \mathbf{w}_1)$ and add edge $(\mathbf{w}_i, \mathbf{m}_j)$.
2. If element (i, j) of \mathcal{E} for $i, j > 1$ is a negative value k' , it means that we have extra k' edges between women with i partners and men with j partners. To remove these extra edges we do the following process k' times: we find a woman with i partners like \mathbf{w}_i which has a degree- j partner like \mathbf{m}_j , and that at least one of their social friends are not in **SexNet**. Then we find a man like \mathbf{m}_1 which is social friend of \mathbf{w}_i that not in **SexNet**, and also we find a woman like \mathbf{w}_1 which is social friend of \mathbf{m}_j that is not in **SexNet**. Then we do a rewiring: remove edge $(\mathbf{w}_i, \mathbf{m}_j)$ and add edges $(\mathbf{w}_i, \mathbf{m}_1), (\mathbf{w}_1, \mathbf{m}_j)$.
3. In the previous steps, we pushed back nonzero elements in \mathcal{E} to its first row and column, which this causes new nonzero elements in the first row and column. To remove these nonzero values, we have to add or remove small components. For example if element $(1, 1)$ of \mathcal{E} is a positive value k it means that we need a small component of

a woman with i partners whose all partners are degree-1 men, therefore, we simply make this component from the people who are not currently in **SexNet**. n . If element $(1, j)$ of \mathcal{E} is a negative value k it means we have to remove a small component of a man with j partners whose all partners are degree-1 women, therefore, we simply look for such a component and remove it from **SexNet**.

This Phase 3 may not make matrix \mathcal{E} exactly equal to zero, because in its approach the proper nodes may not exist. However, it improves joint-degree distribution of **SexNet**. In the Result Section of Chapter (4), we observe that in practice Phase 3 would not be needed.

Bibliography

- [1] M. W. Adler, I. Weller, and D. Goldmeier. *ABC of sexually transmitted diseases*. JSTOR, 1998.
- [2] J. Dimitrakov. Chlamydia-a journey from embryonated egg to lcr. *The Prostatitis Foundation*, viewed, 9, 2011.
- [3] E. Torrone, J. Papp, H. Weinstock, C. for Disease Control, P. (CDC), et al. Prevalence of chlamydia trachomatis genital infection among persons aged 14–39 years united states, 2007–2012. *MMWR Morb Mortal Wkly Rep*, 63(38):834–838, 2014.
- [4] cdc. <http://www.cdc.gov/std/chlamydia/hedis.htm>. Accessed: 2010-09-30.
- [5] T. A. Farley, D. A. Cohen, and W. Elkins. Asymptomatic sexually transmitted diseases: the case for screening. *Preventive medicine*, 36(4):502–509, 2003.
- [6] E. L. Korenromp, M. K. Sudaryo, S. J. de Vlas, R. H. Gray, N. K. Sewankambo, D. Serwadda, M. J. Wawer, and J. D. F. Habbema. What proportion of episodes of gonorrhoea and chlamydia becomes symptomatic? *International journal of STD & AIDS*, 13(2):91–101, 2002.
- [7] T. C. Quinn, C. Gaydos, M. Shepherd, L. Bobo, E. W. Hook, R. Viscidi, and A. Rompalo. Epidemiologic and microbiologic correlates of chlamydia trachomatis infection in sexual partnerships. *Jama*, 276(21):1737–1742, 1996.
- [8] M. S. Cohen. Sexually transmitted diseases enhance hiv transmission: no longer a hypothesis. *The Lancet*, 351:S5–S7, 1998.
- [9] S. D. Datta, E. Torrone, D. Kruszon-Moran, S. Berman, R. Johnson, C. L. Satterwhite, J. Papp, and H. Weinstock. Chlamydia trachomatis trends in the united states among persons 14 to 39 years of age, 1999–2008. *Sexually transmitted diseases*, 39(2):92–96, 2012.
- [10] S. L. Gottlieb, R. C. Brunham, G. I. Byrne, D. H. Martin, F. Xu, and S. M. Berman. Introduction: the natural history and immunobiology of chlamydia trachomatis genital infection and implications for chlamydia control. *Journal of Infectious Diseases*, 201(Supplement 2):S85–S87, 2010.
- [11] S. L. Gottlieb, D. H. Martin, F. Xu, G. I. Byrne, and R. C. Brunham. Summary: The natural history and immunobiology of chlamydia trachomatis genital infection and implications for chlamydia control. *Journal of Infectious Diseases*, 201(Supplement 2):S190–S204, 2010.

- [12] S. D. Hillis and J. N. Wasserheit. Screening for chlamydia: a key to the prevention of pelvic inflammatory disease. *New England Journal of Medicine*, 334(21):1399–1401, 1996.
- [13] J. Lan, A. van den Brule, D. Hemrika, E. Risse, J. Walboomers, M. Schipper, and C. Meijer. Chlamydia trachomatis and ectopic pregnancy: retrospective analysis of salpingectomy specimens, endometrial biopsies, and cervical smears. *Journal of clinical pathology*, 48(9):815–819, 1995.
- [14] M. D. PEARLMAN and S. G. MCNEELEY. A review of the microbiology, immunology, and clinical implications of chlamydia trachomatis infections. *Obstetrical & gynecological survey*, 47(7):448–461, 1992.
- [15] L. Westrom. Effect of pelvic inflammatory disease on fertility. *Venereology: official publication of the National Venereology Council of Australia*, 8(4):219–222, 1995.
- [16] L. Weström. Sexually transmitted diseases and infertility. *Sexually transmitted diseases*, 21(2 Suppl):S32–7, 1993.
- [17] M. R. Golden, M. Hogben, H. H. Handsfield, J. S. S. LAWRENCE, J. J. Potterat, and K. K. Holmes. Partner notification for hiv and std in the united states:: Low coverage for gonorrhea, chlamydial infection, and hiv. *Sexually transmitted diseases*, 30(6):490–496, 2003.
- [18] L. M. Niccolai, K. A. Livingston, A. S. Laufer, and M. M. Pettigrew. Behavioural sources of repeat chlamydia trachomatis infections: importance of different sex partners. *Sexually transmitted infections*, 87(3):248–253, 2011.
- [19] H. Ward and M. Rönn. The contribution of stis to the sexual transmission of hiv. *Current Opinion in HIV and AIDS*, 5(4):305, 2010.
- [20] G. I. J. Rours, L. Duijts, H. A. Moll, L. R. Arends, R. de Groot, V. W. Jaddoe, A. Hofman, E. A. Steegers, J. P. Mackenbach, A. Ott, et al. Chlamydia trachomatis infection during pregnancy associated with preterm delivery: a population-based prospective cohort study. *European journal of epidemiology*, 26(6):493–502, 2011.
- [21] T. R. Eng, W. T. Butler, et al. *The hidden epidemic: Confronting sexually transmitted diseases*. National Academies Press, 1997.
- [22] K. E. Rogstad. *ABC of sexually transmitted infections*, volume 194. John Wiley & Sons, 2011.
- [23] C. F. Turner, L. Ku, S. M. Rogers, L. D. Lindberg, J. H. Pleck, and F. L. Sonenstein. Adolescent sexual behavior, drug use, and violence: increased reporting with computer survey technology. *Science*, 280(5365):867–873, 1998.
- [24] S. O. Aral. Sexual behavior in sexually transmitted disease research. an overview. *Sexually transmitted diseases*, 21(2 Suppl):S59–64, 1993.
- [25] C. for Disease Control, P. (CDC, et al. Update: barrier protection against hiv infection and other sexually transmitted diseases. *MMWR. Morbidity and mortality weekly report*, 42(30):589, 1993.

- [26] ChildTrend. <http://www.childtrends.org/?indicators=condom-use>. Accessed: 2014-07-22.
- [27] M. Reece, D. Herbenick, V. Schick, S. A. Sanders, B. Dodge, and J. D. Fortenberry. Condom use rates in a national probability sample of males and females ages 14 to 94 in the united states. *The journal of sexual medicine*, 7(s5):266–276, 2010.
- [28] R. B. Rothenberg and J. J. Potterat. Strategies for management Of sex partners. 1990.
- [29] D. Cotton, D. Higgins, B. Person, and W. Darrow. Cdc behavioral interventions. 1994.
- [30] D. K. Eaton, L. Kann, S. Kinchen, S. Shanklin, J. Ross, J. Hawkins, W. A. Harris, R. Lowry, T. McManus, D. Chyen, et al. Youth risk behavior surveillance-united states, 2009. *Morbidity and mortality weekly report. Surveillance summaries (Washington, DC: 2002)*, 59(5):1–142, 2010.
- [31] S. Del Valle, H. Hethcote, J. M. Hyman, and C. Castillo-Chavez. Effects of behavioral changes in a smallpox attack model. *Mathematical biosciences*, 195(2):228–251, 2005.
- [32] S. Y. Del Valle, J. M. Hyman, H. W. Hethcote, and S. G. Eubank. Mixing patterns between age groups in social networks. *Social Networks*, 29(4):539–554, 2007.
- [33] J. M. Hyman and J. Li. Behavior changes in sis std models with selective mixing. *SIAM Journal on Applied Mathematics*, 57(4):1082–1094, 1997.
- [34] J. M. Hyman and J. Li. Disease transmission models with biased partnership selection. *Applied Numerical Mathematics*, 24(2):379–392, 1997.
- [35] J. M. Hyman, J. Li, and E. A. Stanley. The differential infectivity and staged progression models for the transmission of hiv. *Mathematical biosciences*, 155(2):77–109, 1999.
- [36] J. M. Hyman, J. Li, and E. A. STANLEY. The initialization and sensitivity of multi-group models for the transmission of hiv. *Journal of theoretical Biology*, 208(2):227–249, 2001.
- [37] J. M. Hyman, J. Li, and E. A. Stanley. Modeling the impact of random screening and contact tracing in reducing the spread of hiv. *Mathematical biosciences*, 181(1):17–54, 2003.
- [38] J. M. Hyman and E. A. Stanley. Using mathematical models to understand the aids epidemic. *Mathematical Biosciences*, 90(1-2):415–473, 1988.
- [39] J. M. Hyman and E. A. Stanley. The effect of social mixing patterns on the spread of aids. In *Mathematical approaches to problems in resource management and epidemiology*, pages 190–219. Springer, 1989.
- [40] J. M. Hyman and E. A. Stanley. A risk-based heterosexual model for the aids epidemic with biased sexual partner selection. In E. E. Kaplan and M. Brandeau, editors, *Modeling the AIDS Epidemic*, pages 331–364. Raven Press, 1994.

- [41] C. L. Althaus, J. Heijne, A. Roellin, and N. Low. Transmission dynamics of *Chlamydia trachomatis* affect the impact of screening programmes. *Epidemics*, 2(3):123–131, 2010.
- [42] J. Clarke, K. White, and K. Turner. Exploring short-term responses to changes in the control strategy for *Chlamydia trachomatis*. *Computational and mathematical methods in medicine*, 2012, 2012.
- [43] M. Kretzschmar, Y. T. van Duynhoven, and A. J. Severijnen. Modeling prevention strategies for gonorrhea and *Chlamydia* using stochastic network simulations. *American Journal of Epidemiology*, 144(3):306–317, 1996.
- [44] M. Kretzschmar, R. Welte, A. Van den Hoek, and M. J. Postma. Comparative model-based analysis of screening programs for *Chlamydia trachomatis* infections. *American journal of epidemiology*, 153(1):90–101, 2001.
- [45] N. Low, A. McCarthy, J. Macleod, C. Salisbury, R. Campbell, T. Roberts, P. Horner, S. Skidmore, J. Sterne, E. Sanford, et al. Epidemiological, social, diagnostic and economic evaluation of population screening for genital *Chlamydia* infection. *Health technology assessment (Winchester, England)*, 11(8):iii–iv, 2007.
- [46] K. Turner, E. J. Adams, D. LaMontagne, L. Emmett, K. Baster, and W. Edmunds. Modelling the effectiveness of *Chlamydia* screening in England. *Sexually transmitted infections*, 82(6):496–502, 2006.
- [47] S. Y. Del Valle, J. M. Hyman, and N. Chitnis. Mathematical models of contact patterns between age groups for predicting the spread of infectious diseases. *Mathematical biosciences and engineering: MBE*, 10:1475, 2013.
- [48] A. Azizi, L. Xue, and J. M. Hyman. A multi-risk model for understanding the spread of *Chlamydia*. In *Mathematical and Statistical Modeling for Emerging and Re-emerging Infectious Diseases*, pages 249–268. Springer, 2016.
- [49] S. Busenberg and C. Castillo-Chavez. A general solution of the problem of mixing of subpopulations and its application to risk-and age-structured epidemic models for the spread of AIDS. *Mathematical Medicine and Biology*, 8(1):1–29, 1991.
- [50] P. Van den Driessche and J. Watmough. Reproduction numbers and sub-threshold endemic equilibria for compartmental models of disease transmission. *Mathematical biosciences*, 180(1):29–48, 2002.
- [51] J. Heffernan, R. Smith, and L. Wahl. Perspectives on the basic reproductive ratio. *Journal of the Royal Society Interface*, 2(4):281–293, 2005.
- [52] J. J. Sylvester. XIX. a demonstration of the theorem that every homogeneous quadratic polynomial is reducible by real orthogonal substitutions to the form of a sum of positive and negative squares. *Philosophical Magazine Series 4*, 4(23):138–142, 1852.
- [53] L. M. Arriola and J. M. Hyman. Being sensitive to uncertainty. *Computing in Science & Engineering*, 9(2):10–20, 2007.

- [54] L. Arriola and J. M. Hyman. Sensitivity analysis for uncertainty quantification in mathematical models. In *Mathematical and Statistical Estimation Approaches in Epidemiology*, pages 195–247. Springer, 2009.
- [55] C. A. Manore, K. S. Hickmann, S. Xu, H. J. Wearing, and J. M. Hyman. Comparing dengue and chikungunya emergence and endemic transmission in a. aegypti and a. albopictus. *Journal of theoretical biology*, 356:174–191, 2014.
- [56] A. Azizi, K. Ríos-Soto, A. Mubayi, and J. M. Hyman. A risk-based model for predicting the impact of using condoms on the spread of sexually transmitted infections. *Infectious Disease Modelling*, 2(1):100–112, 2017.
- [57] Z. Feng, A. N. Hill, A. T. Curns, and J. W. Glasser. Evaluating targeted interventions via meta-population models with multi-level mixing. *Mathematical Biosciences*, 2016.
- [58] C. M. Lescano, E. A. Vazquez, L. K. Brown, E. B. Litvin, D. Pugatch, P. S. S. Group, et al. Condom use with casual and main partners: Whats in a name? *Journal of Adolescent Health*, 39(3):443–e1, 2006.
- [59] B. Beadnell, D. M. Morrison, A. Wilsdon, E. A. Wells, E. Murowchick, M. Hoppe, M. R. Gillmore, and D. Nahom. Condom use, frequency of sex, and number of partners: Multidimensional characterization of adolescent sexual risk-taking. *Journal of Sex Research*, 42(3):192–202, 2005.
- [60] C. L. Althaus, K. M. Turner, B. V. Schmid, J. C. Heijne, M. Kretzschmar, and N. Low. Transmission of chlamydia trachomatis through sexual partnerships: a comparison between three individual-based models and empirical data. *Journal of The Royal Society Interface*, page rsif20110131, 2011.
- [61] K. M. Turner, E. J. Adams, N. Gay, A. C. Ghani, C. Mercer, and W. J. Edmunds. Developing a realistic sexual network model of chlamydia transmission in britain. *Theoretical biology and medical modelling*, 3(1):3, 2006.
- [62] P. J. Kissinger. Expedited partner therapy for sexually transmitted diseases—are we there yet? *Sexually transmitted diseases*, 41(11):695–697, 2014.
- [63] S. A. Colgate, E. A. Stanley, J. M. Hyman, S. P. Layne, and C. Qualls. Risk behavior-based model of the cubic growth of acquired immunodeficiency syndrome in the united states. *Proceedings of the National Academy of Sciences*, 86(12):4793–4797, 1989.
- [64] O. Diekmann, J. A. P. Heesterbeek, and J. A. Metz. On the definition and the computation of the basic reproduction ratio r_0 in models for infectious diseases in heterogeneous populations. *Journal of mathematical biology*, 28(4):365–382, 1990.
- [65] C. W. Kabiru and P. Orpinas. Correlates of condom use among male high school students in nairobi, kenya. *Journal of School Health*, 79(9):425–432, 2009.
- [66] A. Azizi, J. Dewar, and J. Mac Hyman. Using an agent-based sexual-network model to guide mitigation efforts for controlling chlamydia. *bioRxiv*, page 233239, 2018.
- [67] P. Kissinger. Check it! a seek, test and treat pilot study of methods for community recruitment of hard-to-reach men for chlamydia and gonorrhea screening and expedited treatment. In *2014 National STD Prevention Conference*. CDC, 2014.

- [68] J. Green, N. Schmidt, J. Latimer, T. Johnson, U. Aktaruzzaman, E. Flanigan, Y. Olugbade, S. Bangel, G. Clum, A. Madkour, et al. The influence of partnership type and characteristics on condom use among young african american women. In *SEXUALLY TRANSMITTED DISEASES*, volume 41, pages S111–S111. LIPPINCOTT WILLIAMS & WILKINS TWO COMMERCE SQ, 2001 MARKET ST, PHILADELPHIA, PA 19103 USA, 2014.
- [69] S. Eubank, C. Barrett, R. Beckman, K. Bisset, L. Durbeck, C. Kuhlman, B. Lewis, A. Marathe, M. Marathe, and P. Stretz. Detail in network models of epidemiology: are we there yet? *Journal of biological dynamics*, 4(5):446–455, 2010.
- [70] S. Eubank. Synthetic data products for societal infrastructures and protopopulations: Data set 2.0. Technical report, Technical Report NDSSL-TR-07-003, Network Dynamics and Simulation Science Laboratory, Virginia Polytechnic Institute and State University, 2008.
- [71] M. Newman. *Networks: an introduction*. Oxford university press, 2010.
- [72] R. Welte, M. Postma, R. Leidl, and M. Kretzschmar. Costs and effects of chlamydial screening: dynamic versus static modeling. *Sexually transmitted diseases*, 32(8):474–483, 2005.
- [73] E. J. Adams, K. M. Turner, and W. J. Edmunds. The cost effectiveness of opportunistic chlamydia screening in england. *Sexually transmitted infections*, 83(4):267–275, 2007.
- [74] B. Andersen, J. Gundgaard, M. Kretzschmar, J. Olsen, R. Welte, and L. Østergaard. Prediction of costs, effectiveness, and disease control of a population-based program using home sampling for diagnosis of urogenital chlamydia trachomatis infections. *Sexually transmitted diseases*, 33(7):407–415, 2006.
- [75] P. Gillespie, C. O’neill, E. Adams, K. Turner, D. O’donovan, R. Brugha, D. Vaughan, E. O’connell, M. Cormican, M. Balfe, et al. The cost and cost-effectiveness of opportunistic screening for chlamydia trachomatis in ireland. *Sex Transm Infect*, 88(3):222–228, 2012.
- [76] T. E. Roberts, S. Robinson, P. M. Barton, S. Bryan, A. McCarthy, J. Macleod, M. Egger, and N. Low. Cost effectiveness of home based population screening for chlamydia trachomatis in the uk: economic evaluation of chlamydia screening studies (class) project. *Bmj*, 335(7614):291, 2007.
- [77] B. B. Hui, D. P. Wilson, J. S. Ward, R. J. Guy, J. M. Kaldor, M. G. Law, J. S. Hocking, and D. G. Regan. The potential impact of new generation molecular point-of-care tests on gonorrhoea and chlamydia in a setting of high endemic prevalence. *Sexual health*, 10(4):348–356, 2013.
- [78] S. Morre, P. Sillekens, M. Jacobs, S. De Blok, J. Ossewaarde, P. Van Aarle, B. Van Gemen, J. Walboomers, C. Meijer, and A. Van den Brule. Monitoring of chlamydia trachomatis infections after antibiotic treatment using rna detection by nucleic acid sequence based amplification. *Molecular Pathology*, 51(3):149–154, 1998.

- [79] T. L. Gift, C. A. Gaydos, C. K. Kent, J. M. Marrazzo, C. A. Rietmeijer, J. A. Schillinger, and E. F. Dunne. The program cost and cost-effectiveness of screening men for chlamydia to prevent pelvic inflammatory disease in women. *Sexually transmitted diseases*, 35(11):S66–S75, 2008.
- [80] C. Gopalappa, Y.-L. A. Huang, T. L. Gift, K. Owusu-Edusei, M. Taylor, and V. Gales. Cost-effectiveness of screening men in maricopa county jails for chlamydia and gonorrhea to avert infections in women. *Sexually transmitted diseases*, 40(10):776–783, 2013.
- [81] M. M. Reagan, H. Xu, S. L. Shih, G. M. Secura, and J. F. Peipert. A randomized trial of home versus clinic-based std screening among men. *Sexually transmitted diseases*, 39(11):842, 2012.
- [82] C. R. Stein, J. S. Kaufman, C. A. Ford, P. A. Leone, P. J. Feldblum, and W. C. Miller. Screening young adults for prevalent chlamydial infection in community settings. *Annals of epidemiology*, 18(7):560–571, 2008.
- [83] T. A. Peterman, L. H. Tian, C. A. Metcalf, C. L. Satterwhite, C. K. Malotte, N. DeAugustine, S. M. Paul, H. Cross, C. A. Rietmeijer, and J. M. Douglas. High incidence of new sexually transmitted infections in the year following a sexually transmitted infection: a case for rescreening. *Annals of internal medicine*, 145(8):564–572, 2006.
- [84] C. F. Dormann, J. Fründ, N. Blüthgen, and B. Gruber. Indices, graphs and null models: analyzing bipartite ecological networks. 2009.
- [85] G. Cimini, A. Gabrielli, and F. S. Labini. The scientific competitiveness of nations. *PloS one*, 9(12):e113470, 2014.
- [86] M. Boguná and R. Pastor-Satorras. Class of correlated random networks with hidden variables. *Physical Review E*, 68(3):036112, 2003.
- [87] P. Mahadevan, D. Krioukov, K. Fall, and A. Vahdat. Systematic topology analysis and generation using degree correlations. In *ACM SIGCOMM Computer Communication Review*, volume 36, pages 135–146. ACM, 2006.
- [88] M. E. Newman. Mixing patterns in networks. *Physical Review E*, 67(2):026126, 2003.
- [89] S. Eubank, H. Guclu, V. A. Kumar, M. V. Marathe, A. Srinivasan, Z. Toroczkai, and N. Wang. Modelling disease outbreaks in realistic urban social networks. *Nature*, 429(6988):180–184, 2004.
- [90] G. D’Agostino, A. Scala, V. Zlatić, and G. Caldarelli. Robustness and assortativity for diffusion-like processes in scale-free networks. *EPL (Europhysics Letters)*, 97(6):68006, 2012.
- [91] O. Williams and C. I. Del Genio. Degree correlations in directed scale-free networks. *PloS one*, 9(10):e110121, 2014.
- [92] P. Erdős and A. Rényi. On random graphs. *Publicationes Mathematicae Debrecen*, 6:290–297, 1959.

- [93] F. Chung and L. Lu. Connected components in random graphs with given expected degree sequences. *Annals of combinatorics*, 6(2):125–145, 2002.
- [94] C. G. M. Mihail and E. Zegura. The markov chain simulation method for generating connected power law random graphs. In *Proceedings of the Fifth Workshop on Algorithm Engineering and Experiments*, volume 111, page 16. SIAM, 2003.
- [95] M. Molloy and B. Reed. A critical point for random graphs with a given degree sequence. *Random structures & algorithms*, 6(2-3):161–180, 1995.
- [96] I. Stanton and A. Pinar. Constructing and sampling graphs with a prescribed joint degree distribution. *Journal of Experimental Algorithmics (JEA)*, 17:3–5, 2012.
- [97] G. Amanatidis, B. Green, and M. Mihail. Graphic realizations of joint-degree matrices. *arXiv preprint arXiv:1509.07076*, 2015.
- [98] É. Czabarka, A. Dutle, P. L. Erdős, and I. Miklós. On realizations of a joint degree matrix. *Discrete Applied Mathematics*, 181:283–288, 2015.
- [99] M. Gjoka, B. Tillman, and A. Markopoulou. Construction of simple graphs with a target joint degree matrix and beyond. In *Computer Communications (INFOCOM), 2015 IEEE Conference on*, pages 1553–1561. IEEE, 2015.
- [100] K. E. Bassler, C. I. Del Genio, P. L. Erdős, I. Miklós, and Z. Toroczkai. Exact sampling of graphs with prescribed degree correlations. *New Journal of Physics*, 17(8):083052, 2015.
- [101] A. A. Boroojeni, J. Dewar, T. Wu, and J. M. Hyman. Generating bipartite networks with a prescribed joint degree distribution. *Journal of Complex Networks*, 5(6):839–857, 2017.
- [102] M. Latapy, C. Magnien, and N. Del Vecchio. Basic notions for the analysis of large two-mode networks. *Social networks*, 30(1):31–48, 2008.
- [103] U. Brandes. On variants of shortest-path betweenness centrality and their generic computation. *Social Networks*, 30(2):136–145, 2008.
- [104] L. C. Freeman. Centrality in social networks conceptual clarification. *Social networks*, 1(3):215–239, 1978.
- [105] P. S. Bearman, J. Moody, and K. Stovel. Chains of affection: The structure of adolescent romantic and sexual networks1. *American journal of sociology*, 110(1):44–91, 2004.
- [106] D. A. Schult and P. Swart. Exploring network structure, dynamics, and function using networkx. In *Proceedings of the 7th Python in Science Conferences (SciPy 2008)*, volume 2008, pages 11–16, 2008.
- [107] M. E. Newman. The structure and function of networks. *Computer Physics Communications*, 147(1):40–45, 2002.
- [108] S. L. Hakimi. On realizability of a set of integers as degrees of the vertices of a linear graph. i. *Journal of the Society for Industrial and Applied Mathematics*, 10(3):496–506, 1962.

Biography

The author was born in Boroojen in 1984 year and graduated from Amir Kabir University with MSc in 2009. The author started the PhD program at the Tulane University mathematics department in August 2012, eventually completing the program in May 2018.